Functional Effects of a Neuromelanin Analog on Dopaminergic Neurons in 3D Cell Culture: Biomaterials for Modeling Neurodegenerative Disease

A thesis submitted by

William R Collins

in partial fulfillment of the requirements for the degree of

PhD

in

Pharmacology and Experimental Therapeutics

Tufts University

Sackler School of Graduate Biomedical Sciences

February 2019

Advisor: David L Kaplan, PhD

Abstract

Neurodegenerative diseases have been declared the 'coming epidemic of the 21st century' and remain largely underfunded research outside of philanthropic organizations. However, the challenge of therapeutic development is more fundamental stemming from the lack of human physiologically-relevant research models. A prime example of this can be found in Neuromelanin (NM), the dark pigment which comprises the substantia nigra pars compacta (SNpc). Found predominantly in primates, NM binds neurotoxic compounds and transition metals. Extraction of NM from the cortex is labor intensive, protein contaminated and often provides low yields. On the other hand, synthetic melanins possess limited metal binding characteristic of true biological melanin. Researchers have even ventured so far as to extract NM from humans for use in animal cell culture models.

Using our existing 3D brain model we incorporated a NM analogue to dopaminergic cultures to add physiological relevance. Here we describe extraction, characterization and incorporation of *sepia melanin* as a functional replacement for NM in our 3D cultures. It was found that this NM analogue chelated transition metals unlike synthetic melanin. The iron-precipitate (Fe-NM) exhibited tailorable properties of particle diameter and ellipticity with ultrasonic dissociation. Furthermore, the product produced peroxides (H_2O_2) via Fenton chemistry (n=24, p<0.001, Peroxide Assay) and depleted antioxidants and nutrients from cell culture (n=8, p,0.05, GSSH Assay).

The 3D model was made 'human relevant' by making use of Lund's Human Mesencephalon (LUHMES) dopaminergic (DA) cells. We investigated the effects of this extracted NM and its precipitate on electrical activity by Local Field Potential (LFP) measurements and correlated the results against metabolic assays. We concluded that NM reliably reduces the activity of these neurons roughly two fold (n=22, p<0.05,

individual trials). Additionally, free-radicals generated by the precipitate depleted cell nutrients/antioxidants and increased the carbonylated proteins (~8 Fold Increase, $p<0.05$) suggesting oxidative damage to the proteome.

NM plays a fundamental role in disease progression. Theory regarding means by which NM may expedite neurodegeneration/dysregualtion within the human cortex is elaborated on including: (1) neurotransmitter oxidation (2) Neuromodulation (3) metallostasis. Future directions describing further experiments on neuro-inflammation, materials advancements, methods standardization and bioreactor integration are provided.

Dedication

This work is dedicated to my family who has supported me over the late nights and set-backs. My mom, who reminded this was the kind of work I always wanted to do no matter how difficult. My Dad, who recounts childhood stories of 'potion making' attempts and the mess that followed. My brother, who has stood by me through hard times and reminded me there is a world outside of the lab. My grandmother, for moral support. My beautiful wife, who works in STEM education and regales me with stories of her student's sense of enjoyment in tinkering and generally puts up with me.

Were it not for my grandfather's brain cancer; my godfather's affliction with Parkinson's and grandmother's affliction with dementia I likely would not have pursued neuroscience research. Lastly, this is dedicated to my grandfather and namesake who passed away in his 100th year just before the thesis came to an end.

In the future I hope to put family as a priority.

Acknowledgements:

First would like to thank the committee: Dr. Emmanuel Pothos (Manos) who has aided me innumerable times. Dr. Greenblatt, who serves as a perfect foil to my experimental meanderings. Dr. Fiorenzo Omenetto (Fio), who guided me in silk production and graciously provided an office at Scitech. I have great confidence that Dr. Nieland will carry on research pertaining to 3D models for neurodegenerative disease. Dr. Lovett will continue to guide the neuro-group's new exploits. Most of all would like to thank David Kaplan without whom this would not have been possible. In my reaching outside the Boston campus for greener pastures (both literally and figuratively) David was good enough to take a gamble on me.

The most notable contributions to this work were made by undergraduate students Kevin Kapner, Alex Jeremiah, Nick Hartman and Carlos Lopez-Rodriguez. Chief among them was Kevin without whom I would have quit out of frustration years ago. Additional students who contributed include: Chandler Glass, Eric Metaj, Camilla Gil, Roger Gu, Suraj Shah and Ian Jones. Contributions of fellow graduate students are duly noted as well including: Will Cantley, Disha Sood, Ash Sundarakrishnan and Tom Dixon. Guidance was also provided by post-doctoral scholars Yu-Ting Dingle and Volha (Olga) Luidanskya. Technicians Christopher Lucaj, Danielle Morrow and Peter Andrew of the Stephen Moss lab were and invaluable source of tissue for conducting studies.

Support staff were essential to the completion of this work including Milva Ricci, Carmen Preada and Laura Place (BME) and staff Karen Hatch (PPET). Martin Hunter provided support on Leica SP8 and SP2 confocal microscopes. Chuang Du provided assistance on electrophysiology. I am indebted to my colleagues Nic Rouleau and Mattia Bonzanni for assistance in editing the manuscript and collaborating on data. The bioreactor system can be partially ascribed to the help of Dr. Brian Timko of Tufts BME.

Ad-hoc graduate student therapists included: Annie Golding, Eleana Manousiouthakis, Jon Grasman, Dana Cairns, Ilya Rodionov and Olga Luidanskya providing moral support.

Former academic guides (Brandeis) include: Greg Petsko, Eve Marder, Irv Epstein, Jeff Agar, Don Katz and James Ragona (Sharon). Former research mentors (Foster Miller/QNA) include: Dr. Yongwoo Lee, Dr. Kin Chiu, Dr. Steve Weiss, Phil Bogue, Andy Riecker and John Larouco.

Multi-electrode Array (MEA) results were supported by Axion Biosystems and efforts of the Timko lab. This work was supported by the NIH Tissue Engineering Resource Center TERC (R01NS092847, P41EB002520), the W.M. Keck Foundation and the Allen Discovery Center at Tufts University is gratefully acknowledged.

Table of Contents

List of Tables

List of Figures

List of Copyrighted Materials

Kaxiras, E., Tsolakidis, A., Zonios, G., Meng, S. Structural Model of Eumelanin. *Physical review letters*, **97**(21), (2006).

Du, C., Collins, W., Cantley, W., Sood, D., & Kaplan, D. L. Tutorials for electrophysiological recordings in neuronal tissue engineering. *ACS Biomaterials Science & Engineering*, **3**(10), 2235-2246 (2017).

Sulzer, D. C., Cassidy, G., Horga, U.J., Kang, S., Fahn, L., Casella, G., Pezzoli, J., Langley, X.P. Hu, and Zucca, F.A.. Neuromelanin detection by magnetic resonance imaging (MRI) and its promise as a biomarker for Parkinson's disease. *NPJ Parkinson's disease*, **4**(1), 11. (2018).

Kim S., Thiessen, P.A., Bolton, E.E., Chen, J., Fu, G, Gindulyte, A., Han, L., He, J., He, S., Shoemaker, B.A., Wang, J., Yu, B., Zhang, J., Bryant, S.H., PubChem Substance and Compound databases. *Nucleic Acids Res*, **44**, (D1):D1202-13 (2016).

Peritore, Carina. Axion Biosystems (personal email communication 09-10-18) Email regarding usage of data collected during Maestro Multi Electrode Array (MEA) experiment visit at Tufts University, Medford.

Materials Copyrighted under Creative Commons

List of Abbreviations

5-HIAA, Hydroxy indole acetic acid;
AADC, Amino Acid Decarboxylase;
AD, Alzheimer's Disease;
ADP, Adenosine Diphosphate;
ASYN, Alpha-synuclein;
ATP, Adenosine Triphosphate;
AUC, Area under the curve;
B3T, Beta-3-tubulin;
BCA, Bichinoic Acid;
BDNF, Brain Derived Neurotrophic Factor;
BTC, Benzene Trichloric acid;
CA, Colorimetric Assay;
COMT, Catechol O-Methyl Transferase;
CPG, Central Pattern Generators;
CSF, Cerebrospinal Fluid;
DA, Dopamine/Dopaminergic;
DAPI, 4',6-diamidino-2-phenylindole;
DAT, Dopamine Transporter;
db-cAMP, di-butyryl cyclic AMP;
DBH, Dopamine beta hydroxylase;
DHI:DHICA, Dihydroxy indole: Dihydroxy indole carboxyl acid;
DLS, dynamic light scattering;
DOPAC, 3,4-Dihydroxyphenylacetic acid;
DPBS, Dubellco's Phosphate Buffered Saline;
DRD2, Dopamine Receptor D2;
DSM, Diagnostic and Statistics Manual;
ECM, Extracellular Matrix;
ELISA, Enzyme Linked Immunosorptive Assay;
EPI, Epinephrine;
EPR, Electron Paramagnetic Resonance;
FA, Fatty Acid;
FTIR, Fourier-transform infrared spectroscopy;
GDNF, Glial Derived Neurotrophic Factor;
GP, Globus palladius ; HDAC, Histone Deacetylase;
HEPES, Hydroxyethyl-piperazine-1-ethanesulfonic acid;
HPLC, High Pressure Liquid Chromatography;
HVA, Homovanillic acid;
IBS, Irritable bowel syndrome;
ICP-MS, Ion Coupled Plasma Mass Spectrometry;
LB, Lewy Bodies;
LC, Locus coeruleus;
LFP, local field potential;
LUHMES, Lund's Human Mesencephalon;
MAO, Monamine oxidase;
MCH, Melanin Concentrating Hormone;
MOF, Metal Organic Framework;
MOPS, Morpholino-propanesulfonic acid;
MPP+, Methyl-phenylpyridinium;
MPPP, methyl-phenyl-propionoxypiperidine (Desmethylprodine);

MPTP, 1-methyl-4-phenyl-1,2,3,6-tetrahydropyridine;
MRI, Magnetic Resonance Imaging;
MS, Mass Spectrometry;
NEPI, Norepinephrine;
NM, Neuromelanin;
NMDA, N-Methyl-D-aspartic acid;
NO, Nitric Oxide;
NT, Neurotransmitter;
PD, Parkinson's Disease;
PSP, Progressive Supranuclear Palsy;
RN, Raphe Nucleus;
RNS, Reactive Nitrogen Species;
ROS, Reactive Oxygen Species;
SEM, Scanning Electron Microscope;
SN, Substantia nigra;
SOD, Super Oxide Dismutase;
STN, Subthalamic nucleus;
SYN, Synaptophysin;
TBI, Traumatic Brain Injury;
TH, Tyrosine hydroxylase;
TSE, Transmissible Spongiform Encephalopathy;
TTX, Tetrodotoxin;
UPDRS, Unified Parkinson's Disease Rating Scale;
VMAT, Vesicular Monamine Transporter;
WNT, Wingless integrated;
WST-1, Water Soluble Tetrazolium;

Chapter 1. Introduction

The original work described here was developed by Dr. Min Tang-Schomer and was the basis for this research. Dr. Tang-Schomer's fundamental approach paved the way for all ongoing research on traumatic brain injury (TBI) and for emphasis to be placed on the neurodegenerative disease state [1]. These tissue engineering innovations were further advanced by Dr. Chwalek in video publication that documented the stages of silk processing and cell seeding with primary cortical neurons [2]. The work of Dr. Sood furthered integration of extracellular matrix (ECM) component derived from primary tissue. Greater proliferation and connectivity of primary cortical neurons could be identified with embryonic derived ECM [3]. Here we aim to further advance disease relevance of neural tissue engineered models by integrating the pigment neuromelanin (NM) a naturally occurring human disease relevant biomaterial.

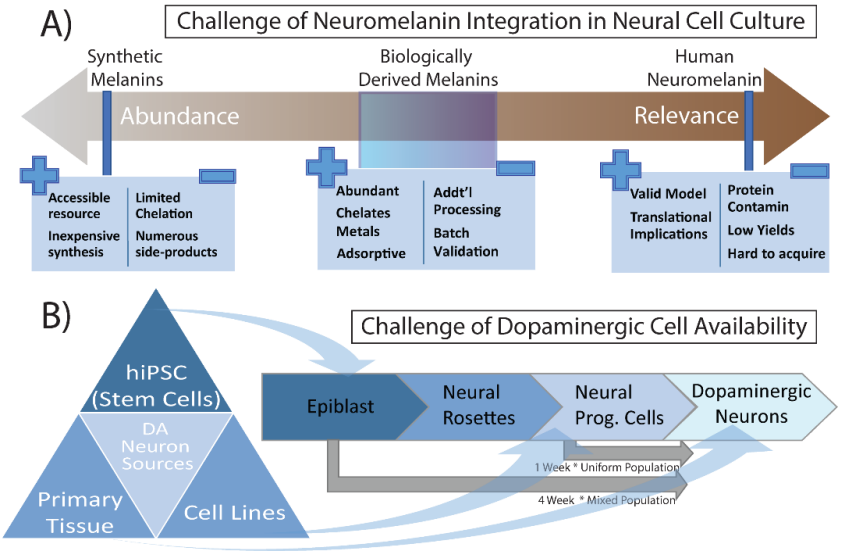

Figure 1.1 Schematic of Challenges in Sourcing Materials & Cells for PD Models

In development of PD models relevant to the human SN the challenges for investigators are twofold. (A) Gathering the necessary NM for incorporation into cell culture or finding suitable alternatives. (B) Having access to dopaminergic neurons which can be derived from: stem cells, primary tissue, or cell lines; of which stem cells may present lineage control issues or long durations of differentiation and primary tissues would provide low yields. Biologically derived melanin coupled with a human cell line was selected for this study.

Much of what we have come to learn regarding the human brain revolves around tragic but otherwise informative accidents guided by curiosity (i.e. Phineas Gage, early phrenology). The story of NM and Parkinson's is no different; driven by the discovery of neurotoxins which have an affinity for NM (See Figure 1.3) but providing models with acute effects that undermine how the disease progresses organically (See Figure 1.4).

1.1 Survey of Neuromelanin and the *Substantia Nigra*

NM was first described by Cajal as early as 1838 and was considered a highly unusual part of the brain even then as it has remained a subject of interest since [4]. While there has been vigorous debate regarding NM's biological synthesis methods it is often regarded to be the product of oxidation and internal rearrangement of dopamine (DA) to quinone and indole derivatives followed by reduction and cyclization [5, 6]. However, the dopaquinone (DAQ) derivatives are thought to be cytotoxic resulting in protein aggregation of alpha-synuclein by the interaction with thiol groups [7, 8].

The structural properties of NM have been elucidated due in large part to the investigative work of Meng and Kaxiras [9, 10], among many other respectable scientists. Mechanistic synthesis of NM is ascribed in part to the efforts of organic chemists Wakamatsu, Ito and colleagues [5]. A thoroughly abridged version of this interaction can be found in Figure 1.1A which references the convergence of dihydroxy-indole (DHI) derivatives during biological synthesis and illustrates the binding of proteins. Subsequent vacuolar ingestion and cross reaction with fatty acids described by Luigi Zecca, David Sulzer, Fabio Zucca and colleagues [11] illustrated in Figure 1.1B as NM aggregates. A comprehensive review of the synthesis, interactions and permutations of DA in broader context to NM can be found in the work of Meiser et al. "Complexity of dopamine metabolism" (2013) [12] and Schreoder et al. "Using Sepia melanin as a PD model to describe the binding characteristics of neuromelanin" (2015) [13].

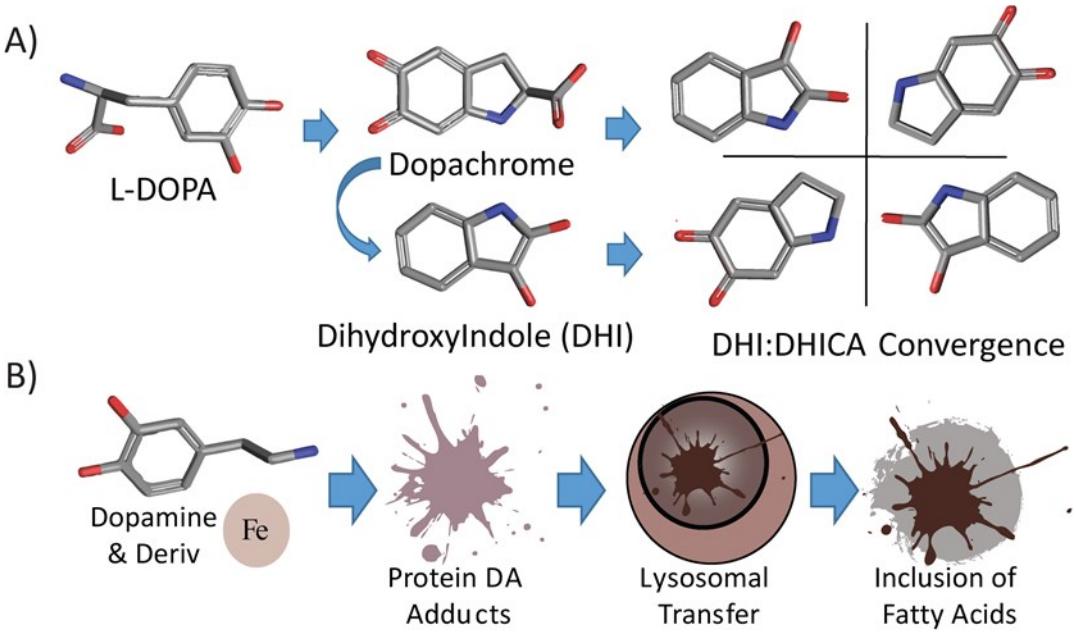

Figure 1.2 Schematic Neuromelanin Biological Synthesis and Protein Interaction

(A) Existing models of NM assume that a series of internal arrangements result in a product derived from dopachrome which when internally reduced, then converges into a structure analogous to that of NM. (B) Additionally, the conversion of DA and its close derivatives to DAQ facilitates the binding of the catecholamine to various proteins which are subsequently gathered by the lysosome only to be combined with other complex protein and fatty acid mixtures and synucleopathies ultimately yielding variable aggregate products. Adapted with permission from: Nucleic Acids Res. 44, Kim S., Thiessen P.A., Bolton E.E., Chen J., Fu G., Gindulyte A., Han L., He J., He S., Shoemaker B.A., Wang J., Yu B., Zhang J., Bryant S.H., PubChem Substance and Compound databases, D1202–D1213, (2016) [14]. Changes include: (A) vectoring, recoloring and overlay of molecules; changes in (B) include vectoring Dopamine molecule.

The understanding of NM's interactions with both the lipidome and proteome is the subject of ongoing research which pertains to specialized NM organelles that accumulate a diverse array of proteins over the lifetime of an individual (Figure 1.2 B) described as Lewy bodies (LB) [15]. Interaction of NM and the proteome result in an immense diversity of associated proteins for which patients who exhibit similar neurological outcomes may present a diverse array of associated proteins (i.e. Tau, β-amyloid in addition to α-synuclein) [16]. This has led investigators to explore clinical overlap between PD and other neurodegenerative conditions like dementia clinically defined as PD with dementia (PDD) [17]. However, the diversity of NM associated

proteins, coupled with varying clinical outcomes (i.e. PDD), comorbidities and genetic risk factors associated with PD (See Table 1.4) have confounded specific diagnostic biomarkers of disease for PD investigators [18] and slowed the development of treatments[19] for lack of a comprehensive diagnostic criteria and approaches.

Advances in modelling PD have emerged from neurotoxic compounds (See Table 1.1) but many investigators have found this acute neurotoxic approach misleading for screening therapeutic compounds for a disease progression that can be >10 years in development [20]. For this reason a 'paradigm shift' in drug discovery has been suggested [21] revolving around human relevant tissue modelling [22] in the third dimension [23] in efforts to account for discrepancies between neurotoxic PD models and clinical development of PD therapeutics.

1.1.1. 'The Case of Frozen Addicts': Established Neurotoxic Models

A good deal of what we know about PD is based around an unfortunate but serendipitous accident that occurred in the 1980's (See Figure 1.3), colloquially known as the 'case of the frozen addicts', as recounted by medical doctor William Langston [24]. One afternoon in the Santa Clara, CA County ER, a rash of adults under forty years of age came in exhibiting the resting tremor of PD patients. It was found that all victims had injected the synthetic opioid drug methyl-phenyl-propionoxypiperidine (MPPP). The drug was traced back to its origin and the product was found to be methyl-phenyl-tetrahydropyridine (MPTP) [25]; the product of a failed organic synthesis. In the months following discovery, it was found MPTP had an affinity for the substantia nigra (SN), due to the presence of neuromelanin (NM) and that MPTP's metabolite Methyl-phenylpyridinium (MPP+)[26], acts on complex-I of the mitochondrial matrix and indirectly acts in 'uncoupling' the electron transport chain [27]; creating a sustained

source of free radicals which caused extensive damage to the dopaminergic (DA) neurons and the manifestation of PD symptoms [28].

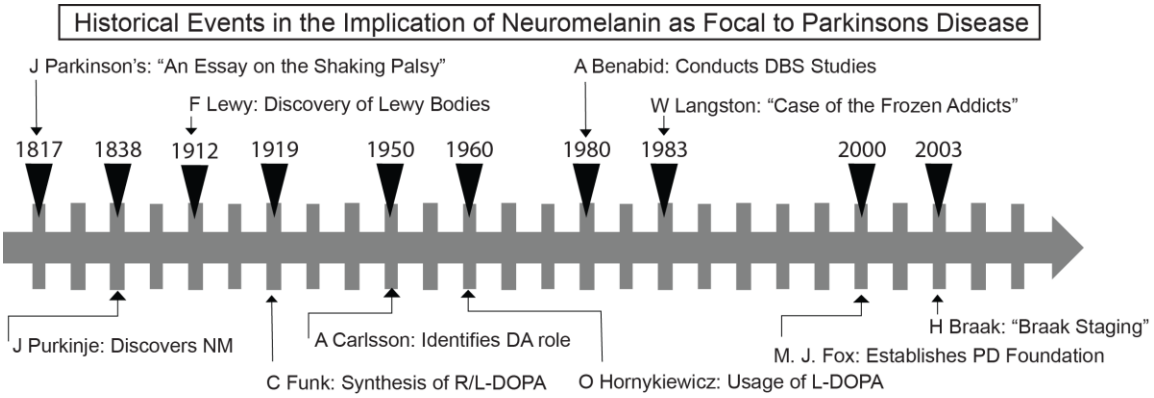

Figure 1.3 Historical Events Regarding Neuromelanin

Above the major events in the discovery of NM in context to PD are summarized. Events most relevant to this introduction include: (1) William Langston's encountering neurotoxic MPTP (1983) and (2) Heiko Braak's identification of staging events in PD progression (2003). The extended timeline of L-DOPA's discovery (~50 years) and its current usage today are noted. Therapeutic investigation for neurodegenerative conditions could be further expedited through tissue engineered models.

While the discovery of MPTP was beneficial for PD research it presents an immense potential to mislead the scientific community regarding disease etiology as it is an acute neurotoxin that lacks the finesse of 'organic' clinical disease progression [20]. The assumption that MPTP mechanisms are capable of being universally generalized to PD illustrates pre-conceived notions regarding causality, as inducing neurotoxicity is an acute/crude means of accomplishing a PD model [20]. Nevertheless, the 'case of frozen addicts' pointed researchers in the direction of the *substantia nigra* (SN), the focal point of this research pertaining to NM [24]. MPTP and MPP+ implicated a variety of other neurotoxins as causal in the development of PD many of which are classified as pesticides and insecticides following the wake of Rachel Carson's 'Silent Spring' [29].

Some of these neurotoxic insecticides and pesticides are illustrated in Table 1.1 in addition to neurotoxic metals that can be found in Table 1.2.

Curiously enough, it was found that the MPTP neurotoxic mechanism worked on specific animal models (i.e. predominantly primate models) due to NM presence [30] as younger rat models would be resilient to the toxic effects and were resilient to neurotoxic effects [17]. Some researchers have gone so far as to extract NM from the human cortex and incorporate it into experimental models [31] which is both labor intensive and provides low yields (0.15mg per SNpc) [32] the product of which is often contaminated with protein [13]. For investigators without ample access to a morgue and persistence in engaging a university ethics board, NM serves as a 'limiting reagent' in reconciling translational models [33].

Over time the list of implicated neurotoxic compounds in PD expanded and mechanistic understanding of the disease did as well [20]; in part due to improvements in transgenic techniques [36]. During this time the revolution in genomics identified key genes implicated in PD but the majority of cases fall under the guise of 'idiopathic' or unknown origin [37] suggesting environmental factors are causal in PD development.

Neurotoxin	Abbrev.	Mech. of Action	CAS No.	Cit.
methyl-phenyl-tetrahydropyridine	MPTP	Compl-I Mito	28289-54-5	[24]
tri-hydroxy-phenethylamine or hydroxydopamine	6-OHDA	Neural Excitoxicity	1199-18-4	[34]
Rotenone or Tubatoxin	N/A	Compl-I Mito	83-79-4	[26]
tetrahydroisoquinoline or Norsalsolinol	NorSAL	DNA Damage	34827-33-3	[35]
Dimethyl-bipyridinium or Paraquat	N/A	Compl-I/III Mito	1910-42-5	[26]

Table 1.1 Established Neurotoxins Relevant to Neuromelanin

The majority of cellular mechanism of action of the established neurotoxins pertain to the mitochondrial uncoupling. An important distinction is that of 6-OHDA which acts primarily as an excitotoxic chemical and NorSAL which causes genomic damage. Neurodegeneration comprises more than acute neurotoxic damage and implicates genomic damage and proteasome turnover as well.

Many of the neurotoxic compounds found in Table 1.1 exhibit affinity for NM and contribute to the increased vulnerability of the SN relative to other parts of the cortex [38, 39]. However, the relationship between NM, neurotoxic drugs and transition metals requires further elucidation [40] in which metal chelation may displace NM bound xenobiotic drugs thereby causing a targeted release in the SN. Proposed means of characterizing these interactions can be found in the Future Directions (Section 3.4.5. pg. 78) which considers metal displacement as it pertains to chemical affinity.

While the neurotoxic effects of pesticides were becoming active research topics, research pertaining to the impact of metals on the nervous system had been established (See Table 1.2). It is generally accepted that lead (Pb), cadmium (Cd) and mercury (Hg) are among the most pernicious targets of the CNS [41] leading to dysregulation of the immune system and demyelination [42, 43].

Metal		Disease Implicated	Additional Symptoms	Ref.
Cadmium	Cd	Itai-Itai Disease, Anosmia	Blood Acidity, Gout	[44]
Mercury	Hg	Minamata & Young's Disease	Demyelination, Autoimmunity	[45]
Manganese	Mn	Lou Gherig's (similar)	Irritability, Motor Dysfunction	[44]
Nickel	Ni	Behavioral Deficits	Inflammation, Dermatitis	[46]
Copper	Cu	Wilson's Disease	Anemia, Jaundice	[47]
Lead	Pb	Cognitive/Learning Deficits	Neuropathy,Blood pressure	[48]

Table 1.2 Metals Implicated in CNS Toxicity

Metals have been long established poisons of the nervous system. Lead and mercury are perhaps the most widely known neurotoxic element but numerous other seemingly innocuous transition metals are capable of inducing cytotoxic damage as well. In many cases exposure results in neurodevelopmental and neuroendocrine disruption that extends beyond the scope of this work.

A wide array of cellular mechanisms are perturbed by these transition metals (See Table 1.2) pertaining largely to: voltage activated channels, ion transport mechanisms, neurotransmitter release and synthesis and excitotoxicity [49]. A comprehensive review

can be found in Sadiq et al., “Metal Toxicity at the Synapse” (2012). Aspects of metal homeostasis or ‘metallostasis’ as it pertains to cell viability is illustrated in the Discussion (See Table 3.1). Further investigation of the role of ‘metallostasis’ as it pertains to PD is an ongoing research topic [50, 51] and worth pursuing if it were to yield organometallic therapeutics capable of reinstating cell homeostasis. However, the existing means of PD treatment is L-DOPA, discovered in the 1950’s (See Figure 1.3), which remains a mainstay of therapeutic intervention to this day.

1.1.2. ‘Awakenings’: L-DOPA and Current Therapeutics

L-DOPA was originally derived as a natural product fava beans as early as 1913 by Torquato Torquati before further isolation and characterization by Markus Guggenheim [52] The original chemical synthesis of racemic mixture D/L-DOPA was executed by Barger and Ewans in 1911 [52]. However, stereo-selective synthesis of L-DOPA was not developed until William Knowles perfected an organometallic catalyst for scalable production of the drug for which the Nobel prize was awarded [53].

L-DOPA (or Levodopa) gained popular renown due in part to the book ‘Awakenings’ by Dr. Oliver Sacks (1933-2015) [54]. During an outbreak of encephalitis in the 1920’s several patients were given an experimental drug L-DOPA which caused them to miraculously emerge from a comatose state [54]. Later, the work of Arvid Carlsson, George Cotzias and Oleh Hornykiewicz emphasized L-DOPA’s use in treatment of PD [55].To this day one of the most common forms of PD treatment involves co-formulation of the drug with a COMT inhibitor under the trade name ‘Sinemet’ [56]. As it became evident that dopamine (DA) was focal to the development of PD symptoms further efforts to design drugs around the DA metabolism were pursued [12]. Some of the therapeutics are intended to mitigate hallucinations or extra-pyramidal symptoms (See Table 1.3) of

the treatment regieme but the key therapeutic target mechanism has remained largely unchanged for many years [18].

TARGET	CLASS	TRIVIAL NAME	Cite
Central Nervous System	Neurotransmitter Precursor	Tyrosine Suppl.	[12]
		L-DOPA	[57]
	Dopamine D2 Agonist	Bromocriptine	
		Apomorphine	[17]
		Cabergoline	
		Ropinirole	
		Rotigotine	
Periphereal Nervous System	MAO-B Inhibitor	Rasagline	
		Selegline	
	COMT Inhibitor	Entacapone	[56]
		Tolcapone	
	Decarboxylase inhibitors	Benserazide	
		Carbidopa	
Extrapyramidal Symptoms	Anticholinergic Antimuscarinic	Benzatropine	[58]
		Diphenylhydramine	

Table 1.3 Established Drugs Pertaining to DA Metabolism in Parkinson's

The table illustrates that existing therapeutics are focused on supplementing the DA pathway both by reducing degradation (i.e. COMT and MAO-B inhibitors) and increasing NT precursors or mimicking DA effects (i.e. Precursors and D2 Agonists). Other means of addressing the fundamental challenges of PD (i.e. neuroprotective compounds rather than mitigating the condition) require further validation due to insubstantial clinical research at the time this research was published.

PD treatments primarily seek to mitigate the symptoms of disease and are not curative of the underlying cause despite extensive efforts in developing neuroprotectants for PD [18, 30, 59] often the condition is too advanced. Despite decades of investigation L-DOPA remains a mainstay of PD treatment though clinicians debate if the compound is best delayed until later stages of the disease [57] theoretically to slow the rate of progression. A promising new approach making use of selective calcium ion channel blocker, isradipine, [60] can be found in the Discussion section (3.3. Local Field Potential pg 64) in terms of emerging treatments. Additionally, tissue engineered constructs and stem cell methods have been explored as well (See Section 1.4).

1.1.3. 'Braak to the Future'[1]: Model Advancements

To contrast differences between the PD experimental model (Section 1.1.1.) and what is clinically known about disease progression the complexity of PD emergence throughout the brain is illustrated in Figure 1.4. While the olfactory bulb and brain-stem (rhombencephalon) are not often thought to be implicated in neurodegenerative disease both play a prominent role in the early stages of disease progression. In accordance with the 'Braak Stages' of Parkinson's disease (See Figure 1.4) progression Lewy body pathologies tend to emerge in the pons/medulla and olfactory bulb well before the shaking gate and resting tremor emerge [61]. Anosmia, loss of smell, is considered one of the preliminary indicators of disease progression in both PD and Alzheimer's Disease (AD) [62] which occurs gradually a decade or more before disease onset [63]. For instance, as a population welders were thought to be more prone to neurodegenerative disease perhaps due to their exposure to acetylene and manganese (Mn) derivatives (See Table 1.2) which have been found to be acutely neurotoxic [44, 64].

In keeping with the assumptions of 'Braak stages of PD' there are several leading behavioral indicators that preclude the occurrence of resting tremor and freezing gait [65]. Depression, anxiety, hedonic behavior and affinity for gambling are but a few of the theoretical leading indicators of PD which appear well before motor symptoms [61] in accordance with clinical characterization [66]. The pre-motor areas of the brain are impacted in Stage III (Figure 1.4) when progression affects the SN and motor symptoms begin to accelerate [67]. While evidence for behavioral changes are often anecdotal and circumstantial they remain a crucial portion of the physician evaluation for PD symptomology [68]. The most common of these includes the United Parkinson's Disease

[1] "Braak to the Future" pun is attributed to: Visanji, Naomi P., et al. "The prion hypothesis in Parkinson's disease: Braak to the future." *Acta neuropathologica communications* 1.1 (2013): 2.

Rating Score (UPDRS) system by which the stages of disease progression can be determined [69].

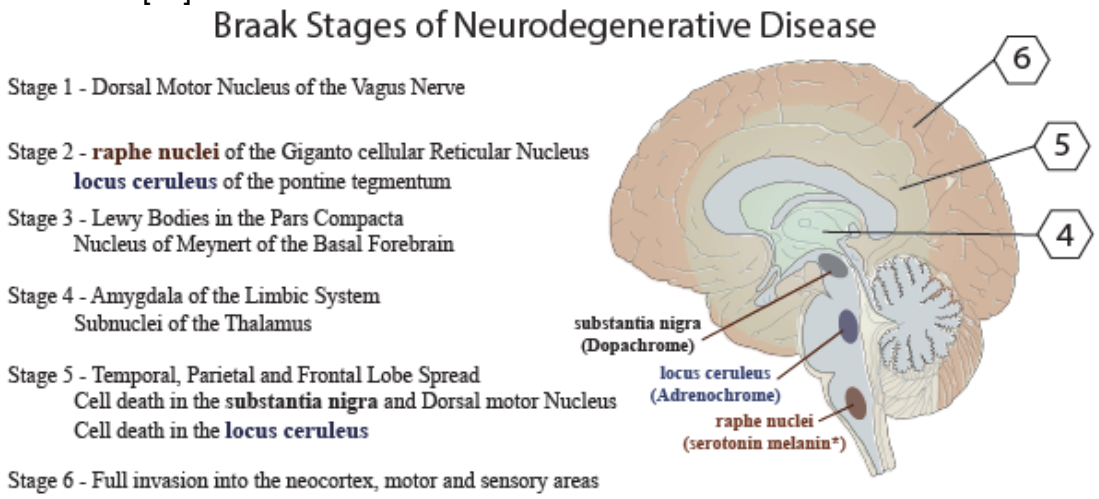

Figure 1.4 Braak Staging Hypothesis of Neurodegenerative Disease

The schematic above highlights the stages of the condition and correspond to histopathological evidence of the disease from post-mortem brains. Of note, the stages highlight the presence in the serotonin rich raphe nucleus (RN) and locus coereuleus (LC) in Stage 2 before presence in the SN. The histopathological stages are thought to correlate with behavioral deficits seen before motor symptoms are evident (Stages 3-6). [70] 'Serotonin melanin' is a theorized molecule structurally linked to melotonin beyond the scope of this work. Adapted with permission from: Creative Commons through Pixabay.com by OpenClipart-Vectors 'Brain'. Changes include: recoloring the brain image; adding reference numbers; highlighting impacted regions of the brain and smoothing lines.

Investigators suspect that PD emerges in the gut and over time is capable of retroactive spread throughout the cortex [71]. This gut-brain interaction is an active research topic which bridges several disciplines pertaining to the microbiota and emerge throughout the large intestine [72]. Braak and colleagues went so far as to correlate bowel movement with PD progression citing epidemiological work of the Honolulu Heart Program (HHP) [66, 73]. While the 'Braak model' has its critics in regards to clinical reproducibility and experimental relevance [74] it remains a guiding series of events for disease progression though investigators debate its implication and timeline [66]. Epidemiological evidence highlights a dual role of genetics (See Table 1.4) and lifestyle-environmental factors as contributory in PD progression from genome wide association studies (GWAS)[21].

1.2 Neurodegenerative Disease Etiology

Regarding lifestyle contributions to neurodegeneration, coffee and tobacco have remained potential neuroprotectants against PD in epidemiological literature [34, 59]. However, research on coffee has predominantly focused on caffeine and neglected the numerous ‘phytochelatins’ present in the beverage [75] which may buffer against free metals in the intestine and protein aggregation [76]. Comparative studies of caffeinated/decaffeinated coffee have remained largely inconclusive perhaps due to such discrepancies of study design emphasis.

1.2.1 Epidemiology and Genes Implicated in PD

From a population perspective PD effects predominantly males over females by a factor of ~2; although this is gender difference is dependent on age and environmental factors [77]. Additionally, some correlations have been drawn between onset of menopause and the occurrence of Parkinson’s as well [78]. This consequently led researchers to investigate the relationship between anemia, low blood iron and onset of PD which was ascribed to ‘brain iron overload’ in regards to menopause [79] but has not been more extensively addressed by epidemiologists to current knowledge [80]. The relationship between gender and PD susceptibility merits further investigation as hormones, progesterone and dehydroepiandrosterone demonstrate significant influence on the brain function and connectivity [63].

Gene	Full Name	Effect	Associated Conditions	Cite
ASYN	Alpha-synuclein	Synaptic rearrangement	Multiple system atrophy	[16]
		SNARE complex chaperonin		
LRRK	Leucine Rich Repeat Kinase	Mitochondrial membrane	Crohn's Disease	[81]
		Shortening of dendritic spines		
		Chaperone mediated autophagy		
GBA	β-Glucocerebrosidase	Associated w. lysosomal membrane	Lysosomal Storage; Gaucher's	[17]
		Recognition and hydrolysis		
PRKN	Parkin	Mitochondrial Dysfunction	Glioblastoma; Colorectal cancer	[82]
		Ubiquitin proteosome		
PINK	PTEN -induced putative kinase 1	Depolarized mitochondria	Mitochondrial dysfunction	[83]
		Induction of autophagy		
DJ-1	Protein deglycase	α-Syn aggregation via chaperonins	Metal induced cytotoxicity	[26]
		Prevents Cu & Hg toxicity; ROS sensor		

Table 1.4 Genes Implicated in Parkinson's Disease and Categorization

Above are the major genes found in the hereditary and genetic-risk associated forms of PD. The table is intended to illustrate that co-morbidity includes a variety of metabolic and lysosomal storage disorders which revolve around the mitochondria, proteome, synaptic bed and vesicle trafficking mechanisms. A substantial portion of the diagnosed cases of PD may not possess any of the major genes implicated leading some to be considered 'risk factors' and not always directly causal to the disease state.

Table 1.4 illustrates the genes implicated in PD, which collectively appear to be implicated in four primary cell interaction sites: Mitochondria, Lysosome, Synaptic Bed and vesicular trafficking (i.e. Golgi & ER)[72, 84]. Additionally, the genes in question demonstrate co-morbidity with a diverse array of metabolic, lysosomal storage and inflammatory disorders suggesting an inter-relatedness between the proteome and subsequent neurodegeneration [15, 85]. While this work focuses primarily on NM and

transition metal exposure it is presumed that similar mechanism of action would occur in the disease state [86, 87] (i.e. increased proteosomal turnover, ubiquitination).

1.3 Means of Investigation

As the variety of metabolic, proteosomal and inflammatory implications are too non-descript for clinical investigation a review of known indicators in disease is provided (Table 1.5). However, many of the biomarkers described require longitudinal study validation before being considered reliably diagnostic [88]. Post-translational modification and alternative splicing, as it pertains to PD [63, 89], may comprise the difference between accurate and misleading diagnostic criteria and if reliant on antibodies which cannot distinguish these nuances [90] then important distinctions regarding disease progression may go largely unnoticed. For instance, gaseous neurotransmitters like NO cannot be readily validated given their transient nature as free radicals (See Section 3.3.2. pg. 61).

1.3.1. Clinical Biomarkers

In the past clinical evidence regarding PD has focused around the UPDRS clinical test describing both the behavioral and physiological symptoms of the disease [69]. While there is benefit in clinical evaluation, often the disease has become far more advanced than when preventative measures would be beneficial. Increasingly, research has turned to markers extracted from cerebrospinal fluid (CSF) and blood serum to provide earlier indications of disease [91].

One of the unique challenges encountered in determining early stage biomarkers is the identification of ‘post-translational’ modification and ‘alternative splicing’ of genes which may elude such established tests as ELISA’s due to the target-specificity of capture antibodies [90]. These forms of ‘post-translational modification’ may take several

forms but generally encompass (1) Addition of functional groups (i.e. Phosphorylation) [92, 93] (2) and structural changes (i.e. disulfide bridges and protein splicing) [94, 95].

Sometimes post-translational modifications are more subtle, for instance there are several varieties of the enzyme super oxide dismutase (SOD) which depend on the variety of catalytic metal present (i.e. SOD1 is Cu-Zn and SOD2 is Fe-Mn) [83, 96]. As could be imagined the absence of key metal catalysts could result in a substitution (i.e. Fe for Mg) which would therefore affect the binding substrate and reaction kinetics, substitution of Fe in metallo-enzymes with other metal co-factors is generally conducted under conditions of 'metal starvation' [97] (See Table 3.1).

Source	Marker	Means of Detection	Citation
Serum & CSF	Oligomerized Alpha-Synuclein	ELISA	[94]
	Nitrotyrosine	HPLC	[98]
	Uric Acid	HPLC	[98]
Lysate	Ubiquitin	ELISA, MS	[99]
CSF	8 Hydroxydoexyguanosine (8-OHdG)	HPLC	[98]
	metallothioneins (MT1, MT2, MT3)	ELISA, CA	[63]
	Coenzyme Q10	HPLC	[63]
	Glutathione	CA, HPLC	[63]
Cortex	Serotonin	HPLC, CA	[63]
	Dopamine	HPLC. CA	[100]
CSF	DJ-1	Chip-Assay	[101]
	Fractalkine	Chip-Assay	[32]
	alpha-synuclein	Chip-Assay	[32]

Table 1.5 Biomarkers Regarding Neurodegenerative Disease Progression

Notable diagnostic biomarkers established in clinical literature and their primary means of quantification. HPLC – High Pressure Liquid Chromatography; ELISA – Enzyme linked immunosorptive assay; CA - colorimetric assay; MS - Mass spectrometry. Many of the means of detection have redundancies (i.e. MS and Chip-Assays) but those selected have a lower detection threshold.

One of the challenges of PD research is that the proteins implicated often undergo structural modification which may render antibody binding substrates ineffective [102].

As these antibodies are (1) batch dependent (2) require validation and (3) may not be specific to the region of interest suggesting more extensive quality control measures than many academic labs have undertaken [102, 103]. In conclusion, the field PD biomarkers remains somewhat ambiguous and thus may be subject to 'fishing expedition' investigation without supporting clinical imaging and cell culture models.

1.3.2. NeuroImaging and Electrophysiological Techniques

Electron Paramagnetic Resonance (EPR) is a form of spectroscopy capable of observing the difference in spin states of metal ions and has been applied to the SN and LC of PD patients [104, 105]. Modified versions of EPR spectroscopy is capable of observing transition states of alpha-synuclein [106]. NM extracted from the human mesencephalon was analyzed with EPR spectral analysis as well and it was revealed that a pool of 'peculiarly organized' iron (Figure 1.5) demonstrated 'superparamagnetic' behavior which can now be directly observed with EPR techniques [107, 108]. Paramagnetic materials like chelated NM exhibit a strong dipole moment which tend to interact with free radicals also possessing dipoles (i.e. Nitric oxide and peroxides)[109]. Details of the interaction between nitric oxide (NO) free radicals and NM aggregates are relevant to post-translational modification [110] (See Figure 4.3)

Figure 1.5 illustrates that in advanced stages of the disease metals accumulate within the organelles of the human brain. This suggests that not only is a great deal of NM present but large quantities of iron can be found as well [15] in disorganized aggregates. It is speculated that chemical reduction (i.e. alkyne to alkane groups) or internal rearrangements may contribute to the inefficiency of the proteome to degrade proteins or fatty acids [111] that have been structurally modified [50] as the enzymatic cleavage sites would likely be inactivated by oxidation.

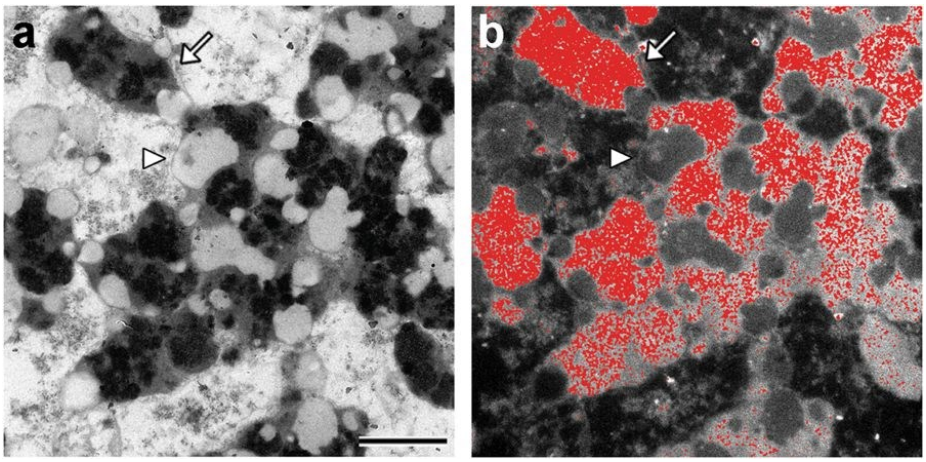

Figure 1.5 Neuromelanin Detection by Magnetic Resonance Imaging (MRI)

Iron distribution in NM-containing organelles of human SN (89 y.o.) revealed by using electron spectroscopic imaging. In the left panel (a) transmission electron microscopy indicates the classical morphology of NM-containing organelles: these organelles contain large amount of dark NM pigment (arrow) strictly associated with lipid bodies (arrow head). The iron distribution map was created by electron spectroscopic imaging (b) and revealed that large amounts of iron (red spots) are localized into the NM pigment of the organelles, consistent with the ability of NM pigment to scavenge iron forming stable complexes. Electron spectroscopic imaging was performed using a LEO 912AB electron microscope. Scale bar = 1 μm. Reprinted with permission from: NPJ Parkinson's Disease, 4, Sulzer D., Cassidy C., Horga G., Isaisa I. and Zecca L., Neuromelanin detection by magnetic resonance imaging (MRI) and its promise as a biomarker for Parkinson's disease, 1-13, (2018). [15]

Collectively this illustrates that bound iron has a catalytic role in generation of superoxide radicals which concurrently interact with nitric oxide (NO) to form more reactive peroxynitrite [112] capable of modifying aromatic amino acid residues (i.e. nitrotyrosine) [97, 113] and nitrosothiols (i.e. SNO-proteins) [110] thereby supporting the catalytic role of iron accumulation in neurodegeneration.

1.3.3. Electrophysiological Techniques

Local Field Potential (LFP) technique was originally developed as a recording technique for ascertaining synchronized input from neural networks by fluctuations in action potential activity. Early work on the technique focused on neuro-oscillations and was correlated against membrane potential fluctuation [114, 115]. These oscillations were predominantly categorized according to those of the beta (12.5 to 30Hz) and

gamma (25-100 Hz) waveforms [116]. Major considerations for LFP concern the: (1) the geometric arrangements of cells (2) synchronized input and (3) band-pass filtering as it pertains to background noise [117].

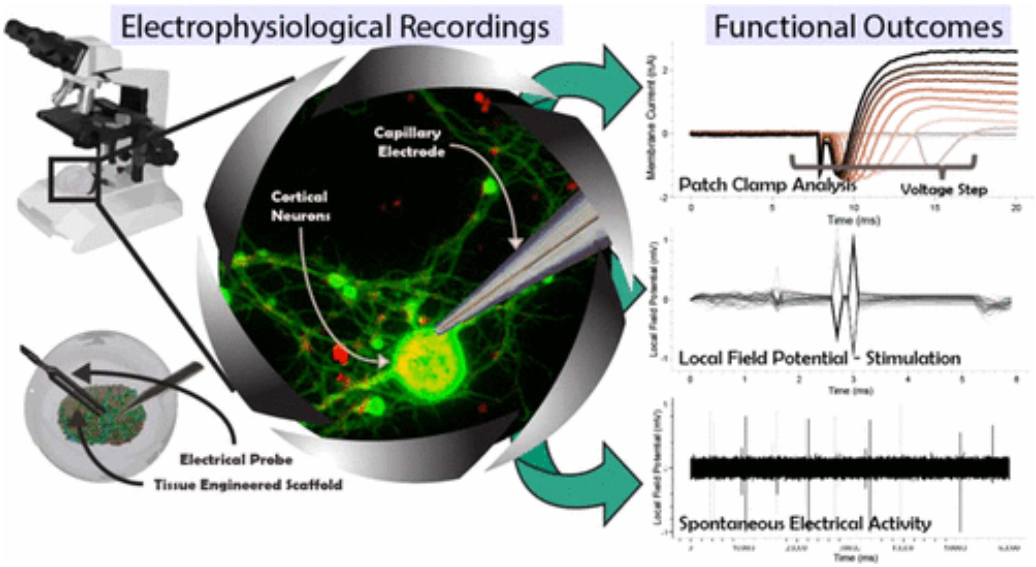

Figure 1.6 Electrophysiological Recordings Schematic

Schematic of Electrophysiological Measurements depicting patch-clamp results (top-right) and local field potential (bottom-right). Electrical stimulation can be applied to induce firing as can be seen in the 'stimulation' figure (middle right). Reprinted with permission from: ACS Biomaterials Science., 10, Du C, Collins W., Cantley W., Sood D., Kaplan D.L., Tutorials for electrophysiological recordings in neuronal tissue engineering, 3-10, (2017) [117].

From a phenomenological perspective the oscillatory network behaviors capable of being recorded through electrophysiological methods for resting tremor are thought to emerge from 'attractor networks'; simply put an attractor is a dynamical system within which global trends emerge from a diverse variety of 'chaotic' or non-synchronous starting conditions [118]. Synchronous behavior, as it pertains to PD, is the result of neural network cohesion and has been a subject of tissue engineering efforts for decades in efforts to recover the SN from neurodegeneration (See Table 1.6).

1.4 Existing Substantia Nigra Tissue Engineering Models

The following highlights the means by which 3D scaffolds can be characterized.

(1) Tissue Dimensionality		
2D	Advantages	Disadvantages
Glass Slides	Well established	High Stiffness, X-Y plane Limts
2.5D	Advantages	Disadvantages
Slice Physiology	Physiological relevance	Narrow time window
Microfluidic Chip	Comparmentalization, discrete application	Labor intensive; scalability issues; proof-of-concept
3D	Advantages	Disadvantages
Organoids	Exhibit diverse morphology	Necrotic core, Lineage control
Scaffolding	Controlled spatial architecture	Imaging & Visualization
Hydrogels	Tuneable hardness index	Oxygen permability
(2) Extracellular Matrix Components		
Source	Advantages	Disadvantages
Primary Tissue	Extensively Available Physiologically relevant	Time consumptive limited yields
E. Coli & Yeast Derived Proteins	Highly Scaleable Cost effective	Many proteins are cytotoxic Some require chaperonins
Biomaterial Derived	Relative Abundance	Sourcing materials often complex
(3) Cell Sourcing - Neuronal Cultures		
Variety	Advantages	Disadvantages
iPSC	Long culture duration	Lineage control and expense
Cell Line	Robust passaging, Low maintenance	Often cancer derived lineage
Primary Tissue	Physiological relevance	Animal housing costs; Limited duration in culture

Table 1.6 Contributory Factors in Tissue Engineered Models of the SN

Disease models are ideally comprised of three components (1) tissue dimensionality (i.e. 2D vs 3D) highlighted according to the variety of surface architecture in 3D (organoids, scaffolds, or hydrogels) (2) Extracellular matrix components (sourced from recombinant, animal or biomaterial sources) (3) Cell sources which may comprise either conditionally immortalized or cancer derived cell lines.

Tissue engineering of the SN has been an active research topic for several decades as grafts of neural stem cells have been successfully conducted with human embryonic stem cells [17]. However, experimental evidence suggests teratoma formation can occur

following stem cell grafting reducing any enthusiasm in an immediate/accessible PD cure [119]. If tissue environmental cues could direct the cell lineage [120] then it may be possible but thus far this has proven far more challenging than it appears [121].

Increasingly, the research field is moving towards 3D human relevant models [122] but progress has been incremental as there are a number of variables at play [123]; all of which must be combined in an appropriate manner. Use of de-celled ECM derived from embryonic and adult brain tissue has shown positive preliminary results in encouraging neuronal survival and re-innervation [3] but requires ongoing further research to validate for human models [124]. Additionally, incorporation of wingless/integrated (WNT) factors into media has been suggested as a means of maintaining stem-like attributes and controlling cell lineage [125]. More is to be done but the biomaterials field is encouraged by the incremental successes of research to expedite neuro-regenerative applications [126].

1.5 Research Directions and Hypothesis

Drawing inspiration from my mentor, Dr. Kaplan, and his work in silk biomaterials I similarly turned to a biomaterial source of melanin. As I discovered with NM, attempting to replicate the properties of silk fibroin would make the most accomplished organic chemists appear amateur [127, 128]. Initial efforts were ‘serendipitous’ as recounted by pouring too much dopamine on a silk sponge (which turned brown) before coming to the realization that neuromelanin could be a viable research topic. Following this ‘eureka moment’ it would have been ill-advised to resume pouring dopamine on silk. In sourcing biomaterials I turned to an unlikely place: to the depths of the sea, to the ancient and venerable squid (Cuttlefish), whose *sepia ink* has been coveted for centuries for its complex melanin pigments.

1.5.1. Research Direction: Benefits of Biologically Derived Neuromelanin

Literature suggested that synthetic melanin was not capable of addressing the diverse challenges of serving as a NM simulant [13] and so efforts were made to find a suitable alternative derived from cephalopod ink (*Sepia Officionalis*). Fortunately, methods describing extraction of water soluble melanin were explored by researchers in nutrition science previously [129]. Unlike the synthetic form of melanin, biologically derived product readily chelated metals and possessed a unique FTIR spectral profile (Figure 2.6 E). What was further needed was: 3D scaffolding, provided by silk fibroin; and a source of dopaminergic neurons, of which the LUHMES were found to be suitable [130].

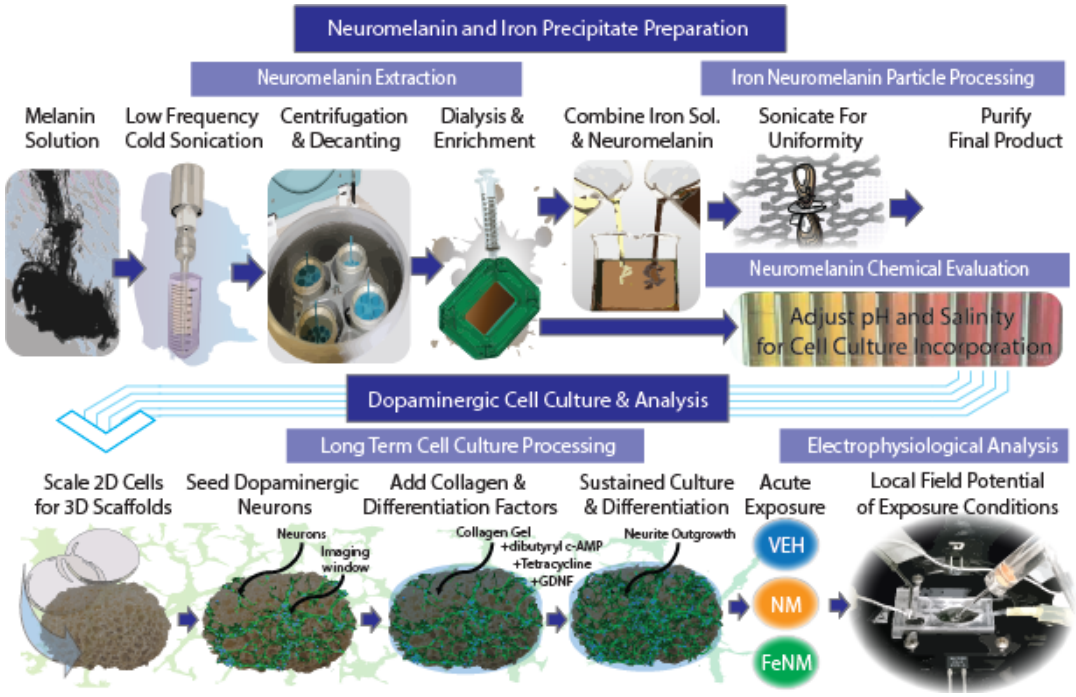

Figure 1.7 Extraction of Neuromelanin and Integration in Cell Culture

Sepia Melanin provided a source of aqeous (aq.) soluble melanin when sonicated under basic conditions as described previously [129]. The product was dialyzed and then took two paths. (1) The NM solution was characterized based on its spectral profile and (2) when combined with a stock solution of Fe the product created a precipitate which could be further processed to provide a defined precipitate (Fe-NM). Following this the LUHMES were grown to a density for 3D cell culture, cast in a collagen gel, and then exposed to Vehicle NM, and Fe-NM before LFP recording.

The extraction of NM from biomaterial sources and use of readily available human dopaminergic cell lines is intended to make the model available to researchers who do not have access to the resources that larger organizations affiliated with hospitals and patient samples might have.

1.5.2. Hypothesis: Neuromelanin as a Catalyst in Dopaminergic Cell Dysfunction

It was hypothesized that that (1) biomaterials (i.e. biologically derived melanins) are a far more suitable source of materials for modelling the substantia nigra than synthetic alternatives and (2) that the electrophysiological phenomena of Parkinsonian symptoms could be elucidated with 3D tissue cultures. Academic literature suggest that NM performs a ‘catalytic’ role in degeneration in context to PD in the conversion of dopaquinones [39]. Additionally, transition metals catalyze chemical reactions resulting in protein aggregation by di-tyrosine cross linking[131]. Collectively this suggest NM and its iron bound form are capable of catalytic reactions that have broader implications in regards to reduction of thiol groups, protein carbonylation and cell viability.

Chapter 2. Functional Effects of a Neuromelanin Analog on Dopaminergic Neurons in 3D Cell Culture

[2] Collins W., Rouleau N., Bonzanni M., Kapner K., Jeremiah A., Du C., Pothos E.N., Kaplan D.L., Accepted to ACS Biomaterials Science & Engineering, 23/11/18

2.1. Introduction

Neuromelanin (NM) has remained an elusive biomaterial for some time due to its unusual presence in the brain. It has been the focus of research due to its contradictory role both as an antioxidant [129] and as an irritant capable of inciting glial-induced neuro-inflammation [132]. However, much of this focus has been on 'synthetic melanin', which is generated by reacting dopamine and peroxide, resulting in a material that lacks many fundamental features of native melanin [13] and uncontrolled polymerization and stereochemistry [133]. These unique qualities include the capacity of NM to chelate metals, most notably iron and copper, thereby reducing the potential for generation of free radicals by 'Fenton chemistry' [134], and also adsorptive properties towards xenobiotics [135].

Melanin is primarily comprised of pheomelanin and eumelanin with chemical properties of UV-absorption, metal chelation and capacitance [136]. Despite the prominence of NM in the clinical literature, the material is challenging to extract from the brain, both in terms of solvents involved and the limited resulting yield [13]. To complicate matters, NM is also especially pronounced in human SNpc above other primates [137], further complicating the isolation and study in terms of procurement. In contrast, synthetic melanin presents different functional properties than 'biologically derived' melanin [13] and a number of poly-dopamine derivatives in an uncontrolled reaction [13, 133]. The challenge in extraction of endogenous NM drives the need for alternative options in order to formulate 3D tissue models of disease states towards physiologically-relevant functional scaffolds [22].

The 'biologically derived' form of melanin can be extracted from lyophilized cephalopod (*Sepia Officinalis*) ink and contains a complex mixture of derivatives of dopamine and is theorized to have the structure of hemi 5,6-dihydroxyindolequinone and

hemi 5,6-dihydroxyindole 2-carboxylic acid (DHI:DHICA) [9]. The binding affinity of this NM simulant (NM-sim) includes an extensive array of alkali and transition metals [138]. In contrast to the biologically-drived material, synthetic melanins preparations and chemically different and also vary based on method of preparation, ranging from incubation with tyrosinase to oxidation of tyrosine with hydrogen peroxide [13]. All of these synthetic NM preparations demonstrate a lower quantity of carboxylic acid groups than the biologically derived forms [13]. Furthermore, biological sources, like pigments derived from hair or eyes, are more likely to contain protein contaminants than those derived from cephalopod ink [139]. Sepia melanin was therefore selected as a suitable source of NM for studies of brain-related functions in vitro in the present work [13].

To explore the potential effects of this NM-sim and its metal-bound analogues (Fe-NM-sim) on neurological functions, 3D tissue analogs are needed. Silk protein-based scaffolds have supported tissue engineering studies providing benefits of mechanics, processing and biocompatibility [140], and as a support matrix for neural tissue studies [141] [142]. To generate in vitro 3D tissue systems for the study of the SNpc, we modified our prior 3D tissue-engineered brain-like constructs [143, 144]. For the present studies, LUHMES were utilized, as these cells have previously been used in both 2D and 3D tissue models [130, 145] to investigate cellular mechanisms of Parkinson's disease. While induced pluripotent stem cells (iPSC) are favorable for long-term studies LUHMES cells serve as reliable, conditionally immortalized, dopaminergic cells capable of differentiation and consistent passaging [146] for evaluation of neurotoxic compounds related to PD [147]. Post-differentiation, LUHMES are also electrically active, produce dopamine, alpha-synuclein, and express the necessary markers for a mature dopaminergic neuronal phenotype [130] [146]. In previous studies, LUHMES cells were grown in neurospheres in the absence of scaffolding containing exogenous extracellular

matrix (ECM) like NM in 3D as addressed in this study[147, 148]. In the present study, our objective was to use the prior 3D brain tissue engineering model to approximate the cyto-architecture the cortex, with the incorporation of the extracellular matrix in a 3D microenvironment along with the LUHMES to emulate the dopaminergic phenotype [130].

A distinction between the SNpc of persons of advanced age is the absence of NM and increased metal content, which correlates with presence of PD symptomology [149]. Furthermore, the interaction of transition metals with NM can result in the depletion of nutrients and antioxidants, with a concurrent increase in tissue oxidative damage [150, 151]. These metabolic outcomes suggest irreparable cellular damage, primarily in the form of nitrosylation and carbonylation, which are incremental and primarily observable indirectly via ubiquitination as a measurement of proteosomal turnover [152, 153]. Free radical scavenging compounds like glutathione (GSSH), which form the crux of cellular defenses against mitochondrial reactive oxygen species (ROS), are rendered inert by complexation with transition metals [154]. While iron-neuromelanin (Fe-NM) complexation may limit the free-metal content of the brain, a catalytic role may still persist in causing oxidative damage to neurons.

To bridge the gap between clinical needs and in vitro PD research demands, here we incorporated Sepia melanin (NM-sim) as a functional replacement for NM within 3D silk scaffolds seeded with LUHMES dopaminergic neurons. The goal was to assess the effects of the various NM-sim conditions on electrical network activity through local field potential (LFP). Additionally, depletions of general antioxidants, glutathione loss, production of peroxides, and consequent increase in carbonylation were examined in the 3D tissue systems. These efforts were directed towards establish initial 3D tissue engineered models for studies of Parkinson's disease.

2.2. Experimental – Materials and Methods

2.2.1. Neuromelanin Processing.

Melanin extraction from Sepia ink was adapted reproduced from established methods [129]. Sepia melanin (Sigma, St Louis, MO USA) was sonicated using a tip probe (SjiaLab, Zhejiang, China) in a basic solution of 3M NaOH (Sigma, St Louis, MO USA) a 4°C for 30 min at the lowest possible setting (10% Power). Both aqueous (aq.) soluble and insoluble precipitates remained after sonication and the aq. soluble portion was decanted and dialyzed with 2K MWCO Slide Cassettes (ThermoFisher, Waltham, MA USA), enriched by air drying under continuous flow to highest opacity then frozen and lyophilized. To form 'Iron-Neuromelanin' (Fe-NM) precipitate the NM stock solution was combined with a 1M solution of ferric (3+) chloride in a 1:5 ratio of 1M $FeCl_3$ solution and saturated NM solution. The precipitate was again sonicated then washed and 3X with DI water and dialyzed with mini-dialysis device (3.5K MWCO) (ThermoFisher, Waltham, MA USA) to remove free metals and unreacted product before lyophilization to acquire a mass. (See Figure 2.6 Figure 4.1 for additional details).

2.2.2. Silk Sponge Preparation.

To form sponges, the silk fibroin was extracted from cocoons of the Bombyx mori silkworm using a 30 minute extraction protocol, after salt leached sponges were prepared as we have described previously [155] and cut to dimensions of 6mm diameter with 2 mm height and 2 mm internal window. Silk sponges were treated with poly-ornithine solution 50 ug/mL (Sigma, St Louis, MO USA) overnight followed by human fibronectin 10 ug/mL (Roche, Basel Switzerland) for 12hrs prior to cell seeding to support cell adhesion [1]. To further improve cellular adhesion the sponges were

incubated in DMEM:F12 media at 37^{O}C (30 min) before aspiration and seeding of undifferentiated cells.

2.2.3. Cell Culture.

Lund's Human Mesencephalon cells (LUHMES, ATCC: CRL-2927) were grown to 80% confluence in growth media DMEM:F12 (Lonza, Portsmouth, NH USA) supplemented with N2 (Thermo Waltham, MA) and basic Fibroblast growth factor bFGF (50 µg/mL) on coated T-175 flasks prior to seeding [130]. LUHMES were seeded on silk sponges using 100 uL suspension of complete DMEM:F12 at a density of 25M cells per mL dropwise in a 96 well plate. Following this silk sponges were cultured overnight, as well as in 2D controls (100K cells/mL) to observe differentiation and to assess cellular health. Rat derived type-I collagen gels (2 mg/mL BD science, San Diego, CA, USA) were cast by combining 880 uL collagen: 100 uL 10X Media-199: 2 ul NaOH (3M) with dibutyryl cAMP (db-cAMP 10mM) (Sigma, St Louis, MO USA) and Glial Derived Neurotrophic factor (GDNF 20 ng/mL) (Sigma, St Louis, MO USA) prior to casting in the silk sponges. Media was additionally supplemented with tetracycline (50 µg/mL), GDNF (100 ng/mL), and db-cAMP (50 mM) to foster a dopaminergic lineage from the cells [130]. For the cell preparations, the LUHMEs were grown in the undifferentiatied state in T-175 flasks before transition to 3D. When 80% confluent, the cells were passaged, seeded on the coated silk scaffolds and incubated before differentiation. Differentiation was conducted by casting a collagen gel with GDNF and db-cAMP, followed by a 7 day culture prior to LFP recording and exposure to the control (CTRL), NM-sim and Fe-NM-sim study groups.

2.2.4. Scanning Electron Microscopy.

Samples of sponges were dried, mounted and sputter coated with a SC7620 Mini Sputter Coater (Quorum Technologies, Lewes UK). Following 30 seconds of gold sputter coating, the samples were placed in the SEM chamber of a Zeiss Sigma Field Emission Scanneing Electron Microscope (FESEM) (Oberkochen, Germany). Similarly, Iron-NM aggregates were air dried and mounted on carbon tape after which the particles were sputter coated as above and analyzed for particle size and morphology.

2.2.5. Immuno-staining & Microscopy.

Silk sponges and glass slides were fixed using 4% paraformaldehyde (PFA) (SCB, Santa-Cruz CA USA) in DPBS for 30 min after which sponges were washed 3X with 1X DPBS. Blocking was conducted with 10% goat serum (ThermoFisher, Waltham, MA USA) before permeabilizing with a dilute solution of Triton X-100 (0.2% in DPBS) preceding the addition of primary antibodies. Primary antibody against Beta-3-tubulin – B3T (Sigma, St Louis, MO USA) was used at a dilution of 1:1000 in blocking buffer. Primary stain conditions were overnight (2-8^{o}C) with working concentrations of 1:500 in blocking buffer. Following washing of the of unbound primary antibodies, secondary staining was conducted using Alexafluor 568/488 for 3-4 hrs at 37^{o}C with working concentrations of 1:250. Fluorescent microscopy was conducted using a Keyence BZ-X700 fluorescent microscope (Keyence, Itasca, IL USA) equipped with Texas red (TXR – 595 nM), Green fluorescent protein (GFP – 475 nM) and Diamidino-2-Phenylindole (DAPI-461 nM) dichroic filters. Confocal imaging was conducted using a Leica SP8 confocal microscope (Leica, Lawrenceville, GA USA) using the same staining.

2.2.6. Water Soluble Tetrazolium WST-1.

To account for variations between 3D scaffolds (i.e. seeding density and viability) WST-1 was used as a 'post-hoc' test to follow electrophysiological recordings. Recorded samples were placed in a 24 well dish with 1mL of WST-1 media (Complete DMEM:F12 with 10% WST-1) for 24 hours and read on a spectrophotometer. Results were normalized against the mean of the data-set and correlated against electrophysiological measurements.

2.2.7. Electrophysiology.

Spontaneous neural firing was conducted using local field potential (LFP) with pulled capillary electrodes using a Sutter P-97 (Novato, CA USA) for resistance 20-40 MΩ. Recordings were conducted on an Axon instrument data recorder equipped with an Intan digital amplifier. Analysis was conducted using the Axon instruments (Sunnydale, CA USA) Clampfit and Clampex software and analysis was conducted with SPSS v.20. For recordings, sponges were placed in an extracellular bath solution prepared with (mM): 130 NaCl, 1.25 NaH2PO4, 1.8 MgSO4, 1.6 CaCl2, 3 KCl, 10 HEPES-NaOH, 5.5 glucose, pH 7.4 warmed to physiological temperature before use. Each sample batch consisting of n=21 scaffolds with LUHMES cells was exposed to either NM (10 mg/mL; 10 uL), NM-Fe suspension (5 mg/mL; 20 uL), or DPBS (20 uL) injected directly into the sponges. Electrophysiological measurements for each batch began immediately following the group injection period. The measurement period consisted of 6 hours of serial measurement *of individual scaffolds* where each trial consisted of a 5 minute baseline recording of alternating conditions to account for order effects (i.e. control, NM, Fe-NM, repeat). A water soluble Tetrazolium (WST-1) metabolic assay was conducted

as a post-hoc analysis to account for differences in exposure time. All samples were individual scaffolds, and no repeat measures were collected.

2.2.8. Patch Clamp.

Patch clamp experiments in the whole cell configuration were carried out at day 7 and 11 of differentiated LUHMES cells. Neurons were superfused at room temperature with an external solution containing (mM): 130 NaCl, 1.25 NaH_2PO_4, 1.8 $MgSO_4$, 1.6 $CaCl_2$, 3 KCl, 10 Hydroxyethyl-piperazine-ethanesulfonic acid (HEPES)-NaOH, 5.5 glucose, pH 7.4. The pipette solution was composed (mM): 130 K-Asp, 10 NaCl, 5 EGTA-KOH, 2 $MgCl_2$, 2 $CaCl_2$, 2 ATP (Na-salt), 5 creatine phosphate, 0.1 GTP, 10 HEPES-KOH; pH 7.2 capacitance was used as a measure of the cell size after the application of 20 ms hyperpolarizing -10 mV voltage step (0 mV holding potential). A voltage clamp ramp protocol from -100/100 mV (100 ms duration) was used to identify the presence of the sodium current peak; the sodium peak amplitude was defined as the current peak current value relative to the theoretical ramp line. The resting membrane potential (RMP) was recorded in the I/0 configuration. To investigate neuronal excitability, 2,500 ms depolarizing current steps were applied in current clamp mode in 10 pA increments from the resting potential held at −70 mV. Input resistance was extrapolated using first Ohm's Law from the current clamp protocol. The rheobase was defined for each neuron as the minimal amount of injected current of infinite duration able to induce an action potential.

2.2.9. Subcellular Fractionation/Extraction.

Lysis and extraction of proteins from the scaffolds was conducted to acquire the 'cytoplasmic' contents of the scaffolds and accomplished using a combination of flash-freezing and mechanical isolation, followed by subcellular fractionation. Two fractions

were isolated and characterized including (1) cytosolic and (2) nuclear using Nuclear Extraction (NE-PER™) extraction buffer (Thermo, Waltham MA) and Halt protease inhibitor cocktail was added (Thermo, Waltham MA USA). In brief, sponges were flash frozen in liquid nitrogen and then pulverized using glass beads during mechanical isolation in cytoplasmic extraction reagent. Subsequent stages of isolation were conducted per the "Nuclear and Cytoplasmic Extraction Reagent" manufacturer instructions. Product concentrations were quantified using a BCA (Thermo, Waltham MA). Protein was precipitated using a 20% (V/V) Trichloroacetic acid (TCA) solution (Sigma, St Louis MO USA) when deemed necessary by the manufacturer for metabolic assays.

2.2.10. Metabolic and Quantitative Assays.

Primary assays included: (1) Bichinoic acid (BCA) protein quantification assay (Thermo, Waltham, MA), (2) Glutathione assay (Cayman Chem., Ann Arbor, MI), (3) Protein Carbonylation assay (Cayman Chem., Ann Arbor, MI), (4) ADP/ATP ratio assay (Abcam Cambridge, MA), (4) Hydrogen peroxide assay (Sigma, St. Louis MO), and (5) ELISA assay (Thermo, Waltham MA). The assays were performed on the cytoplasmic fraction of each sample with the exception of: (1) the ADP/ATP assay was performed on phenol-TE:chloroform isolate [156] and (2) the peroxide assay which were conducted with complete DMEM:F12 media (24 hour conditioned). All assays were conducted according to the manufacturer's guidelines and screened for positive and negative experimental controls. Readings are reported as concentration per unit mass (i.e. mM/ug by BCA) where necessary to account for sample variability due to variations in adhesion and cell survival.

2.2.11. qPCR.

Total RNA was extracted from cells using the RNeasy Mini Kit (Qiagen) following manufacture instructions. Total RNA quantification was measured using a nanodrop-2000 spectrophotometer (ThermoFisher, Waltham, MA USA) and 1 µg of total RNA was retro-transcribed to cDNA with the QuantiTect Reverse Transcription Kit (Qiagen) for each experimental group. TaqMan™ Gene Expression Master Mix (ThermoFisher Scientific) was used to perform the qPCR experiments with specific Taqman probes (ThermoFisher Scientific) for each gene of interest. GAPDH and 18S were used as housekeeping genes. The expression level is indicated as 2-ΔCtx100 and the fold increase/decrease is expressed as log2(fold ratio), with the fold ratio defined as the ratio between each gene at day 11 and the undifferentiated cells. Further details regarding qPCR processing can be found in the supplemental.

2.2.12. ELISA.

The sub-cellular protein extracts of silk scaffolds were collected following LFP recordings. The fractions were centrifuged to remove insoluble protein. Before conducting the ELISA samples were quantified by a BCA assay to ensure consistent protein concentrations. The β-Amyloid ELISA (Sigma, St. Louis, MO, US) was conducted according to the manufacturers guidelines. Following quantification by ELISA the individual samples were quantified by BCA to compare. Readings are reported as concentration per unit mass (i.e. mM/ug by BCA) where necessary to account for sample variability due to variations extraction efficiency.

2.2.13. Statistical Analysis.

Analysis of experimental measurements was conducted with PRISM (Graphpad La Jolla, CA). Measurements are expressed as standard deviations from the mean unless otherwise noted. Statistical tests used for analysis of metabolic measurements were t-test adjusted for multiple comparison (Tukey's) with an Alpha=0.05. Analysis of electrophysiological data was conducted with a one-way ANOVA. Electrophysiological analysis was conducted using SPSS v.20 for Local Field Potential measurements.

2.3. Results

The lyophilized Sepia melanin was put into a cold solution of 3M NaOH and sonicated using a tip-probe for 30 min on ice. The solution was centrifuged to isolate the aqueous (aq.) soluble and insoluble fractions after which the aq. was decanted and the dialyzed to remove remaining NaOH. Following this the (1) NM solution and (2) Fe-NM precipitate were generated and characterized. The concentration of the NM solution was evaluated based on based on spectral absorption and adjusted accordingly (i.e. concentrated NM solution absorption was read then diluted with DI water for the absorption corresponding to 5mg/mL). Fe-NM precipitate included a solution of 1M $FeCl_3$ mixed with the NM solution and the product was sonicated for smaller particle size and dialyzed to remove unreacted product which was observed by colorimetric change in the dialysate, and autoclaved/lyophilized to provide a dry weight.

The NM and Fe-NM materials were characterized for absorption spectra, metal content, particle diameter and ellipticity. During processing, the conditions were kept cold to reduce oxidation of the carboxylic acid moieties and particle aggregation. The NM concentration was quantified by absorption spectra whereas Fe-NM was quantified by dry mass following lyophilization. The initial precipitate (Figure 2.1 - gray) exhibited larger

diameters before probe sonication, after which Fe-NM became smaller with sizes that followed a skewed normal distribution (Figure 2.1B - black). The sonicated precipitate was dialyzed to remove excess unreacted material after which the presence of chelated iron was validated with reporter dye Phen-Green (Figure 2.1D). The Fe-NM precipitate was fluorescent with the reporter dye Phen-Green for the presence of Fe^{2+} and particle morphology was amorphous, necessitating analysis of particle ellipticity such that biased distributions were not reported by Dynamic Light Scattering (DLS) (Figure 2.1 B-E).

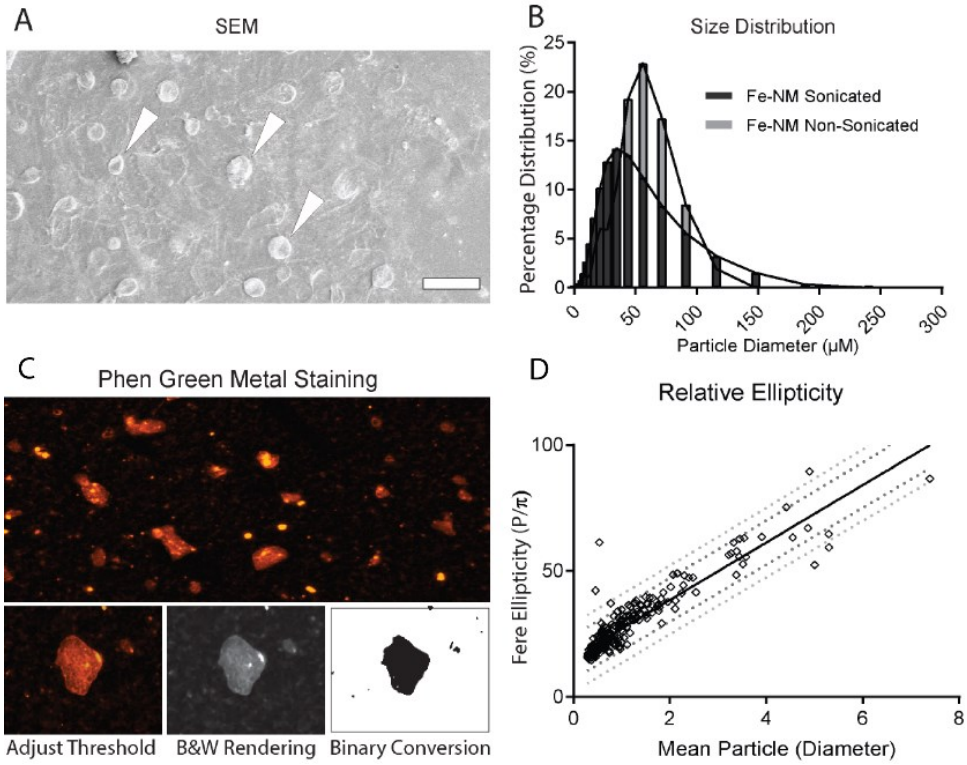

Figure 2.1 Particle Distribution and Analysis

A. Scanning electron microscopy (SEM) image of processed particles (arrows) of the Fe-NM precipitate morphology (Scale 200 μm). B. Dynamic light scattering analysis revealed a change in the particle distribution pre- and post- sonication. Pre-sonicated particles demonstrated more uniform skew (Mean=44.05 μM; Skew=2.007; σ=4.05) whereas sonicated particles had a smaller and less uniform distribution (Mean=27.3 μM; Skew=2.91; σ=5.176) (N=3.). C. The Fe-NM particles stained positive with Phen-Green indicating presence of Fe^{2+} and exhibiting amorphous shapes. D. Image processing to compare particle ellipticity by Feret Value. A correlation between size and ellipticity was observed; the values of ellipticity were expressed as a perimeter to area ratio and demonstrated a linear correlation against particle diameter in which both 90% and 99% predictability lines are shown (N=250 points).

The time-course of differentiation and LFP experimentation can be seen in Figure 2.2 A-B. As the 3D sponge was difficult to visualize without immunostaining, 2D controls were necessary to evaluate cell health during differentiation (Figure 2.2 C). LUHMES cells grew reliably within the 3D scaffolding but exhibited diverse morphology throughout the bulk of the scaffolding (Figure 2.2 GH). Given that neural projections at the inner window of the sponge appeared thicker and more robust (Figure 2.2H) this region was selected for LFP recordings. LUHMES cells in 2D and 3D tissue models were cultured for seven days under differentiation conditions to allow cells to take on a dopaminergic lineage. Due to the higher surface area of scaffolds relative to 2D controls, dopaminergic LUHMES were seeded as undifferentiated cells at a seeding density of 2.5M cells/mL, with 100 µL added to each sponge. Following washes and casting of the collagen gel, the sponges were grown for 7 days in culture (DIC) before LFP measurements. LUHMES were first grown in 2D before 3D (Figure 2.2) to ensure viability. In 2D the growth and differentiation factors (i.e. GDNF, db-cAMP and tetracycline) were incorporated into the media, but in 3D the tetracycline, used for activation of v-myc expression enabling exit from the cell cycle, was put in differentiation media as it was appeared cytotoxic when suspended in the collagen gel. Morphological changes in differentiation were observed based on cellular projections under bright field microscopy. In addition, (1) PCR expression and (2) patch clamp analysis from 2D (Figure 2.5) supported the changes observed, with confirmation of differentiation conducted in 2D.

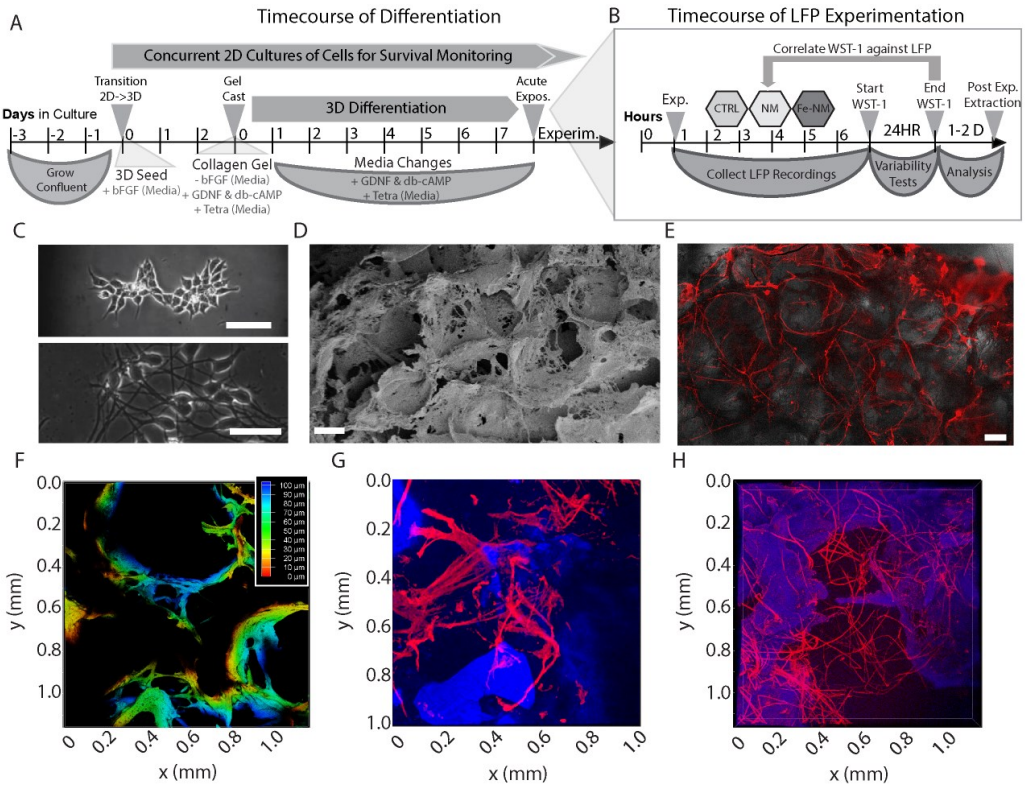

Figure 2.2 Time course of Experiment and 3D validation of LUHMES

A. A time-course of events for differentiation in which cells are grown to confluence and then seeded in both 2D and 3D systems. B. Differentiated LUHMES were exposed to Vehicle (DPBS), NM and Fe-NM before collecting LFP measurements and WST-1 metabolic analysis. C. A comparison of undifferentiated (Day-0) and differentiated (Day-7) LUHMES shows morphological changes during 2D differentiation (Scale 10 uM top and 50 uM bottom). D. Surface of the scaffold imaged by SEM with interconnected pores (Scale 200 µM). E. Broad image of neural projections within the scaffold bulk. F. Topographical map of silk sponge to show pore depth (Axis mm). G. LUHMES cells in the bulk of the sponge in close proximity (Beta-3-tubulin Red, Silk Blue; Scale mm) H. Cells adjacent to the inner window (Beta-3-tubulin Red, Silk Blue; Scale mm).

A one-way analysis of variance (ANOVA) identified significantly different normalized WST-1 values between exposure conditions, $F(2,64)=3.19$, $p<0.05$, $\eta 2=0.09$. Tissue constructs exposed to vehicle only (DPBS) ($M= 1.08$, $SEM=0.60$) expressed elevated normalized WST-1 values relative to the NM+Fe-exposed study group ($M=0.87$, $SEM=0.06$), $t(41)=2.49$, $p<0.05$, $r2=0.13$. There were no significant differences between vehicle- and NM-exposed samples as well as NM- and NM+Fe-exposed samples ($p>0.05$). The results, presented in Figure 2.3A, suggested that NM+Fe-exposed

samples were less viable relative to controls, as inferred by normalized WST-1 values. We concluded that the NM+Fe precipitate was a detrimental to cell viability and neural activity in 3D LUHMES cultures.

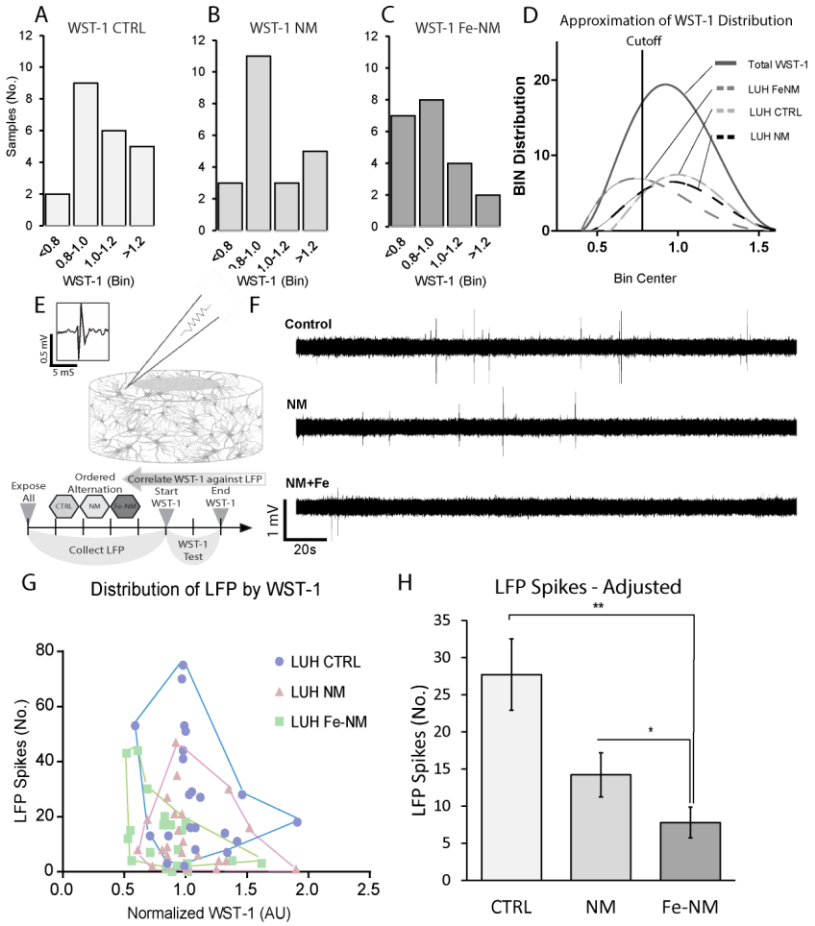

Figure 2.3 LFP Electrophysiology and Correlation with Metabolism.

WST-1 metabolic recordings were collected directly following LFP measurements to account for sample variability. A.B.C. The binned WST-1 results are compiled in comparing the mean distribution of the three experimental groups (CTRL, NM-sim and Fe-NM-sim). Normalized WST-1 results (i.e., against the data-set mean) demonstrated reduced cell viability in Fe-NM-exposed samples ($p<0.05$). D. Distribution of the three experimental groups can be seen in comparison to the cumulative results in which a cut-off value was established to screen for low-responders (WST-1=0.80 cutoff) was used to approximateexperimental confidence. E. Recording electrode placement was at the window edge of the sponge over a 6 hour time course of alternating conditions. F. Representative measurements for the Control (CTRL), Neuromelanin (NM-sim) and Iron-Neuromelanin (Fe-NM-sim) conditions. G. When plotted against WST-1 values, further separation was observed between the NM-sim and Fe-NM-sim groups. H. A bar graph of 'adjusted spikes' that have been adjusted for low WST-1 viability (i.e., >0.8), LFP measurements reported more defined separation between experimental groups CTRL-NM ($n=22/19$; $p<0.05$) and CTRL-Fe-NM ($n=22/14$; $p<0.001$) by Students T-Test.

ANOVA identified differences of spontaneous local field potential (LFP) spikes between the exposure conditions, $F(2,64)=6.33$, $p<.005$, $\eta 2=0.17$. When selecting for cases where normalized viability (WST-1) was elevated (z-score>1), the differences were exacerbated, $F(2,24)=7.19$, $p<0.005$, where 40% of the variance was explained by exposure condition ($\eta 2=.40$; Figure 2.3D). Multiple t-tests were computed to determine the major sources of variance with an adjusted $\alpha=0.016$ using the Bonferroni method. Control samples generated more spikes (M=21.08, SEM=3.56) relative to both NM- (M=7.88, SEM=3.61) and NM+Fe-exposed (M=2.20, SEM=0.73) samples with effect sizes (r2) of 0.26 and 0.43, respectively. The results suggested that spontaneous electrophysiological activity was significantly reduced in both NM- and NM+Fe-exposed conditions relative to the controls. We concluded that spontaneous electrical potentials of 3D LUHMES cell cultures were negatively impacted by both NM and NM+Fe precipitate. For further data regarding LFP measurements, please consult the Supporting Information.

Qualitative immunostaining of representative images by confocal shows alteration in the density of the neural network and the expression of beta-3-tubulin of individual neurites in comparing the control and Fe-NM-sim exposed condition (Figure 2.4A-C). A decrease in glutathione (Figure 2-4D) and subsequent increase in media peroxides (Figure 2.4E) was most pronounced in the Fe-NM-sim exposed cultures. This reduction correlated with the increase of the ADP/ATP (Figure 2.4F) and an increase in protein carbonylation (Figure 2-4G). These results suggested oxidative damage to the proteome of the Fe-NM exposed conditions. For further details regarding these markers, refer to the Supporting Information.

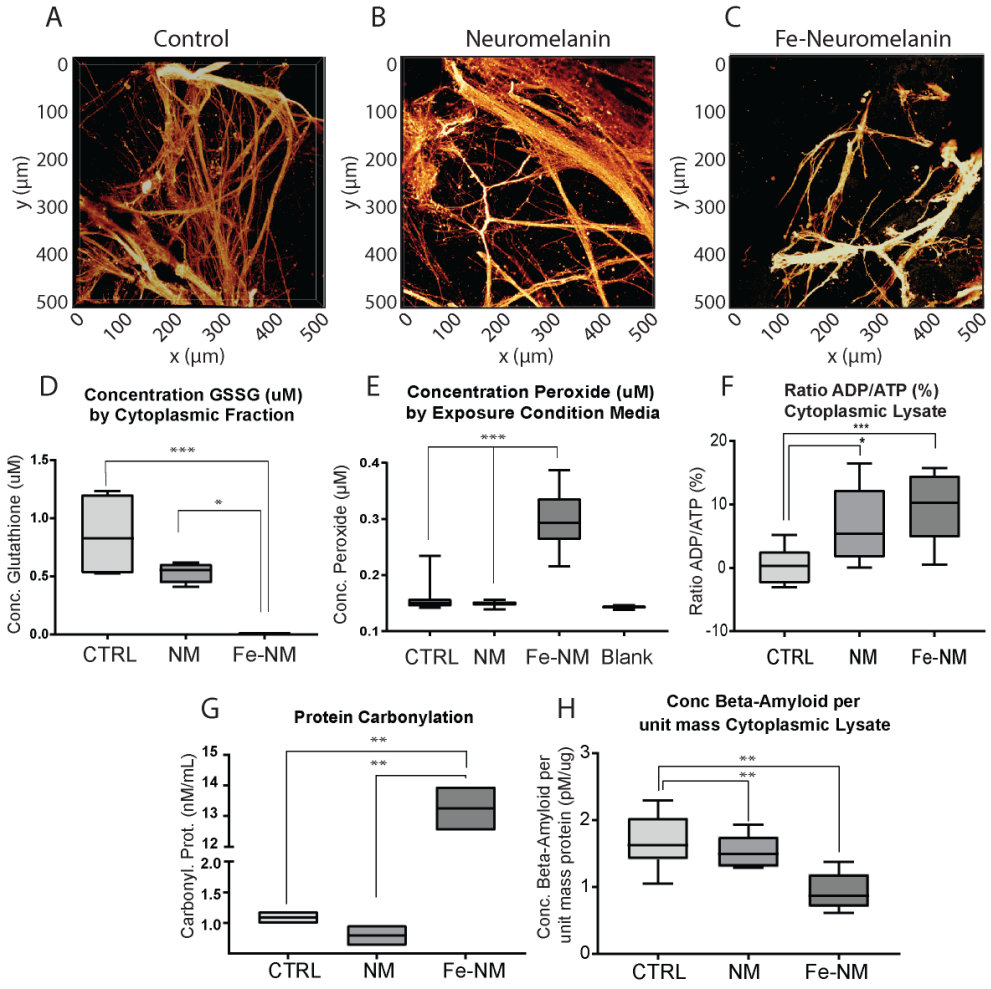

Figure 2.4 Post Exposure Immunostaining and Metabolic Analysis

A-C. The representative images depict immunostained sponges for each of the three conditions (Control, NM and Fe-NM) showing comparable morphology (Beta-3-tubulin; Orange Axis µm). D. The depletion of cytoplasmic glutathione was observed in samples exposed to both NM (n=8; p=0.0124, Multiple Comparison) and Fe-NM (n=8; p<0.001, Multiple Comparison) relative to CTRL conditions (n=8). Tukey's multiple comparison test. E. An increase in peroxides was observed in the Fe-NM media against the control condition (n=24; p<0.001). F. Elevation of the ADP/ATP ration was observed in the NM (n = 8; p=0.0148, Students) and Fe-NM (n=8; p=0.001, Students) against control. G. A difference in Fe-NM exposed protein oxidation was additionally observed, as evidenced by an increase in carbonylation comparing the NM (n=4; p<0.001, Students) and CTRL (n=4; p<0.001, Students) to Fe-NM conditions. H. Beta-amyloid concentration of the lysate indicated a reduction in concentration when normalized against the unit protein of the lysate (i.e. pM Beta-Amyloid per µG lysate) (p<0.001, Multiple Comp.).

2.4. Discussion

NM-sim cooperatively and efficiently binds transition metals, including those likely to be detrimental to cell health [157]. The benefits of metal chelating and ROS scavenging

related to protection of cell functions is key in preventing ‘ferroptosis’ in which cells die due to metal exposure [86, 87]. However, NM’s binding to exogenous pesticides, solvents and other neurotoxins [38] would be problematic in sustained culture as it would contribute to cell attrition in the long term. For instance, the potent neurotoxin and PD induction agent methyl-4-phenyl-1,2,3,6-tetrahydropyridine (MPTP) which is metabolized to create a cytotoxic by-product has an affinity for the pigment as well [39]. Animal models, which lack the same quantities of NM as primates, serve as imperfect models for translational drug studies due to inherent differences between the species [30]. Further investigation of NM-sim binding exogenous neurotoxic compounds like MPTP would be necessary for comparative analysis as it pertains to PD.

The 3D brain-like tissue model presented here has several advantages over traditional tissue models and methods. Human neurons are utilized within a 3D scaffold environment permitting higher cell density than 2D for network formation, and tunable surface chemistry and mechanical properties (i.e. functionalizable and polymeric) when compared to 2D controls [123]. Additionally, the architecture of the scaffolds in these 3D tissue models supports the formation of specialized structures of brain architecture and the 3D scaffold environment allows for more diverse connectivity among the neurons [23]. Lastly, these scaffolds are more accessible than animal models, and also provide biocompatibility with minimal immunogenicity. These features suggest potential for these tissue models for intermediate testing between cell and animal systems.

The Fe-NM-sim precipitate (Figure 2.1 A-B) by morphological appearance is structurally analogous to Lewy bodies (LB), the aggregates commonly encountered in PD, which exhibit abnormal morphology, various size diameters and a dense core surrounded by a halo of alpha-synuclein (ASYN) [16]. To elaborate, dopaminergic neurons possess specialized NM organelles which aggregate proteins and fatty acids

over time contributing to neural dysfunction [15]; these organelles result in LB products. Additionally, histopathological evidence suggests that LBs are stabilized by cytosolic dopamine, bearing resemblance to NM [158]. The Fe-NM aggregates discussed here exhibit aberrant structure and have the potential for tailorable diameters and ellipticity via tuning of sonication parameters (Figure 2.1C). A reduction in glutathione (Figure 2.4D) and subsequent increase in protein carbonlyation (Figure 2.4G) suggests the potential for catalytic activity [159]. Furthermore, the ferrous (2+) iron exhibits paramagnetic properties, thus it is possible that proteins possessing a strong dipole moment would interact with a metal precipitate and be cytotoxic [49]. The intrinsically disordered structure of alpha-synuclein allegedly exhibits such 'promiscuous' dipole interactions based on experimental measurements of Forster resonance energy transfer (FRET) [106] and transition metals have been implicated in catalyzing ASYN oligomerization [159, 160].

On a separate line of inquiry, aberrant electrical activity has been observed in the subthalamic nucleus of PD patients by LFP and encephalography methods as the result of neuronal oscillations [161]. While the LFP measurements found in Figure 2.3 suggest a negative correlation between activity and the presence of NM and Fe-NM, the results also imply a causal relationship between NM and network activity. The "sheet" configuration of NM, which shares π-bonded electrons, is a stacked-planar configuration similar to graphite [13] an organic semiconductor [162]. Furthermore, the chelated form of Fe-NM bears structural similarity to the organometallic catalyst ferrocene ($Fe(C_5H_5)_2$); investigators have previously used a 'beta-sheet breaker' tagged with ferrocene (Fc-KLVFFK6 – Ferrocene-Lys-Leu-Val-Phen-Phen-Lys6) that was used to monitor the aggregation of amyloid beta and contributed to, "breakage of the stacked A-Beta oligomers" [163]. Finally, the addition of other neural cells such as astrocytes and

microglia should also be beneficial in supporting disease relevance. Literature suggests that melanin from *Sepiella Maindroni* is well tolerated when ingested orally and is beneficial for gut microbiota [164]. However, extrapolation of these findings to the brain would be dependent on how 'ramified' microglia might react to exogenous materials (i.e. NM-sim) [43, 165].

Experimental evidence suggests that glutathione is depleted or (Figure 2.4D) as are high energy molecules like ATP (Figure 2.4). High energy phosphate bonds like ATP are generally stabilized by metals (i.e., Mg^{2+} ATP) and would be disrupted by the absence of such metals [166]. Similarly, glutathione interacts with heavy metals and serves to buffer against the oxidative damage [167]. At present it is difficult to ascribe the depletion of glutathione (Figure 2.4D) to such destabilization, but similar phenomena were observed in dopaminergic neurons of PD patients [168]. Exposure to unbound transition metals was correlated with protein carbonylation and proteosomal dysfunction [169]. Protein carbonylaton (Figure 2.4G) is indicative of oxidative damage, including such unstable proteins such as alpha-synuclein (ASYN). The oligomeric, chemically functionalized structure of synuclein is capable of retroactive transport through neural networks [170] in accordance with the Braak staging hypothesis of PD [61].

2.5. Conclusion

It was encouraging that both the NM and Fe-NM contributed to reduction of dopaminergic network firing and a consequent decrease in WST-1 cell viability and LFP measurements. The accessibility of NM to bridge the gap between transition metals (i.e. 'Fe-NM-sim') and tissue engineered models of the disease state appears to be feasible. The reduction in LFP activity due to NM exposure was reproducible across three experimental trials and supported by reduction in WST-1 cell viability. Cell and metabolic based assays supported evidence of free radicals, reduction in glutathione, and protein

oxidation established in literature. Analysis of NM on the kinetics of alpha-synuclein oligomerization would be instructive. Adsorptive properties of NM-sim for exogenous neurotoxins (i.e. MPTP) and the effects of transition metals on solubility of these toxins would be informative regarding PD. Further analysis of the effects of NM on voltage gated channels and to those implicated in long term potentiation (LTP) and long-term depression (LTD) (i.e. NMDA and AMPA receptors) would be merited.

2.6. Associated Content

2.6.1. Supporting Information.

The following files are available free of charge.

S1 – Figure 2.5 Comparison of Molecular and Functional Features of LUHMES

S2 – Figure 2.6 NM Processing Stages and Analysis

S3 – Figure 2.7 Immunostaining Evidence of DA Phenotype.

S4 - Figure 2.8 Comparison of Synthetic and Extracted Melanin's and Timecourse

S5 - Table 2.1. Taqman Primers used in qPCR.

S6 - Table 2.2. Antibodies used in Immunostaining.

S7 – Table 2.3. Relevance of Biomarkers from Main Text

S8 - Table 2.4. Existing 3D Models of the Substantia Nigra and Parkinson's Disease

S9 - Figure 2.8 Comparison of Synthetic and Extracted Melanin's and Timecourse

S10 - Figure 2.9 Experimental Trial and Experimental Condition Groupings

2.6.2. Author Information

Corresponding Author

*E-mail David.Kaplan@Tufts.edu. Tel. +1 617 626 3251. Fax +1 617 627 3231.

Present Addresses

N/A

Author Contributions

The concepts and plans were developed by WRC and DLK. The manuscript was written by WRC and edited by DLK. Experimental data was contributed by WRC, KK, and AJ. Electrophysiological data was provided by NR, CD and MB. The manuscript was written through contributions of all authors. All authors have given approval to the final version of the manuscript.

Funding Sources

Support from the NIH (R01NS092847, P41EB002520), as well as the W.M. Keck Foundation and the Allen Center Foundation is gratefully acknowledged.

Notes The authors declare no competing financial interest.

2.7. Supplemental

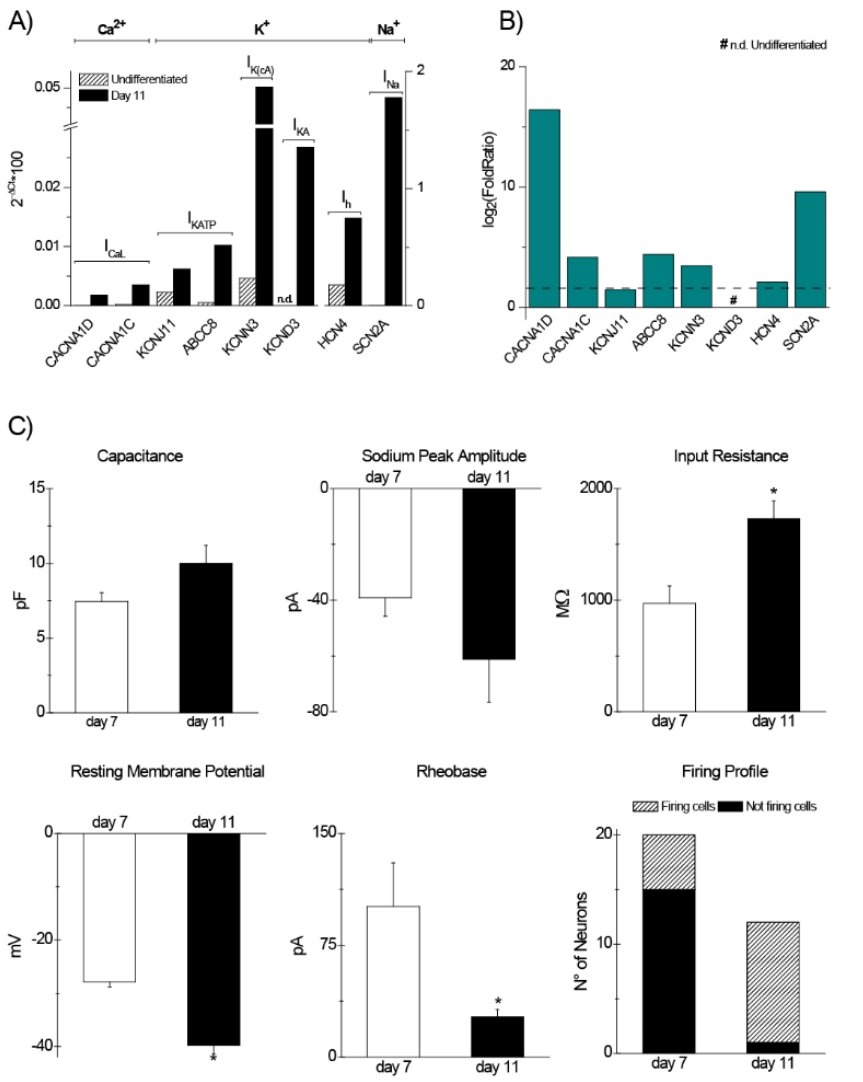

	Day 7			Day 11		
Parameter	Sample size	Mean	S.E.M.	Sample size	Mean	S.E.M.
Capacitance (pF)	19	7.5	0.6	11	10.0	1.2
Sodium peak amplitude (pA)	10	-39.1	6.6	8	-61.1	15.5
Input Resistance (MΩ)	11	970.4	156.5	10	1728.2*	158.0
Resting Membrane potential (mV)	20	-27.9	0.9	11	-39.8*	1.5
Rheobase (pA)	5	101.0	29.2	8	26.9*	5.0

Figure 2.5 Comparison of Molecular and Functional Features of LUHMES

Comparison of the molecular and functional features of LUHMES cells during the 2D differentiation process. **A-B)** The qPCR data compares the undifferentiated and day 11 differentiation conditions. mRNA expression of ion channels and relative fold increase (dash line is the threshold set as Fold Ratio=2) (N=1). **C)** The electrophysiological data compares the day 7 and day 11 of differentiation conditions. Electrophysiological parameters recorded with the patch clamp technique. * $p<0.05$ using Student's T-Test.

Along with chemical communication, mature neurons generate and dynamically integrate electrical signals. To acquire a functional electrophysiological phenotype over the differentiation process of LUHMES progenitor to the dopaminergic state, cells must express a repertoire of ion channels and accessory proteins. To investigate this maturation, we compared by RT-qPCR the mRNA expression levels of 8 ion channels that are the dominant molecular determinants of the main neuronal ionic currents (n=1). After eleven 11 days of differentiation (Figure 2.5A), all subunits except KCND3 increased by 2-fold or more the expression in comparison to the undifferentiated condition (Figure 2.5B). In line with the gene expression data, we observed a maturation of the electrical properties of LUHMES cells (day 7 vs day 11 of differentiation; Figure 2.5C). The input resistance ($p<0.05$) increased as the cells matured over time, concomitant with a significant hyperpolarization of the resting membrane potential and a decrease of the rheobase (injected current necessary to induce the action potential) ($p<0.05$). We did not observe any significant cell size change, as measured by capacitance. Taken together, these data are indicative of a molecular and functional maturation of LUHMES dopaminergic neurons.

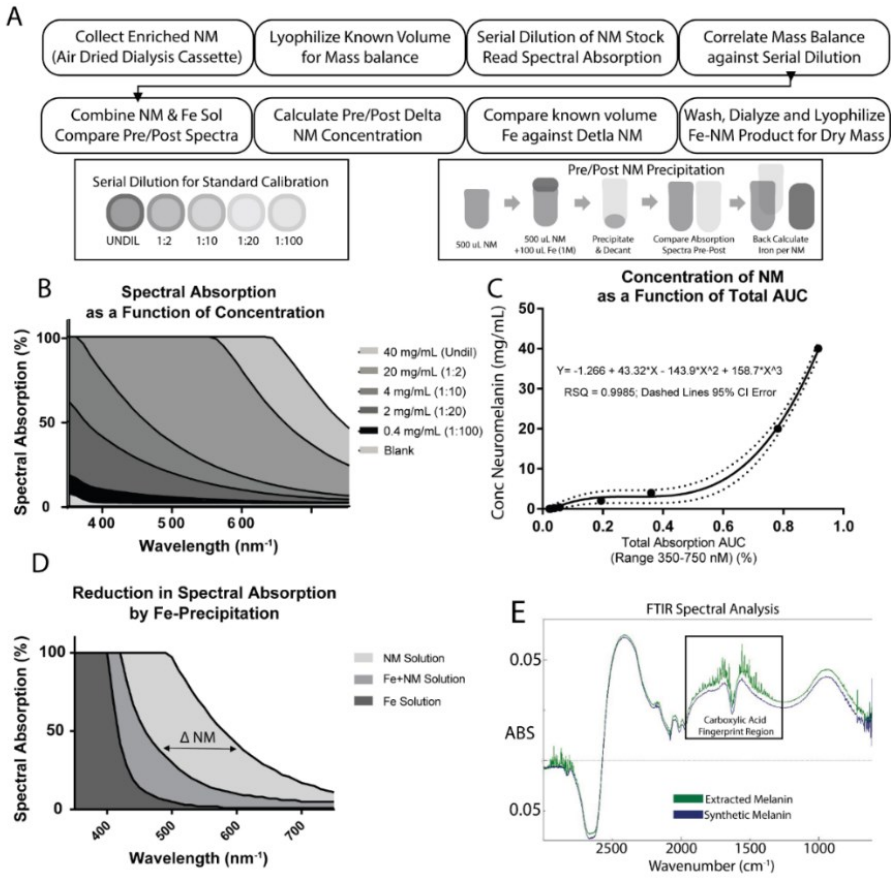

Figure 2.6 NM Processing Stages and Analysis

A. Aq. Melanin solution was enriched by air drying in its dialysis cassette and a known volume (i.e. 10 mL) was frozen and lyophilized for mass balance. The remaining NM solution was diluted in the following manner (1) 1:2 (2) 1:10 (3) 1:20 and (4) 1:100 to establish a calibration and read by its spectral absorption profile. To define the stoichiometric ratio of Fe to NM a 500 uL of NM was combined with 100 uL of Fe Solution (1M) and the pre/post spectral AUC values were compared. The delta was used to estimate the NM precipitated. **B.** The area under the curve (AUC) values allow for quick concentration estimation and follow a hyperbolic function **C.** In estimating the concentration of NM against its total AUC it was found that estimation follows a third order polynomial. **D.** Calculation of the ΔNM is expressed as the difference in area between pre and post Fe precipitation expressed as ΔAUC for the calibration curve **E.** The integrity of NM carboxylic acid groups can be assessed following processing with Fourier Transform IR (FTIR) analysis between1500-1000 cm^{-1}.

The technique for spectral determination of NM allows researchers to indirectly quantify the amount of NM against a known concentration of Fe before precipitation. While the reduction in spectral absorption is not as exacting as chromatography if done reliably can allow quantification of Fe-NM precipitation. Results suggest a stoichiometric ratio of 2 NM to 1 Fe in precipitation.

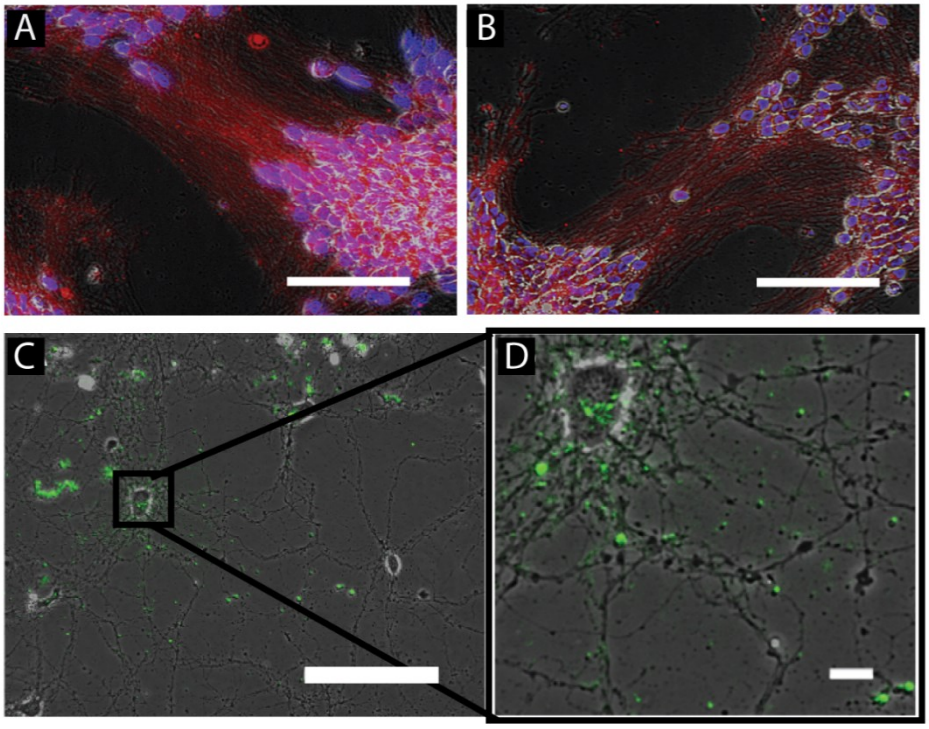

Figure 2.7 Immunostaining Evidence of DA Phenotype.

A.B. The presence of tyrosine hydroxylase (TH –Red; DAPI-Blue; scale 100 uM) and dopamine receptor D2 (DRD2-Red; DAPI -Blue; scale 100 uM) were observed in the D-7 differentiated LUHMES cells, validating the dopaminergic phenotype following one week in culture. D.C. Phen-green, which stains free iron demonstrates a similar punctate staining (Phen-Green – Green; scale 100 uM and 10 uM).

Dopaminergic neurons rely on tyrosine hydroxylase (TH) as the primary means of producing the neurotransmitter dopamine. TH requires iron as a metal catalyst to perform its operations in converting L-DOPA to dopamine. DRD2 receptors suggest that the cells are additionally capable of sensing neurotransmitters in solution. Furthermore, neural cultures that exhibit dendritic beading also stain positive for Phen-Green as well in punctate areas suggesting that free metals may be present here as well.

Gene	Full Name	Assay ID	Entrez Gene ID	UniGene
CACNA1D	calcium voltage-gated channel subunit alpha1 D	Hs00167753_m1	776	Hs.476358
CACNA1C	calcium voltage-gated channel subunit alpha1 C	Hs00167681_m1	775	Hs.118262
KCNJ11	potassium voltage-gated channel subfamily J member 11	Hs00265026_s1	3767	Hs.248141
ABCC8	ATP binding cassette subfamily C member 8	Hs01093752_m1	6833	Hs.54470
KCNN3	potassium calcium-activated channel subfamily N mem. 3	Hs01546821_m1	3782	Hs.490765
KCND3	potassium voltage-gated channel subfamily D member 3	Hs00986860_m1	3752	Hs.666367
HCN4	hyperpolarization activated cyclic nucleotide gated ch 4	Hs00975492_m1	10021	Hs.86941
SCN2A	sodium voltage-gated channel alpha subunit 2	Hs04968321_s1	6326	Hs.93485
18S	Eukaryotic 18S rRNA - Housekeeping Gene	Hs99999901_s1	HSRRN18S	N/A

Table 2.1 Primers used in qPCR

Extraction of LUHMES RNA was conducted according to the manufacturer's guidelines and reverse transcribed into cDNA. All primers were selected exon-spanning wherever possible. For further details please refer to the following: (1) UniGene https://www.ncbi.nlm.nih.gov/unigene or (2) Entrez Gene ID: https://www.ncbi.nlm.nih.gov/gene.

Use of Taqman primers were conducted according to the guidelines of the manufacturer. Where possible primers were selected to be 'exon spanning' to ensure that the RNA in questions was coding and not due to the effects of contamination with genomic DNA. The genes in the table summarize a variety of voltage gated channel related genes which have discrete effects on membrane potential and differentiation. Further replication is encouraged to ensure the results stated here are consistent for investigators before operating on assumptions of reproducibility. Given the implicit costs associated with use of Taqman probes investigators may also pursue use of SYBR Green probes through the Harvard Primer Bank https://pga.mgh.harvard.edu/primerbank for larger studies [171].

Primary Antibodies				
Abbrev.	**Full Name**	**Description**	**Supplier**	**Part No.**
B3T	Beta-3-tubulin	Rabbit polyclonal to beta III Tubulin	abcam	ab18207
DRD2	Dopamine Receptor D2	Anti-Dopamine D2 Receptor antibody	abcam	ab85367
TH	Tyrosine Hydroxylase	Mouse monoclonal to Tyrosine Hydroxylase	abcam	ab129991
Secondary Antibodies				
Abbrev.	**Full Name**	**Description**	**Supplier**	**Part No.**
AF-568	AlexaFlour 568	Goat Anti-mouse & Anti-Rabbit IgG (H+L)	Thermo	A-11004
AF-488	AlexaFlour 488	Goat Anti-mouse & Anti-Rabbit IgG (H+L)	Thermo	A28175

Table 2.2 Antibodies used in Immunostaining

Immunostaining was conducted individually to prevent any occurrence of cross reactivity with poly-clonal antibodies. All staining solutions were concurrently blocked with goat serum blocking buffer to prevent off target effects.

For purposes of reproducibility the antibodies used in immunostaining are provided. It is recommended that investigators validate their antibodies against recombinant targets of interest (i.e. recombinant hTH and hDRD2) at several dilutions with negative controls by western blot to ensure specificity of their primary antibody [172]. As a caution against 'false positives' and 'false negatives' in reporting results best practices in batch validation are advised[173, 174]. For those unaware of the NIH sponsored resources (1) Neuromab (UC Davis) http://neuromab.ucdavis.edu/ and the (2) Hybridoma Bank (University of Iowa) http://dshb.biology.uiowa.edu/ further investigation of dopamine specific markers through these suppliers is merited.

Biomarker	Relevance	Citation
Glutathione	Line of defense against mitochondrial ROS	Lidell 2018
Peroxide	Fenton chemistry generation of free radicals	Robertson 2017
ADP/ATP Ratio	Energy deficits implicit in neuronal dysfunction and dopaminergic death	Sheng 2017
Protein Carbonylation	Irreversable protein denaturation which overwhelms the proteome	Fernandez 2017
Beta-Amyloid Conc.	Protein biomarker implicated in neurodegenerative disease	Scholz 2018

Table 2.3 Relevance of Biomarkers [175-178]

To elaborate on the makers found in Figure 2.4 of the primary manuscript the relevance in regards to PD is expanded upon here. Bio-metals (i.e. Fe2+/Fe3+) are often undermined in regards to neurodegenerative disease as their isolation and detection can be challenging requiring specialized mass spec. techniques (i.e. inductively coupled plasma, ICP-MS) for quantitative results. However, fundamental DA related enzymes like TH often require a catalytic metal to properly perform their necessary functions [174]. Furthermore, many high energy bonds are metal stabilized (i.e. ATP and Mg2+) [166] and were their abundance to be effected by chelation (i.e. by NM-sim) cell metabolism would be biased. Finally, the biological community could benefit from investigation of the burgeoning field of 'organometallics'(like ferrocene or Fe-NM-sim)

which may cause irreparable damage to proteins in the form of carbonylation [179] and be specific to key proteins like alpha-synuclein via dityrosine crosslinking [131, 159].

RESEARCH ARTICLES - Parkinsons 3D Modelling				
No.	CELL LINES	Scaffolding	PD Inductions	Citation
1	C6 Astrocytes PC12 Cells Human iPSC Primary DRG	3D RAFT Scaffold; Collagen Gel	MPP+	O'Rourke 2017
No.	CELL LINES	Scaffolding	PD Inductions	Citation
2	Rat primary w DA induction; H9-hESCs	Micro-TENNS (Agarose base)	N/A	Struzyna 2018
No.	CELL LINES	Scaffolding	PD Inductions	Citation
3	transgenic mice Tg(TH-EGFP) DJ76GSAT	Photolithography Silicone Wafer	MPTP	Lu, 2013
No.	CELL LINES	Scaffolding	PD Inductions	Citation
4	Sprague-Dawley Rat Pups	Organotypic Slice Culture	N/A	Daviaud, 2012
REVIEW ARTICLEs - Parkinsons 3D Modelling				
No.	Focus			Citation
1	3D neural tissue models: From spheroids to bioprinting - integration of technological advancements to supplement the drug discovery platform and challenges thereof			Zhuang, 2018
No.	Focus			Citation
2	Towards artificial tissue models: past, present, and future of 3D bioprinting - Details of printing systems and bio-inks for rapid prototyping of partial relevance to neurodegenerative disease			Arslan-Yildiz, 2016

Table 2.4 Existing 3D Modeld of the Substantia Nigra and Parkinson's Disease

Above additional resources can be found for investigators pertaining to 3D models of PD and tissue engineering for the SN in efforts to treat the disease.[180-185]

Tissue engineering for the treatment of Parkinson's disease is a long established field which coincides with the investigation of stem cells for regenerative medicine. However, as was found following the 'case of the frozen addicts' (i.e. discovery of neurotoxic MPTP) it was found that even successful grafts of neural stem cells would eventually succumb to cell death. Furthermore, lineage control of these stem cells often proves challenging given the complexity of neuro-endocrine cues and extracellular matrix (ECM) interaction to create dopaminergic lineage. The above Table 2.4 summarizes efforts in tissue engineered models of PD with citations.

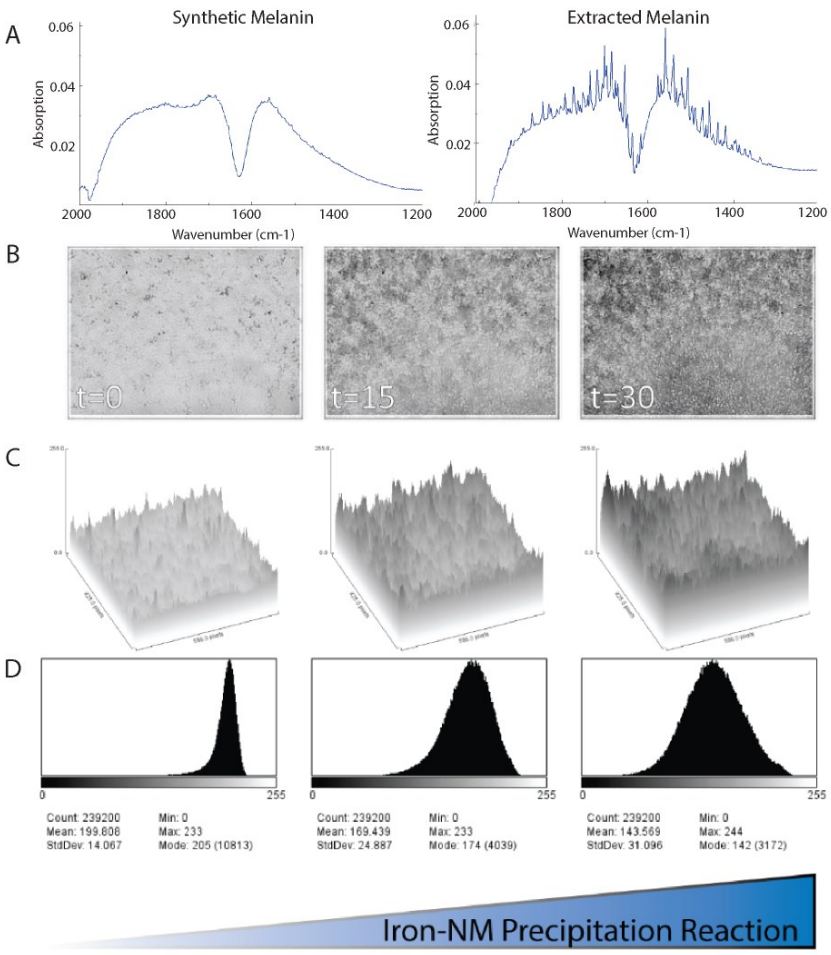

Figure 2.8 Comparison of Synthetic and Extracted Melanin's and Timecourse

A. A comparison of the FTIR spectral profile reveals a stark comparison between the synthetic and extracted melanins in the spectral range of 2000-1200 cm-1. This suggests that there is limited presence of carboxyl groups in the synthetic melanin's which would reduce any capability of metal chelation. B. A time-course of the metal precipitation reaction with iron (i.e. extracted melanin) is shown in black and white (frames t=0; t=15 and t=30 min). C. A 3D rendering of this precipitation in B is illustrated over the course of precipitation for spectral analysis. D. The rate of precipitation was pseudo-quantified by creating a histogram over collected video-frames to allow for kinetic evaluation by evaluation of the AUC values.

Evaluation of the effects of synthetic melanin on cell culture is merited in future studies. However, in regards to iron precipitation of 'synthetic melanin' the investigators have not been able to successfully do so to the same extent as 'extracted melanin' which removes the complexity effects of metal chelation on cell culture.

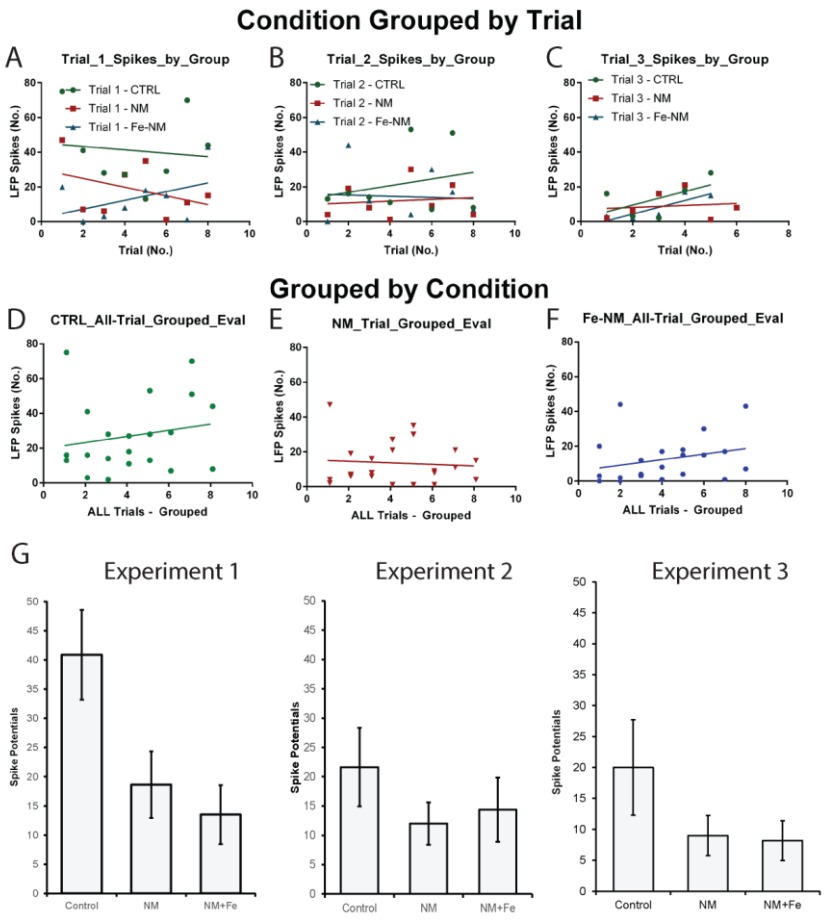

Figure 2.9 Experimental Trial and Experimental Condition Groupings

Results shown in *Figure 2.3* of the main text depict the aggregation of three experimental trials in which individual conditions are color mapped and approximated to ensure that no temporal effects have occurred (i.e. condition specific trending over duration of experiment). **A**. The collective LFP results of Trial 1 **B**. The collective LFP results of Trial 2 **C**. The collective LFP results of Trial 3 (All color coded by experimental condition against the trial order number). **D.** Combined results of all control conditions against trial number **E.** Combined results of all NM-sim conditions against trial number **F.** Combined results of all Fe-NM-sim conditions against trial number. G. All trials can be seen individually error bars are expressed as +- SEM and each experimental condition N=~8.

Collectively the results suggest that differences in experimental groupings replicate across multiple trials and the phenomena of reduced activity by LFP can be replicated independently. Furthermore R-squared values (RSQ) for all slope approximations were below any trend suggesting the phenomena was independent of time (i.e. generally RSQ < ~0.3). The phenomena of NM-sim effects on electrical activity can be observed across multiple experimental trials and replicates.

Chapter 3. Discussion

3.1 Proposed Model: Biologically Derived Neuromelanin and 3D Scaffolding

It can be stated that 'biologically derived' melanins are appreciably better than their synthetic man-made counterparts in regards to metal chelation [157]. The stereochemistry and oligomerization of 'synthetic melanin's and poly-dopamine appear exceptionally challenging to control from an organic synthesis perspective [12, 13, 186]. The conversion of dopamine to dopachrome presumes several resonance stabilized states of which present different nucleophilic attack sites for polymerization [186]. To preserve stereochemistry use of an inorganic catalyst or catalytic substrate would be advisable (e.g. as found in L-DOPA synthesis) [53] but is a dubious assumption for uncontrolled synthetic melanin's [187, 188]. From a synthesis perspective these catalytic substrates are typically kept under highly-regulated conditions to prevent 'catalytic poisoning'[189]. For instance, the synthesis is of pheomelanin is presumed to involve reduction of side products with cysteine residues and are therefore the kinetics are pH dependant [190]. It remains ambiguous how a melanosome incorporates these sulfhydryl groups in the form of cysteine or glutathione residues especially when in presence of free radicals [5, 190].

The silk-NM scaffolding provides addition benefit as the 3D scaffolding permits a higher greater degree of connectivity for neural cultures[1]. Incorporation of cell scaffolding renders these tissue engineered constructs far more representative than their 2D counterparts for applications like electrophysiological measurements[191]. Evidently both NM and Fe-NM disturb neural activity (See Figure 2.3) and cell metabolism of ATP and glutathione (See Figure 2.4). Additional of NM and Fe-NM's effects on membrane potential would be beneficial by patch-clamp validation (See Figure *2.5*) and expression profiling.

3.1.1. Biologically Derived Materials

The level of complexity necessary to replicate the structure of endogenous melanin from an organic synthesis perspective is overwhelming [186] and may yield limited product after sequential steps (i.e. hypothetical yields >30% of starting product). For these reasons 'biologically derived' melanin was pursued as use of 'synthetic melanins' would provide limited stereo-chemical resemblance to NM [13]. While some of the structural permutations of melanin may be contested it can be said definitively that this form of biologically derived melanin chelates iron [40] unlike many of its synthetic counterparts.

It is possible that chelation properties could be ascribed to the interaction of sulfhydryl groups (i.e. cysteine and glutathione) as intermediates in the formation of 'mixed melanins' (i.e. both pheo and eu-melanin) as the result of 'cysteinyldopa' (S-CD) derivatives [5]. Transition metals are notorious for complexing with thiol groups in the form of organometallic clusters in biological conditions especially in context to metallo-enzymes (i.e. Complex I-III of the mitochondrial electron transport chain) [192] and readily deplete glutathione [168]. As was observed in experimental results (See Figure 2.4) glutathione was depleted in both NM and Fe-NM exposed conditions and likely interacted with the NM (Experimental Observations). Confocal video depicting the overlap between Iron (via. Phen Green - Green) and the Synaptic vesicles (via FM-1-43 Red) was added to the supporting content for this document. Further investigation is outlined in the Appendix (See Figure 4.1) to this work.

3.1.2. Disease Implications

A reduction in neural firing can be observed in NM and Fe-NM exposed cultures relative to controls (See Figure 2.3). Additionally, depletion of the necessary antioxidants and nutrients for cell survival was pronounced in the Fe-NM condition (See Figure 2.4). However, the reduction in neural firing could be ascribed to a variety of contributory factors. In the short term (<24 hours) these may include: (1) neurotransmitter precursor molecule deficits (2) neuromodulative activity and (3) metallostasis disturbance (Section 3.2). For the long-term (>24hours) this may comprise: (1) Long-term potentiation (2) Neuroinflammation and (3) Autocrine/Paracrine signaling (Section 3.3).

While DA derived neuromelanin has been the focal point of this research there are other varieties of melanin within the brain. For instance, the LC, which appears blue due to norepinephrine, contains another NM sub variety perturbed by presence of metals [193]. Other transition metals may be catalytic in this process including copper, cobalt, nickel, aluminum as established neurotoxic metals (See Table 1.2)[49].

The PD model described here lacked the contributions of astrocytes/microglia which contribute to the production of nitric oxide and various inflammation makers which spur neurodegeneration [28, 83]. Future models would benefit from the supporting role of astrocytes as they have been found to blunt the effects of neurodegeneration (See) [194]. In efforts to relate NM and Fe-NM to what is known of PD progression we will elaborate on proposed means of neural dysfunction that could be implicated in disease progression (See 3.2. Proposed Mechanisms of Neural Network Dysfunction). The role of Fe-NM on ‘metallostasis’ and implications thereof (See Table 3.1) are beyond the scope of this work but are highlighted. Lastly, improvements regarding biomaterial advancements, co-culture integration and bioreactor device integration can be found in the future directions.

Area	Example	Metal	Citation
High Energy Bond Stabilization	ATP - Mg Stabilized	Mg	[166]
	NAD+ to NADH conversion	Ti, Ni, Cd	[195]
Enzyme Co-factors	Tyrosine Hydroxylase – DA Synthesis	Fe	[196]
	Aconitase	Fe-S	[96]
	Biotin Synthase	Fe-S	[192]
	Complex-I to III mitochondria	Fe-S	[192]
	Catalase	Fe	[197]
Membrane Potential	NMDA Receptor	Mg	[166]
	Voltage gated Channels (CaV1.3)	Cd, Co, Pb	[62]

Table 3.1 Transition Metals and Biological Implications

Metals are often underappreciated in regards to the complex role within biological systems. They serve important catalytic substrate roles in maintaining biological homeostasis and maintaining the functional well-being of the cell. The above table is intended to illustrate the various means by which disturbance in metallostasis would have broad overarching effects on cell health.

The basis for cell metabolism relies a great deal on metal co-factors and dysregulation results in cellular death [198] which is especially true of DA neurons given their energy cost burden [199]. Metals are also closely linked to protein insolubility in animal models and advanced aging [50]. For instance, as stated in Table 3.1 tyrosine hydroxylase requires an Fe catalyst without which it could not convert L-DOPA to DA [196] and it is possible lack of bioavailable Fe could contribute to absence of DA.

3.2. Proposed Mechanisms of Neural Network Dysfunction

Beyond the manuscript (Chapter 2), other theoretical means of neural dysfunction are stated here. Given the inherent complexity of nervous systems there are any number of ways in which transition metal interactions could disrupt the brain's homeostasis (See Table 3.1) [200]. Balance of a feedback control loop as diverse as the neural system can be disturbed in such a manner as to 'over/under dampen' the network [62] as a harmonic oscillator resulting in tremor or locking symptoms in PD [115, 201]. Regarding PD motor-

symptoms, ‘underdamping’ is to ‘freezing’ what ‘overdamping’ is to ‘tremors’ what is relevant is how the system is attenuated when it falls out of balance [202].

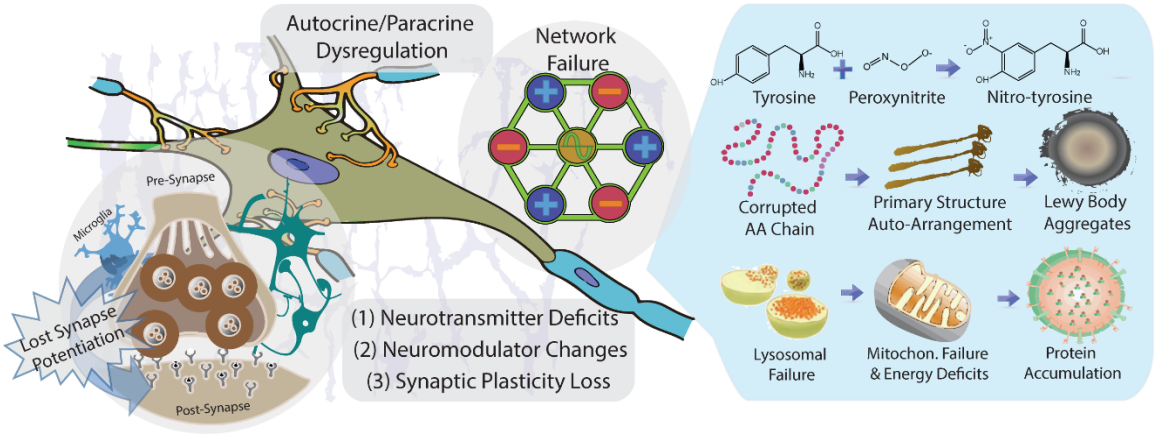

Figure 3.1 Schematic Mechanisms of Dysfunction: Short Long Term

A visual representation of proposed mechanism stages implicated in PD. The left highlights the immediate occurrences of NT loss and disruption of synapse potentiation whereas the right depicts the more gradual evidence of changes to the proteome. Collectively the neural network would be incapable of regaining its homeostasis over time as neurons aged. Adapted with permission from: Creative Commons through Pixabay by OpenClipart-vectors Neuron, Synapse, Mitochondria. Changes to the primary vector graphics include: recoloring and overlay of ‘neuron’; adjusted angle, overlay and re-coloration of ‘synapse’; scaling, re-coloration and vectoring of mitochondria through Illustrator.

Given the limitations of data that was approved for use in this document the proposed mechanisms are largely an interpretation based on clinical literature. However, the neurochemical/chemical mechanisms described are robust phenomena that would likely translate to neurodegenerative implications [26]. Additional efforts to standardize the cell culture environment were undertaken to reduce the variability of biological sampling (See Figure *3.7*) and would be beneficial for future investigators such that they do not encounter difficulties I have encountered.

3.2.1. Neurotransmitter Deficits

We operate on the presumptions that (1) the Braak staging hypothesis is largely correct (2) progression of neurodegenerative disease begins long in advance of motor

symptoms and (3) behavioral symptoms manifest which stem from the gut-brain axis [71]. Accepting these presumptions are true than neurotransmitter deficits may emerge from an absence or modification of neurotransmitter precursor molecules within the gut [203]. The major monoamine neurotransmitters (DA, NE, 5-HT) [204] are derived from a subset of aromatic amino acids (tryptophan, tyrosine and phenylalanine) and in instances of absence, individuals may be disposed to behavioral deficits due to auto-oxidation [113].

Concurrently, gut inflammation is reported in early stages of neurodegenerative disease [203]. Functionally modified versions of these aromatic amino acids (tyr, trp, phen) have been reported in clinical literature[205]; most common is nitrotyrosine, found in elevated levels in the blood serum of PD patients [98]. It was found that incorporation of nitrotyrosine into the culture of dopaminergic neurons caused cellular death [205]. Additionally, when nitrotyrosine was incorporated into cell culture media with PC12 and NT2 cells it was found that the amino acids were incorporated into the cytoskeletal structure and when exposed to primary DA neurons caused a dramatic reduction in TH positive cells [205]. Furthermore, modified nitrotyrosine has been found to be elevated in the SN and LC of individuals exhibiting the symptoms of PD and correlates with robust microglial activity in restraint stress conditions in animal models [206] suggesting a link between stress, sedentary lifestyle and neurodegeneration.

In a similar vein, loss of sleep and appetite preclude PD motor symptoms which correlates with an absence of melatonin [207]. It has been found that melatonin has been perturbed in persons who exhibit early stages of PD and may be preventative in the auto-oxidation of DA [207]. Production of melatonin is closely tied to serotonin given the structural similarities of the two molecules and their concurrent synthesis [208].

Oxidation of serotonin and melatonin to downstream products results in a deficit of these neurotransmitters and the neurological deficits thereof [83].

Absence of bioavailable NT precursors from the gut due to inflammation (i.e. oxidized Tyr, Phe, Trp) could invariably lead to some symptoms observed in PD [204]. The complex relationship between the gut microbiota and the symptoms of PD is an active research topic [71] and may touch upon such concepts as nitrotyrosine in the near future. However, this would suggest therapeutic intervention long before the motor symptoms of PD become apparent and would require consistent maintenance to ensure DA neuronal survival [209].

3.2.2. Neuromodulators

A body of evidence in the field of neuromodulators indicates that free radicals like H_2O_2 act on the GABAergic and ATP-sensitive channels of the brain [210]. The continuous production of H_2O_2 by the mitochondria reveals that depolarization causes an adjustment in the probability of release of dopaminergic neurons via K_{ATP} channels [210]. Another such neuromodulator includes carbon monoxide (CO); a spontaneously occurring 'gasotransmitter' produced by heme-oxygenase and capable of interacting with $K_{Ca,}$ K_{ATP} and various other cationic channels [211]. Some of the voltage sensitive ionic channels susceptible to neuromodulation are addressed in Figure 2.5 A (i.e. KCCN3) but it requires additional replication to substantiate if they are responsive to neuromodulation.

Additionally, the antioxidant glutathione (GSSH) found in Figure 2.4 Post Exposure Immunostaining and Metabolic Analysis, has been identified as a neuromodulator capable of interacting with the NMDA, AMPA and glutamate receptors [212]. Further research suggests that various neurological conditions involve dysregulation of GSSH

including (1) Anti-convulsive effects in epileptic conditions [213] and developmental neuro-immune conditions like autism, schizophrenia and bipolar disorder [214]. The NMDA receptor is fairly ubiquitously expressed throughout the brain and is intricately tied to long-term potentiation at the synaptic level [215].Lastly, hydrogen sulfide (H_2S), is another gaseous neurotransmitter / neuromodulator, that is intimately tied to the abundance of glutathione/cysteine and alkalinity of the neural cytoplasm [216]. H_2S is theorized to be neuroprotective due to its free radical scavenging capabilities and blunts the effects of NO in the inflammation cascade [217].

The effects of NM and Fe-NM on our 3D neural cultures may be more subtle than they appear. Gaseous neurotransmitters (NO, CO, and H_2S) and neuromodulators (GSSH, H_2O_2) are more transient than can be identified by traditional immunostaining techniques and may be implicated in post-translational modification of voltage gated membrane channels. Validation would require concurrent monitoring of neurons exposed to NM and Fe-NM during patch clamp to validate the occurrence of neuromodulation.

3.2.3. Metallostasis and Effect of Catalytic Substrates

Many neurons must maintain a ‘labile-pool’ of iron and other transition metals [218] for use as enzyme co-factors among other applications. To reiterate, the enzyme tyrosine hydroxylase (TH), vital to the conversion of L-DOPA to DA, must have an iron catalyst to work effectively [196] (See Table 3.1). Other such crucial enzymes that require metal co-factors include SOD, Catalase, and Zinc-Finger proteases that are essential metalloenzymes [197] to the workings of the cell but must be tightly controlled to maintain cellular metabolism [219].

In relation to PD this phenomenon includes the oxidative state of the metal co-factors; conversion of the oxidative states of iron (i.e. Fe2+/Fe3+) is another line of inquiry regarding neurodegenerative disease [220]. In a study of scrapie-infected mice it was found that the ferric/ferrous ratio was altered throughout the brain which was ascribed to the astrocytosis and lipid peroxidation from which parallels were drawn to late stage PD [221]. This observation of Fe2/Fe3 ratio has been observed some time ago in the PD field within the SN and Putamen [222].

An experimental observation that was noticed after the fact was that in combining NM and Fe^{3+} solution the remaining precipitate stained with Phen-Green SK which stains Fe^{2+}, suggesting a NM stabilized change in oxidative state. The ratio of ferric/ferrous iron extends beyond PD and has been suggested to play a role in AD and progressive supranuclear palsy (PSP) [223]. Some have speculated that this ratio may result in 'metal starvation' of the cell or that absence of key metals would conflict with cellular transport mechanisms (i.e. symport/antiport mechanisms) and indirectly metal storage to maintain neuronal homeostasis [224].

Pre-existing efforts to isolate NM and incorporate it into cell culture have been made predominantly on synthetic melanins or those extracted from hair, eyes or skin [13]. FTIR data suggests that an abundance of alkyne and carboxyl/carboxylic acid groups (COOH/COO) are present in the extracted form of NM described here (See Figure 2.6 - FTIR Data). These auxiliary carboxylic acid groups (COOH) of Sepia Melanin are capable of binding alkali metal groups as well (Ca, Na, Mg) in a pH dependent manner [157]. Both Ca and Mg are essential in maintaining the membrane potential and are directly manipulated in the brain by astrocytes in the form of 'calcium waves' [225] and correlate with wakefulness states [226]. If interaction between NM and alkali metals is

perturbed it is conceivable this would affect local electrical dynamics through metallostasis as well.

3.3. Local Field Potential

The effects of NM on electrical activity of 3D neural cultures is a focal point of our research and so it is fitting to discuss recent breakthroughs in electrophysiology and PD therapeutics. A notable advancement in the PD field is the research of Dr. Surmeier regarding the neuroprotective effects of isradipine, an L-type calcium channel blocker (CCB) used in treatment of high blood pressure, which has been found to be neuroprotective in neurotoxic 6-OHDA PD models [60]. It was found that DA neurons experience especially thin energy margins due to oxidative phosphorylation and limited Ca^{2+} sequestration in CaV1.3 positive pacemaker DA-neurons for which isradipine is thought to be energy sparing [93]. CaV1.3 is expressed by the gene CACNA1D found in Figure 2.5 but requires additional validation. Additionally, the extensive axonal arborization of DA neurons only further complicates the matter in making action potential propagation highly inefficient [199]. Within the SNc a remarkable subset of 'pacemaker DA' neurons exist due to presence of L-type Calcium Channels (LTCC's), which were previously thought to be exclusively expressed by the sinoatrial node of the heart, but is now an active topic for therapeutic intervention in PD [17]. Efforts to create similar 'pacemaker DA neurons' within the 3D neural culture making use of optogenetic stimulation were attempted but not further pursued (see supplemental video). However, other research groups have elaborated on this concept of DA-pacemaker neurons by integrating different wavelengths and various voltage gated channels [227].

3.3.1. Electrical Activity and Feedback Control Mechanisms

Neuro-oscillatory behavior of the basal ganglia when amplified contributes to the various kinesthetic states in late stage PD [228]. A cohesive ‘beta-band’ (11-30Hz) is required to break-through the elevated threshold necessary to initiate movements and consequently cannot override commands projecting to the motor cortex [202]. However, there remains a good deal of ambiguity regarding whether the synchronization of neuro-oscillatory behavior is causal to the bradykinesia found in late stage PD [228]. Surgical intervention such as a thalamotomy or pallidotomy, in which the tracts adjacent to the SN are neurosurgically ablated, are techniques with the express aim of reducing the symptoms of dyskinesia and tremor by limiting the negative feedback control ‘foci’ at times combined with deep brain stimulation [229]. Similarly surgical ablations were used to mitigate the removal of DBS electrode leads under circumstances in which infection or inflammation have contributed to the removal of electrodes; effectively serving as a back-up should patients be non-responsive to medication management [230].

In considering the DA-pacemaker neurons and emergence of foci efforts at ‘spatial mapping’ of electrical activity were conducted with a multi-electrode array (MEA) during testing with Axion Biosystems (See Figure 3.2) but would require additional validation

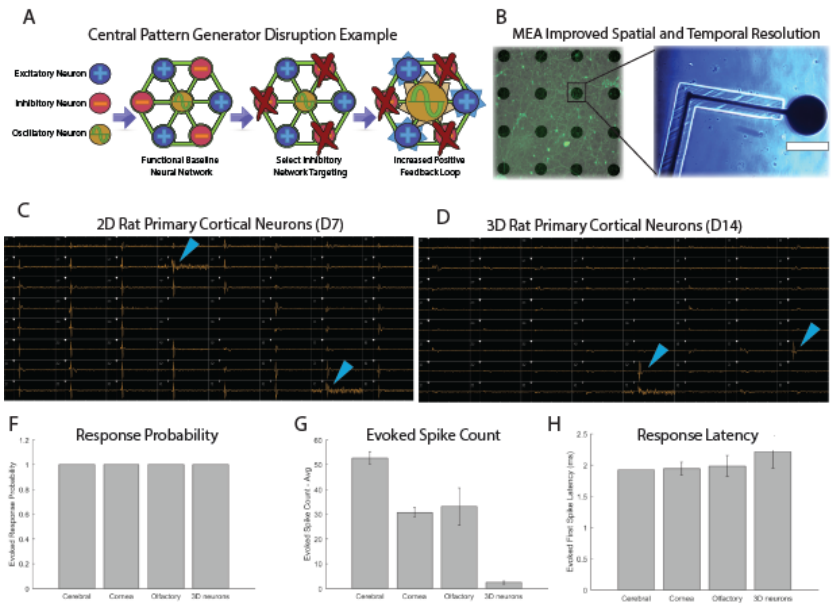

.Figure 3.2 Multi-Electrode Array Activity of 2D and 3D Cultures

(A) A simplified example of a network expressed as nodes in which removal of inhibitory feedback could result in increased positive feedback and potentially oscillation (B) Multi-electrode arrays provides more spatial/temporal resolution with repeat measurements and defined proximity (Scale 100 uM) (C) A 2D rat primary cortical highlights few spiking events (blue arrows) (D) 3D Cortical neurons demonstrated broad electrical activity but only in select cases (blue arrows) (D) Olfactory neurons showed similar activity but fewer occurrences of hysteresis. Major differences between the 2D and 3D cultures were observed in (F) the evoked spike counts and (G) the response latency but further analysis is necessary to validate. Adapted with permission from: Axion Biosystems Maestro MEA system: Tufts site demo (2017). Changes include insertion of C-D and blue arrows; alignment and increased resolution scale of F-G.

Central pattern generators (CPG's) which comprise the most fundamental units of neural circuitry are likely implicated in PD [231] but the connectivity remains undefined. In surgical ablation (i.e. pallidotomy or thalamotomy) CPGs are mechanically modified by selective lesioning whereas in DBS electrode integration stimulation may provide a substitute for CaV1.3 positive oscillatory neurons. Optogenetic stimulation could provide a functional alternative for the CaV1.3 positive oscillatory neuron class within a 3D culture (i.e. temporal control; See Section 3.3) and 3D printing of a substrate could provide defined resolution (i.e. spatial control; SeeFigure 3.2) for the basis of CPG's

which control orchestration of gait and movement [232] and potentially tremor encountered in late stage PD.

Efforts to make the model pharmacologically relevant involved the DA agonist apomorphine (See Table 1.3) as it is classified as both an established therapeutic and emerging neuroprotective compound [59]. The results of a limited study are summarized in Figure 3.3 LFP Measurements and Drug Testing and highlights the study design that integrates electrical stimulation and tetrodotoxin blunting [117]. Additional verification to clarify the proposed neuroprotective effects of Apomorphine merit further investigation.

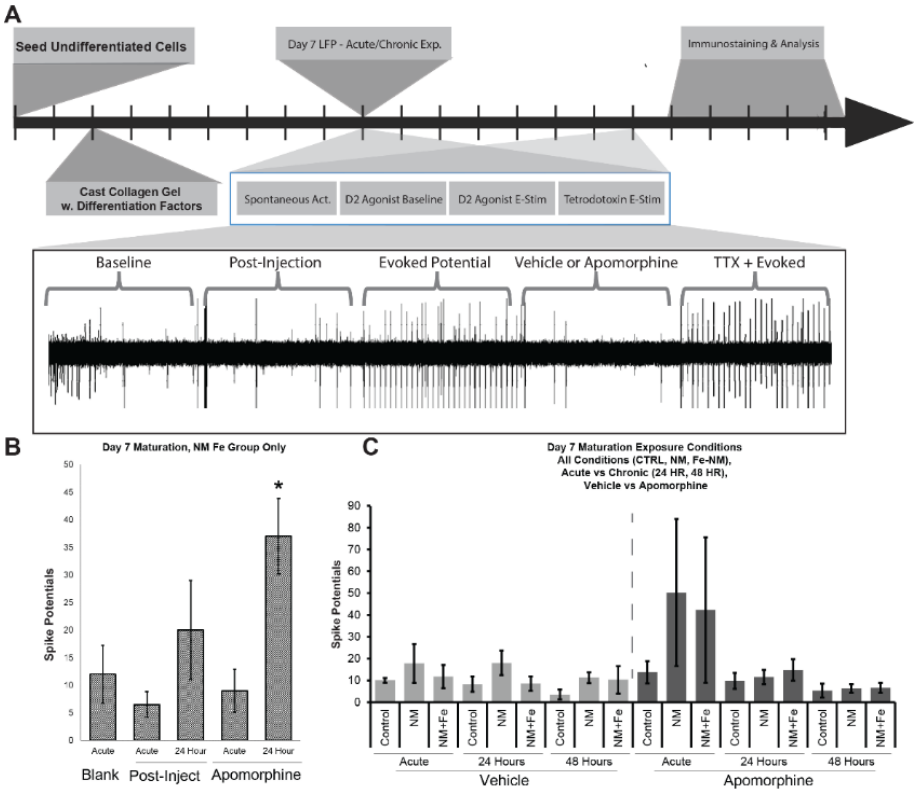

Figure 3.3 LFP Measurements and Drug Testing

(A) Additional electrophysiological tests were conducted using the drug Apomorphine which comprised a baseline and series of evoked injections at both day 7 and day 14 in culture. (B) An analysis of the NM-Fe group revealed differences in the apomorphine groups but would require additional analysis (C) A comparison of the vehicle and apomorphine post exposure to NM and Fe-NM requires further analysis but suggests apomorphine may reduce the effects of NM and Fe-NM exposure. The reader is encouraged to take this analysis lightly given that it is underpowered (n=3; All). Figures (B-C) Completed with assistance by Dr. Nicolas Rouleau.

Previous studies regarding the DA model investigated the effects of Apomorphine. Use of the 3D tissue engineered platform as a means for investigating electrical activity can be explored. If the NM possesses sorptive properties when conjugated to the silk scaffold these effects can be quantified by LFP measurements.

3.3.2. Neuro-Inflammation and Nitric Oxide Release

The model described here lacked the role of microglia which contribute to the production of nitric oxide (NO) and various neuro-inflammation makers (i.e. IFN) contributing to neurodegeneration [132]. By independently investigating the contribution of the brain's immune system in exacerbating protein turnover this process can be elucidated. Furthermore, neurodevelopmental models which contribute to sustained dopaminergic lineage rely on the supporting role of astrocytes and other such supporting cells [226].

Microglia are known to be implicated in PD [158] but additionally in such neuro-affective disorders as schizophrenia [165]. However, it is challenging to establish which microglia have been activated by cellular detritus and which have become dysfunctional by virtue of the experimental model [233]. Microglia produce considerable quantities of peroxides, superoxides and nitric oxide during 'respiratory burst' events; capable of causing de-myelination when concurrent with release of interleukins [43]. Unsurprisingly the NO and H2O2 free radicals cause protein oxidative damage in the form of nitrosylation [234] and carbonylation [169] thereby overwhelming the proteome and resulting in alterations of lysosomal processing and storage [110, 153].

The transient nature of ROS and RNS radicals would be undetectable using traditional histological methods and only evident if actively monitoring NOS-1 and other such enzymes. Similarly, S-nitrosation proteins (SNO-proteins) (See Figure 4.3) are

challenging to isolate and characterize but are implicated in neurodegenerative disease, namely Alzheimer's [235] but additionally Parkinson's following depletion of glutathione [153]. However, the proteome is rife with examples of NO induced oxidative damage as the result of aberrant mitochondrial behavior throughout neurodegeneration literature [110] and may be misleading in disease state causality [236]. Experimental studies that corroborate the interaction of microglia with the Fe-NM precipitate can be found in the Appendix section (See Figure 4.4 and Figure 4.3).

3.3.3. Autocrine & Paracrine Activity: Melanin Concentrating Hormone

Long-term attenuation neural network behavior could also be attributed to neuro-endocrine activity as there are far reaching implications of melanin associated hormones derived from the pituitary gland [237]. It was discovered that the infusion of melanin-concentrating hormone (MCH) (concentrations 4-11 uM) was found to increase hippocampal synaptic transmission of granule cells in the dentate gyrus of Wistar-Rats [237]. In a similar vein, MCH has been evaluated in regards to its role in sleep duration by REM and acetylcholine release when injected into the medial septum of Wistar Rats [238]. It is challenging to anticipate the effects of neuroendocrine hormones associated with melanin like MCH on neural networks to that of NM's effects but interesting that the MCH influences sleep, feeding behaviors, and reproductive behaviors [237]. MCH can be found in select regions of the brain associated with sleep/wakefulness and feeding behaviors within the hypothalamus [239]. Furthermore, MCH expressing neurons directly interact with neurotransmitter production (5-HT, DA, NEPI, Ach) and present the capacity to regulate energy consumption [240]. MCH is expressed selectively throughout the brain (1) in the neocortex (2) throughout the olfactory bulb (3) hippocampus whereas less was expressed in the cerebellum [241]. MCH is also differentially expressed between males and female rat models most notably in the laterodorsal tegmental

nucleus (LDT) adjacent to the LC that is associated with sleep and production of acetylcholine [242]. In summary, neuropeptides and hormones implicated in melanin accumulation (MCH) and are differentially expressed by gender are indirectly tied to neural dysfunction.

3.4. Future Directions

In experimenting with *sepia melanin* we have only scratched the surface of the many diverse forms of melanin that can be incorporated into biomaterials. A cursory investigation of biologically derived melanin in biomaterials literature reveals an enormous diversity of fungal melanin as well [243]. Similar properties of free radical scavenging, thermal tolerance and metal ion binding are reported with fungal melanin; allowing the organisms to survive in extreme environments [244]. It may be possible that the melanin derived from fungi provide a more reliable source of biologically extracted melanin though it is difficult to anticipate how extraction methods may deviate from those described here [129]. Melanin is fundamental to how these organisms/microbes grow in extreme conditions and how they often evade identification by the immune system by continuously changing form [245]. Additionally fungal melanin's possess radically different biological synthesis pathways to those described of NM and perhaps unique metal binging mechanisms as well [246] making them intriguing biomaterials.

3.4.1. Melanin-Silk Horseradish Peroxide Hydrogels

Horseradish peroxidase (HRP)-silk hydrogel derivatives, which exhibit tunable stiffness by dityrosine cross-linking, were originally developed by Partlow and colleagues of the SilkLab [247]. This process of hydro-gelation additionally works with photo-crosslinking agents like riboflavin which acts as a photo-initiator [248]. Additionally, the process works with NM and yields brown opaque gels of similar elasticity to the original

HRP hydrogels (Figure 3.4) (experimental observations). Presently, the mechanism of chemical integration is unknown but it is assumed to be analogous to that of HRP gels provided that NM is cross reacted tyrosine [12], to a limited extent, within which carboxylic acid groups could integrate into the silk structure.

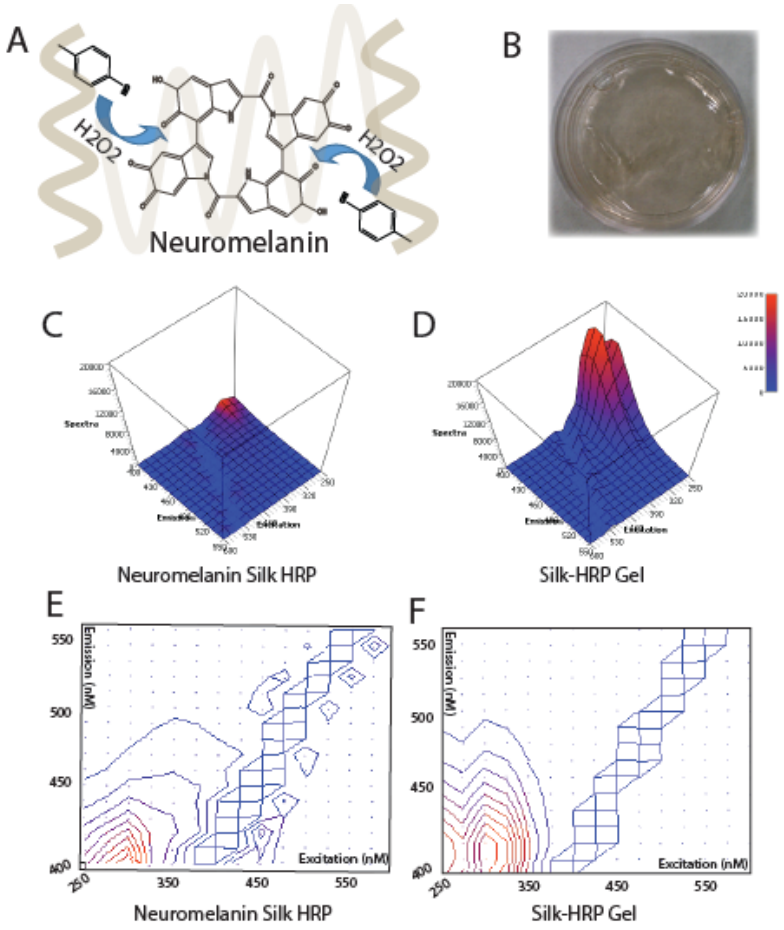

Figure 3.4 Silk-NM Hydrogel

(A) Neuromelanin can function as a linker in Silk-HRP gel as described previously a proposed mechanism can be found above. (B) The NM-Silk HRP gels appear physically brown despite washing with DPBS to remove unreacted product. (C) Excitation-Emission (EX-EM) spectra of the NM-Silk HRP and (D) the Silk HRP gels. A topographical map of the EX-EM profile can be found above for (E) NM-Silk and (F) Silk HRP gels expressed as Excitation (X-axis) and Emission (Y-axis). The blue region corresponds to overlap between the excitation and emission wavelengths (i.e. EX=EM) and screened accordingly. Adapted with permission from: Phys. Rev. Lett. 97. Kaxiras, E., Tsolakidis, A., Zonios, G. and Meng, S., Structural Model of Eumelanin, (2006) [10]. Changes include: redrawing the DHI:DHICA molecule in (A) and overlay with tyrosine crosslinking.

This form of NM-HRP gel could provide a softer substrate for neural cultures as has been explored previously [123, 249]. Additionally, salt-leeched silk scaffolds can be chemically functionalized by the reaction to chemically incorporate the NM provided that the tyrosine residues are chemically available. It remains unknown if metal chelation could still occur through the bulk of the hydrogel or if more complex structures such as the metal organic frameworks (see Section 3.4.2) could be incorporated. Furthermore, if adsorptive properties remain active for these NM-Silk gels it could be used to assess binding affinity of neurotoxins (see Section 3.4.6).

3.4.2. Melanin Metal Organic Frameworks

NM's adsorptive capacity of coupled with its affinity for transition metal linkers is reminiscent of an emerging field in organometallics in metal organic frameworks (MOF) with drug delivery and tissue engineering applications[250]. MOFs were originally developed as materials analogous to zeolites the MOF consist of organic linker molecules comprised of carboxylic acid groups and a transition metal linker [251]. The work was pioneered by Omar Yaghi an immense diversity of MOFs with numerous applications[252]. Poly-dopamine has been proposed as a linker capable of creating super-structure analogous to MOFs [253] but it would appear the biologically extracted melanins have yet to be explored (See Figure 3.5). Some groups have been capable of tethering enzymes like glucose oxidase to these poly-dopamine substrates to serve as reporter enzymes allowing for sustained catalytic activity when encapsulated [211]. A diversity of enzyme linked MOFs have been established and demonstrate reliable enzymatic activity following multiple cycles of use [254]. As materials MOF's have been used for directed drug delivery to macrophages or as a means of enhancing imaging by integrating reporter dyes [255]. Given that microglia comprise one of the most problematic challenges in mitigating the free radical cascade it is natural that they would

be ideal targets for such a delivery platform [256]. Under certain circumstances aldehyde groups are used to covalently link the super-structure, viable alternatives could include glutathione or NADPH given as they are far more biocompatible and would require less purification.

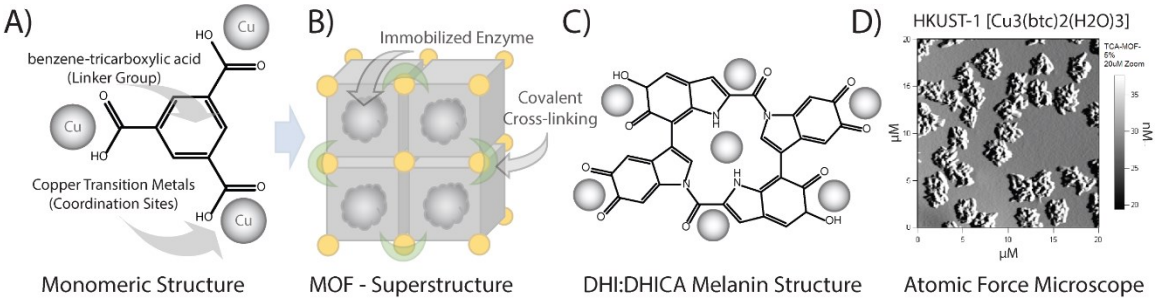

Figure 3.5 Melanin as Metal Organic Framework Linker

(A) HKUST-1 was originally designed making use of benzene-tricarboxylic acid (BTC) and copper to create an organic framework. (B) The crystalline superstructure of MOF's is capable of enzyme encapsulation and chemical crosslinking. (C) Similarly the DHI:DHICA structure of melanin could interact with various metals alkali and transition metals and could be developed as a MOF platform (gray spheres indicate metal site). (D) Atomic force microscopy (AFM) imaging of HKUST-1 reveals complex surface architecture but additional X-ray diffraction would be merited for such experiments. Hypothetically the DHI:DHICA monomer could be used for similar applications to that of TCA used in the original HKUST-1 MOF. Adapted with permission from: Phys. Rev. Lett. 97. Kaxiras, E., Tsolakidis, A., Zonios, G. and Meng, S., Structural Model of Eumelanin, (2006) [10].Changes include redrawing the DHI:DHICA structure shown in panel (C).

Such hybrid-MOF materials would otherwise be only tangentially relevant to research described here but experimental observation suggested that during LFP data collection the resistance of the electrode would increase dramatically if touching a Fe-NM (Figure 2.3; unpublished results). As some MOF's have the potential to act as supercapacitors [257, 258] suggesting electrochemical interactions and it was speculated that the relationship between organic frameworks and the Fe-NM precipitate may be connected. It is additionally speculated that a MOF immobilized enzyme could be used as a real-time detection mechanism for phagocytosis [259].

3.4.3. Astrocytes and Microglia Incorporation into the PD Model

The complexity of the 3D NM model is lacking in absence of supporting cell types of the microglia and astrocytes. Microglia contribute to the release of inflammatory cytokines (IL-1, IL-6, TNF-α, and IFN-γ) [43] which are detrimental to neuronal survival and mount an immune response against NM [260]. Over time microglia become increasingly reactive with age often resulting in increased vulnerability of activation [165]. Furthermore, the notable increase in inducible nitric oxide synthase enzymes of microglia in presence of NM [31] suggests a causal link between protein nitrosylation and NM following apoptosis of DA neurons [110]. During respiratory burst events the release of superoxides generated by microglia [206] can interact with NO resulting in more sustained peroxynitrite (ONOO-) radicals that are collectively more active and longer lasting [112]. Generation of ROS and inflammatory cytokines is further exacerbated when coupled with phagocytosis resulting in a cascade of complications in cellular metabolism [83]. Research suggest that co-culture of DA-neurons and astrocytes is capable of mitigating neurodegeneration of LUHMES within *in vitro* models [194] but it remains to be seen how the three cellular components (astrocytes, microglia and DA-neurons) would interact in 3D cultures. For this purpose a system of controlled interactions must be devised to integrate NM [209] given its inherent effects on neuro-inflammation.

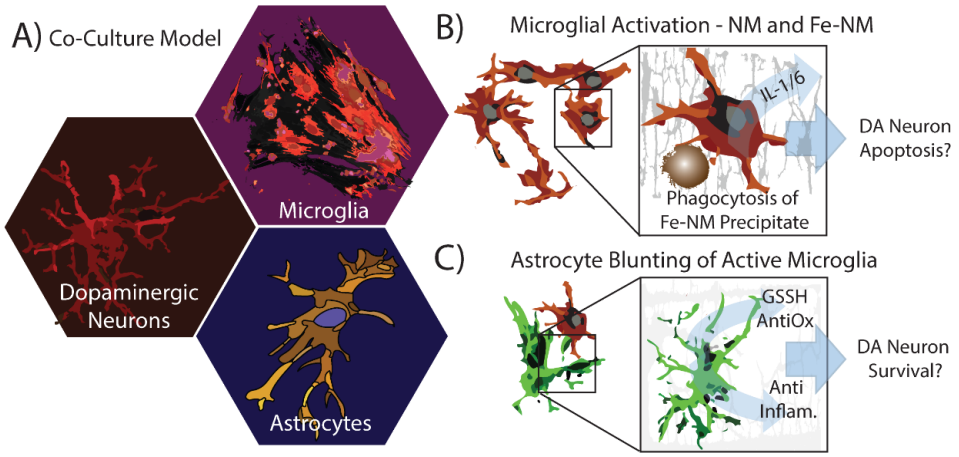

Figure 3.6 Astrocyte and Microglial Interactions

(A) In a controlled co-culture model two components would be combined and defined before integration (i.e. Astrocyte and DA neuron; Astrocyte and Microglia etc.) to ensure that combining all three factors did not have undue effects. (B) In a hypothetical example microglia exposed to Fe-NM may produce inflammatory cytokines which could then be exposed to DA neurons and identified. (C) Additionally combining astrocytes and microglia may blunt an inflammatory reaction when exposed to DA neurons.

Controlled interactions between the populations of the dopaminergic neurons and astrocyte and microglial populations would provide a means of defining the factors implicated in PD and how NM or Fe-NM may exacerbate to this interaction as found in rotenone induced PD models as well [261]. A broad evaluation of the hormones, cytokines and cell signaling molecules can be accomplished with an antibody array to select preliminary biomarkers to be further pursued (See Figure 4.3 Modelling of NeuroInflammatory Response). ‘Bottom-up’ engineering approach with this model is advantageous as it allows investigators to parse variables in a controlled fashion [2, 262] unlike complexity of ‘top down’ transgenic animal models [19].

3.4.4. Bioreactor and Cell Culture Standardization

Substantial investments of time are required in the feeding and splitting of cultures [263]; especially when conditioned media and feeder layers are required [122, 264]. When factoring in the time required in coating the lead time to a viable culture can be several weeks before results can be anticipated [122]. Additionally, the inherently high

degree of variability in biological samples coupled with the challenge of human error in reproducibility has remained an understated difficulty of biological research [90, 265]. As stated previously, advantages of this tissue engineered model over traditional transgenic animal models underscores the ability to control all variables of extracellular matrix integration, nutrient exchange and neurotrophic factors.

Controlling the variables of O2, pH, flow-rate and temperature allows for real-time monitoring of factors that contribute to cell survival [266]. Furthermore, many 3D cell cultures require regular administration of neurotrophic factors to maintain survival [267, 268]. Thankfully a breadth of information and accessible electronics platforms through the Arduino and Rasberry Pi has orchestrated accessible development in bioreactor technologies [269]. Both platforms were originally designed for educational purposes but have since gained traction as tools for scaled down bioreactor fabrication [270]. Efforts to develop a supporting platform for long-term cell culture maintenance were conducted in hopes of improving reproducibility.

The effects of persistent oxygen deprivation on the brain, referred to as brain ischemia, lead to a reduction in activity, and increase in lactate/pyruvate ratio as can be observed by PET imaging [271]. As the core of the 3D scaffold can become dense with neurons it would be imperative that O2 concentration be sufficient to diffuse to the bulk of the sponge or it may become anoxic [272]. Additionally, many of the growth/differentiation factors necessary to maintain a neural lineage have limited duration in culture which may be as little as 12 hours or less and would benefit from continuous infusion from a perfusion system (Figure 3.7 Standardized Bioreactor for Cell Culture Schematics - A). An advantage of the dual syringe is that it allows for liquid dilution by independently changing the injection rates of two syringes. Lastly, it is anticipated that sensor drift will occur over time due to bio-fouling. For this reason a

valving configuration to wash and calibrate was integrated (Figure *3.7* – F and I). The wash solution contained 1% formic acid to remove build-up at the catalytic substrate.

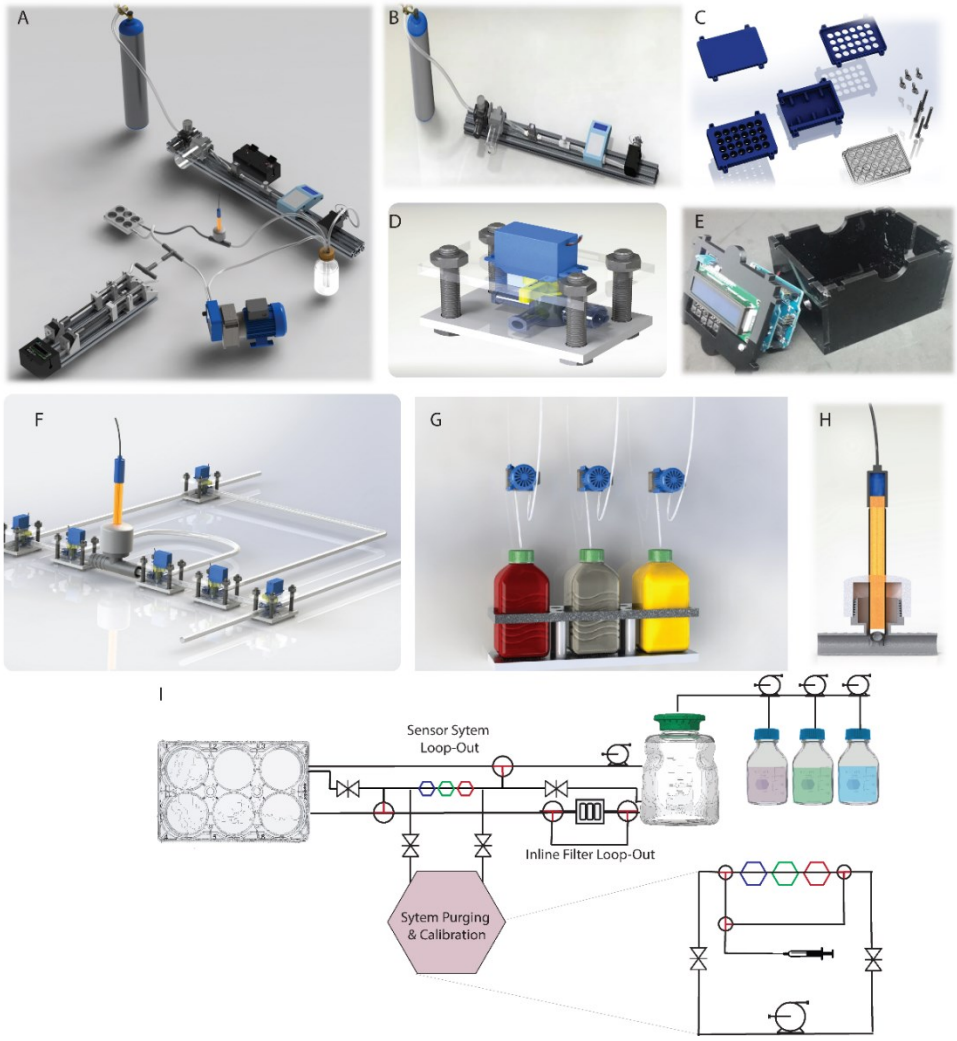

Figure 3.7 Standardized Bioreactor for Cell Culture Schematics

(A) The system is comprised of a dual auto-injector, peristaltic pump, inline sensor system and gas delivery system. (B) The delivery system is comprised of a tank, pressure regulator, needle valve, mass flow controller and electronic valve. (C) The light integration system to be used for optical stimulation (D). The valving is comprised of 3 way valves with servo motors affixed on top of them the (E) LCD display and control board for system automation. (F) Integrated valving controls – capable of measuring bioreactor inlet and outlet O2, pH and temp measurements and backflush. (G) Stock solutions can be made in advance and diluted accordingly (i.e. 10X DMEM combine with FBS solution and dilute) (H) Sensor integration capable of integrating O2 sensors, pH sensors, and temperature sensor into the platform. (I) A valving diagram showing inline purge system and various 'loop-out' positons. Prototyped and coded with assistance of Kevin Kapner, Nick Hartman and Carlos Lopez-Rodriguez.

Figure 3.7 was intended to automate and standardize the process of cell culture integration and reporting to provide real-time reporting to investigators but could not be brought to completion. If efforts to create 'disease relevant' tissue engineered models are to succeed it is imperative that both cell culture (Figure 3.7 A) and reporting/interpretation of data (Figure 4.5) are to be standardized for reproducibility.

3.4.5. Binding Affinity Evaluation: Melanins, Xenobiotics and Transition Metals

Adsorptive properties of NM for such diverse neurotoxic compounds as pesticides and antibiotics has been established clinically [38]. This is ascribed to the stacked planar secondary structure configuration of NM which possesses a gap capable of being displaced by small molecules [13, 39]. Established researchers in the NM field suspect that the release of exogenous neurotoxic compounds can be caused by interaction with alkali and transition metals [11, 40] causing release into the surrounding area and subsequent neurotoxic effects.

Provided that the NM-Silk HRP hydrogel could have comparable density to that of the cortex such that small molecules could move freely the kinetics of adsorption and desorption could be evaluated on an individual basis (See Figure 3.8). A similar approach can be found in plasma protein binding, by which a drug in question can be exposed to varying concentrations of globular proteins to assess the affinity of the molecule [273]. Similar techniques have been conducted with melanin and chloroquine and metoprolol to observe release kinetics following site activation and binding [274]. However, a portion of the literature pertaining to melanin binding is applied to the pigments of the eye and thus not directly applicable to NM [275].

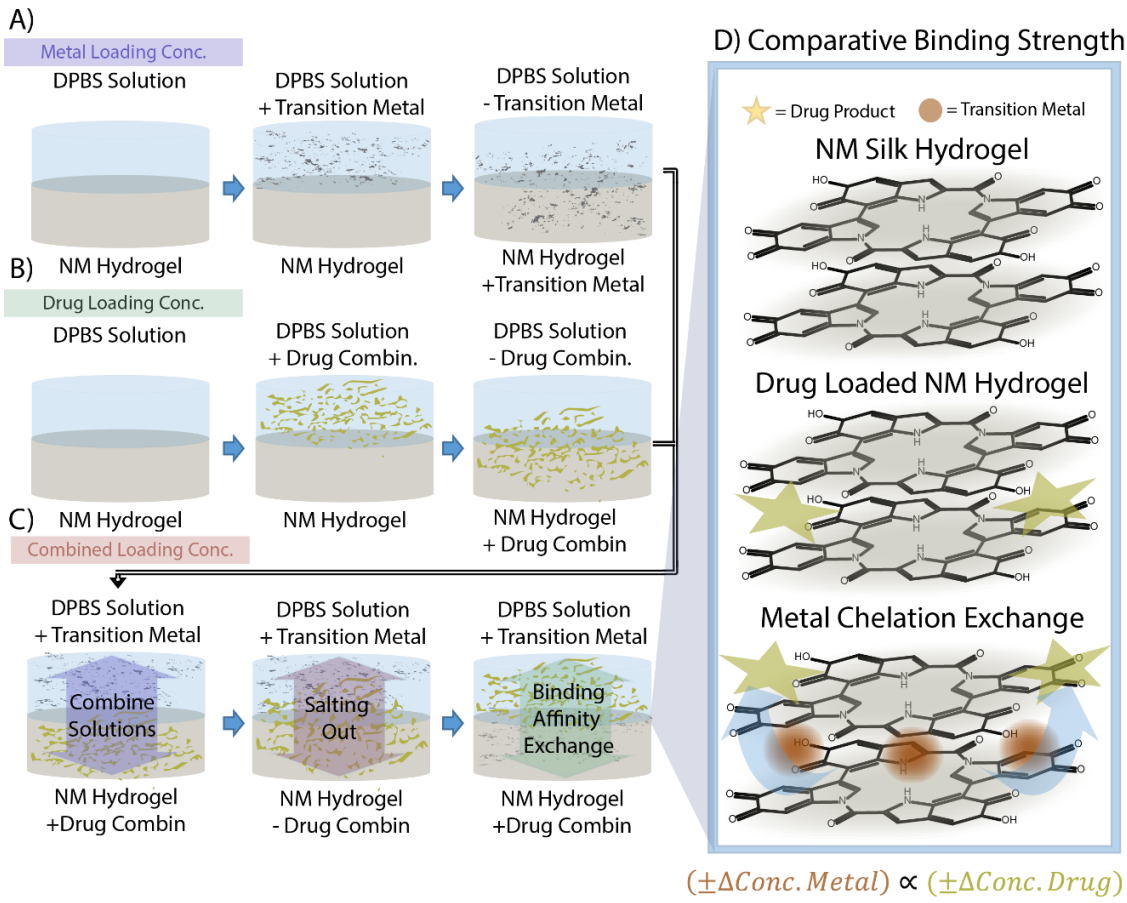

Figure 3.8 Binding Affinity of Neurotoxic Compounds and Transition Metals

To assess the binding kinetics of various neurotoxic drugs to NM for high throughput applications the following steps may be conducted. (A-D) (1) Bind NM to silk in a hydrogel (2) Evaluate if metal chelation can occur through this silk hydrogel (3) establish 'loading capacity' of gel for various metals (4) create new gels and load with compound of interest (i.e. tetracycline) (5) again evaluate metal chelation and (6) assess if 'salting out' has occurred in which binding metals causes the release of the compound of interest. A schematic of this interaction can be found in (D) expressing how competitive interactions could result in the displacement of neurotoxic compounds. (E) Additionally, assuming use of a 96 well plate format this procedure could be multiplexed to define known interactions of (1) NM and drug loading, (2) NM and metal loading and lastly (3) drug and metal loading for a known NM concentration.

It is possible that the interaction between NM and transition metals results in a release of neurotoxic drugs accumulated over a lifetime [17, 38]. Should this be the case

it would be worthwhile to know the affinity of a drug for NM [40] and how this may affect adsorption capacity [40, 157]. Should there be a chemical displacement relationship between NM, transition metals and neurotoxic drugs [276] it would be beneficial to know the implications in a human relevant representative model as it would allow modelling of release of neurotoxic drugs (See Figure 3.8).

3.5. Conclusions

Despite several decades of research, NM remains a biomaterial of interest given its exclusive presence in select animal models like primates [30]. In some regards NM is a 'limiting reagent' for investigators conducting physiologically relevant research on cellular mechanisms involved in PD [95]. For instance, some academic literature goes so far as to extract NM from deceased human patients to then be used with animal derived models or for chemical analysis [31, 32, 260]. In doing so, yields were estimated to be 0.15g per each SNpc sufficient for a limited number of experiments [85]. For investigators that (1) do not have ample access to a morgue for human tissue (2) do not have the resources and personnel to extract/pool the quantities derived from several human cortices or (3) find extraction of human NM ethically dubious; alternatives must be provided capable of metal chelation. This would allow more researchers to address fundamental in vitro questions. For instance, Lewy Bodies, which have long been the focal point of PD research, differ considerably between patients and how to ascribe these differences remains unclear [17]. Links between PD and dementia (i.e. PDD) suggest a more complex causal relationship than genetic factors alone could account for [84].

A substantial amount of research has been undermined and left out in this analysis concerning the mechanistic underpinnings of how NM and Fe-NM may correlate with development of PD. This is largely a shortcoming of the author that (1) neurotransmitter

HPLC data (2) RT-PCR data (3) ELISA and (4) Immunostaining data did not reach a meaningful conclusions to support this work. That being said, it is concluded that NM and Fe-NM could act as a 'bio-inorganic catalyst' in neurodegenerative disease changes occur in the proteome during neurodegeneration leading to a marked increase in ubiquitination [277].

Histology of post-mortem brains of PD patients reveals small protein aggregates akin to those encountered in AD, huntingtons (HD) [72, 278] and transmissible spongiform encephalopathies (TSE) [94]. However, these 'proteinaceous infectious particles' have unusual chemical properties for aggregation (i.e. many are resistant to traditional decontamination methods of autoclave [279, 280] and the kinetics of fibrilization suggest extremely slow progression in absence of a catalyst or co-operative binding [281]. Transition metals have been suggested to contribute to this progression [218] implicating bio-organic metal catalysis in α-synuclein aggregation by di-tyrosine linking [131]. The resilience of Fe-NM to autoclave and structural similarities to the neurotoxic organometallic catalyst ferrocene [282] suggesting 'metallocenes' may have unique protein degradation methods [283, 284].

Chapter 4. Appendix

4.1. Flow Diagram for Processing Stages of NM Extraction

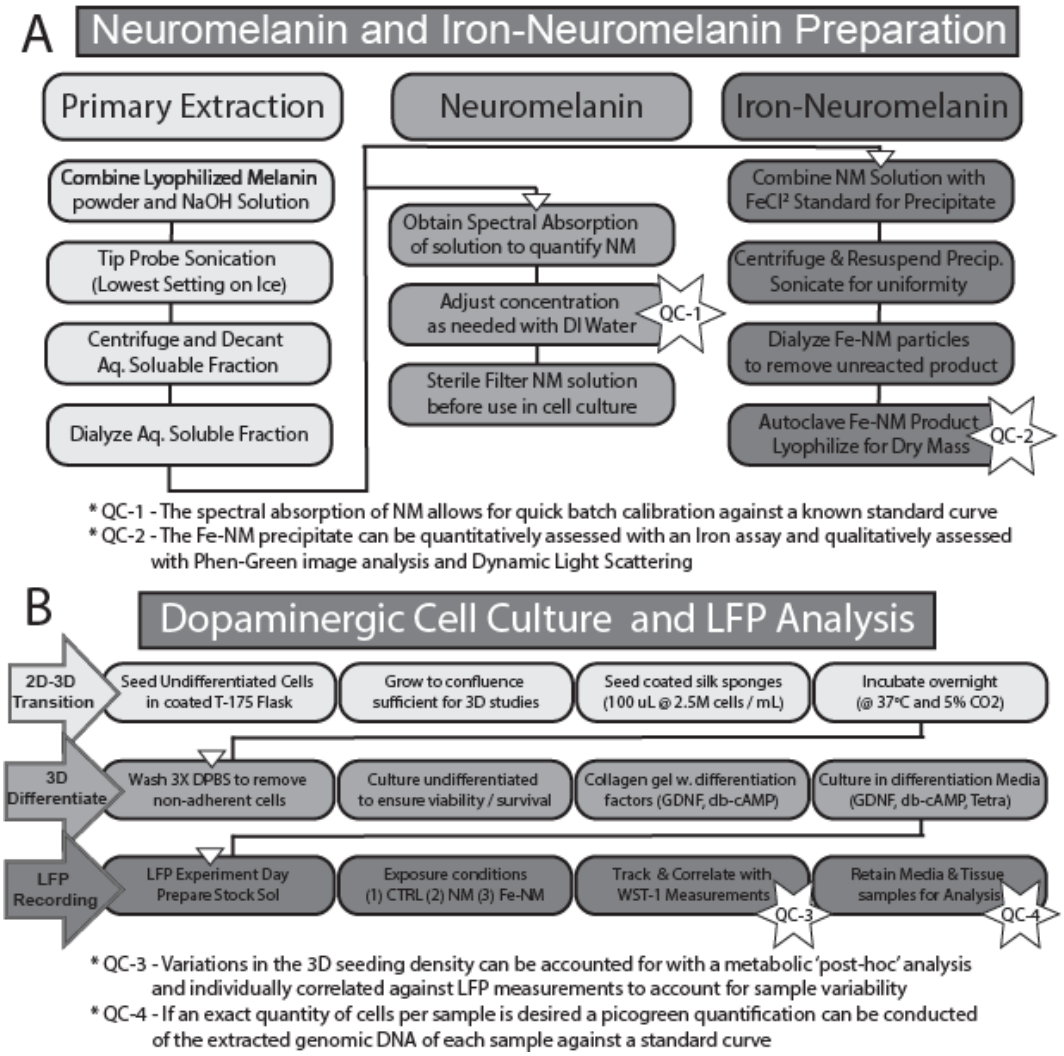

Figure 4.1 Flow Diagram of Processing Stages for Extraction of NM

A more in depth flow diagram of processing methods are provided to supplement those found in the manuscript. Additional quality control 'QC' measures are suggested to ensure comparable product is extracted. While not addressed in the body of the text investigators may benefit from use of thermogravimetric analysis (TGA) and a particle counter to characterize the Fe-NM precipitate. Additionally, post-hoc measurements beyond the WST-1 values described could include picogreen quantification of the extracted genomic DNA following collection of measurements.

4.2. Supporting Electrophysiological Data and Challenges

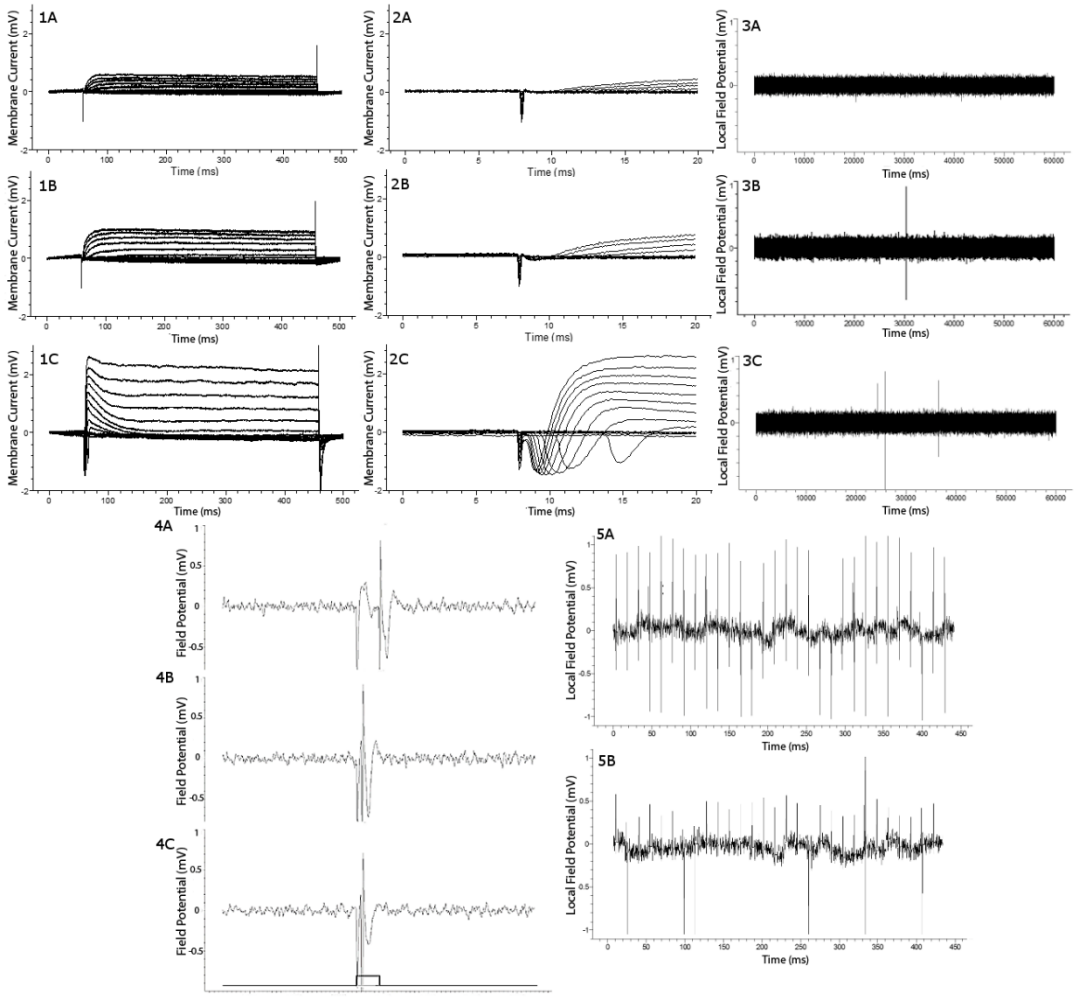

Figure 4.2 Additional Electrophysiology

(1A) Undifferentiated LUHMES patch clamp, (1B) Differentiated LUHMES patch clamp, (1C) Rat cortical neurons patch clamp, (2A) Undifferentiated LUHMES inward voltage gated channels (2B) Differentiated LUHMES inward voltage gated channels (2C) Rat cortical neurons inward voltage gated channels (3A) Undifferentiated LUHMES Local Field Potential Measurements (2 weeks), (3B) Differentiated LUHMES Local Field Potential Measurements (2 weeks), (3C) Rat cortical neurons Local Field Potential Measurements (2 weeks), (4A) 20V 5 mSec evoked Stimulus evoked action potential on LFP, (4B) 20V 1 mSec evoked Stimulus evoked action potential on LFP, (4C) 20V 1 mSec evoked Stimulus blunted with Tetrodotoxin a voltage gated sodium channel blocker, (5A) Evoked Local Field Potential on silk sponge, (5B) Evoked Local Field Potential on neuromelanin silk sponge.

The LUHMES cell line was found to be challenging to patch in 2D due to shearing from glass slides and sustained exposure to tetracycline. While the cells proliferate and differentiate in 3D investigators are encouraged consider other cell models if they wish to correlate against 2D patch results and have cultures beyond ~4 weeks.

4.3. Markers of Interest for PD Investigators

Tier	Approach	Means of Analysis	Anticipated Functional Outcome
1 Validation	Confocal Imaging	Immunostaining	Neuronal: ↓Beta-tubulin: Network Degradation; Loss of connectivity
			Dopaminergic: ↑TH&DRD2: Dopaminergic phenotype; NT Production
			Synaptic: ↓Synaptophysin; Gephyrin; PSD-95
			Stemness: ↓SOX2, ↓KLF4, ↓TERT,
		Real-Time Cell Viability	Fluo-4: ↑ Synchronous behavior;
			FM-143: ↓ Synaptic uptake; ↓vesicular release
			JC-1 & Mitotracker: ↓Mitochondrial voltage marker
	Neurotransmit. production	EC-HPLC	Dopamine Derivatives & Catacholamine: ↓DA, ↓NEPI, ↓EPI, ↑5HT, ↑5HIAA, ↑HVA, ↑DOPAC
		LC-MS/MS	Excitation/Inhibiton: ↓GABA, ↑L-glutamate
	Electrophysiol.	Local Field potential	Neural Activity: ↑ Spontaneous action potential
		Patch Clamp	Voltage gated channels:↑Inward voltage gated channels
Tier	Approach	Means of Analysis	Functional Outcome
2 Phenotypic Disease	Proteomics	ELISA Assay	↑ protein turnover (ubiquitination); ↑Genomic instability of histone modification (H2AX); ↑Increase in aggregates (α-Synuclein)
		Western Blotting	↑inflammation markers (iNOS, CD-11b); ↑Mitochondrial proteins implicit in apoptosis
		Mass Spec	↑ enzymatically degraded oligomers (i.e. α-Synuclein; & Tau)
	Expression Profile & Epigenetics	RT-PCR	RNA Profile↓tyrosine hydroxylase (TH), ↑monoamine oxidase (MAO), ↑catachol-o-methyltransferase (COMT) ↑ alpha syn ↑iNOS, ↑TGF-beta, ↑SOD-1, ↑Catalase, ↓TNF-A, ↓GSH
		Genomic Methylation	Methylation:↓ASYN, ↑SYN, ↓TH, ↓VMAT, ↑DAT
	Metabolic Assays	WST-1 Assay	general cell metabolism: Production of NADH
		Cell Meter (Nitric Oxide)	Oxidation: Colorimetric nitric oxide plate reader assay
		GSH-Glo (Glutathione)	ROS Scavenging: Compensatory increase/decrease in cell antioxidants to free radicals relative to exposure
Tier	Approach	Means of Analysis	Functional Outcome
3 Tertiary Markers	Electrophysiol.	Carbon Fiber Amperometry	Substantiate electrical properties of synaptic release
		Local Field Potential	↓Spontaneous action potential
		Patch Clamp	↓Inward voltage gated channels
	Metabolic Assays	Lactate Dehydrogenase	↑Lactate Dehydrogenase; ↑anoxia, ↑oxidative damage
		Thioredoxin reductase	↑Glycogen Synthase Kinase 3-beta activity assay
	Expression Profile	RT-PCR	Vessicle Synthesis: ↑DAT, ↓VMAT, ↑SERT, ↑SNAP-25
			Cell Survival: ↓SOX2, ↓KLF4, ↓TERT, ↓LRRK2

Table 4.1 Experimental Variables of Interest to the 3D Neuromelanin Model

The above table was intended as a guide to validate the phenotype and then progress into markers of the PD disease state. Redundnancies in (1) proteomics (2) RT-PCR (3) electrophysiology and (4) metabolic assay validation are provided to ensure that no false positive results would be reported. The complexity of PD is far more elaborate than the mechanisms described here and in the interest of aiding other researchers

4.4. Preliminary Evidence of Neuroinflammation and Apoptosis in Microglia & Astrocytes

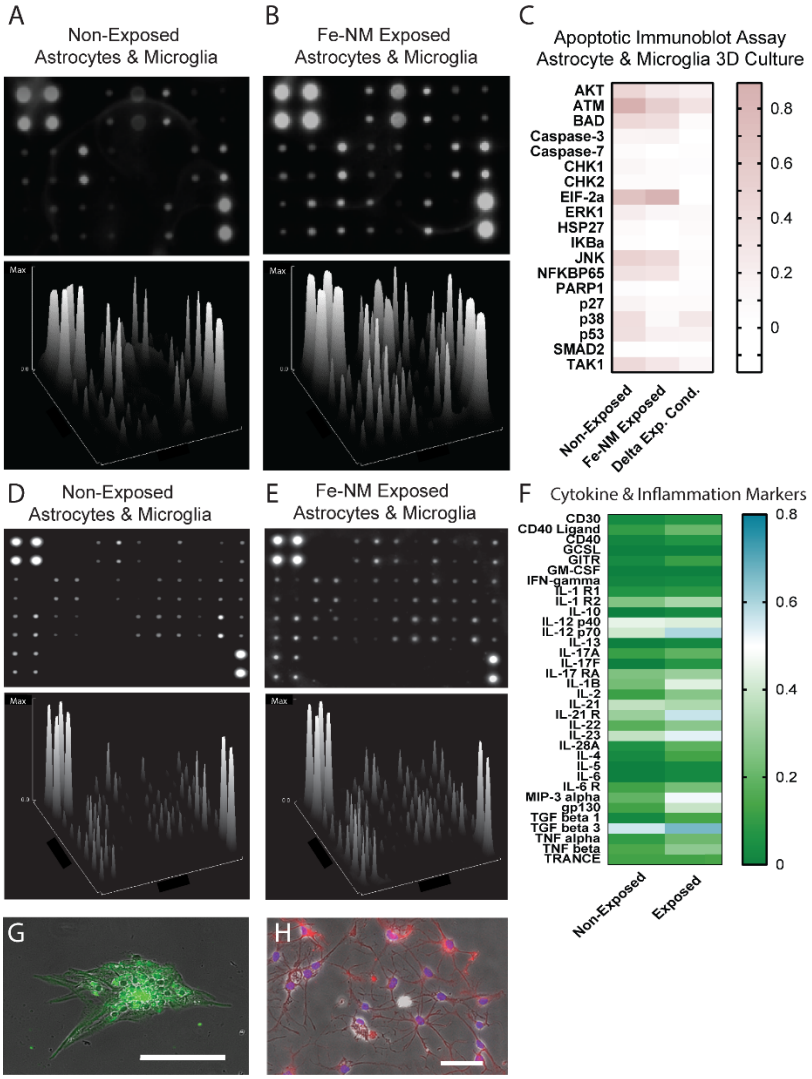

Figure 4.3 Modelling of NeuroInflammatory Response

Combined 3D cultures of Astrocytes and Microglia were exposed to either vehicle or 50 uG of the Fe-NM precipitate. Replicates of each biomarker were provided according to the map provided by the supplier (A-B). The provided immunoblot assays were quantified by electrochemical luminescence (ECl) normalized and quantified with by spectral density using Image-J. The positive control served as the metric against which blots were measured and quantified by a heat map as a basis of comparison (C). Additional markers of cytotoxicity would include inflammatory cytokines in presence and absence of the Fe-NM precipitate. An immuno-array of established inflammatory cytokines was prepared to compare (F) Non-Exposed and (G) Exposed Astrocyte and microglial cultures to establish which cytokines appear increased in presence of the irritant (Figure G). Lastly evidence of S-nitrosylated proteins (G) can be observed as well as positive immunostaining for (H) nitric oxide synthetase (iNOS red) from concurrent 2D studies.

4.5. Schematic of Integrated Neuro-Inflammation and Free Radicals in PD

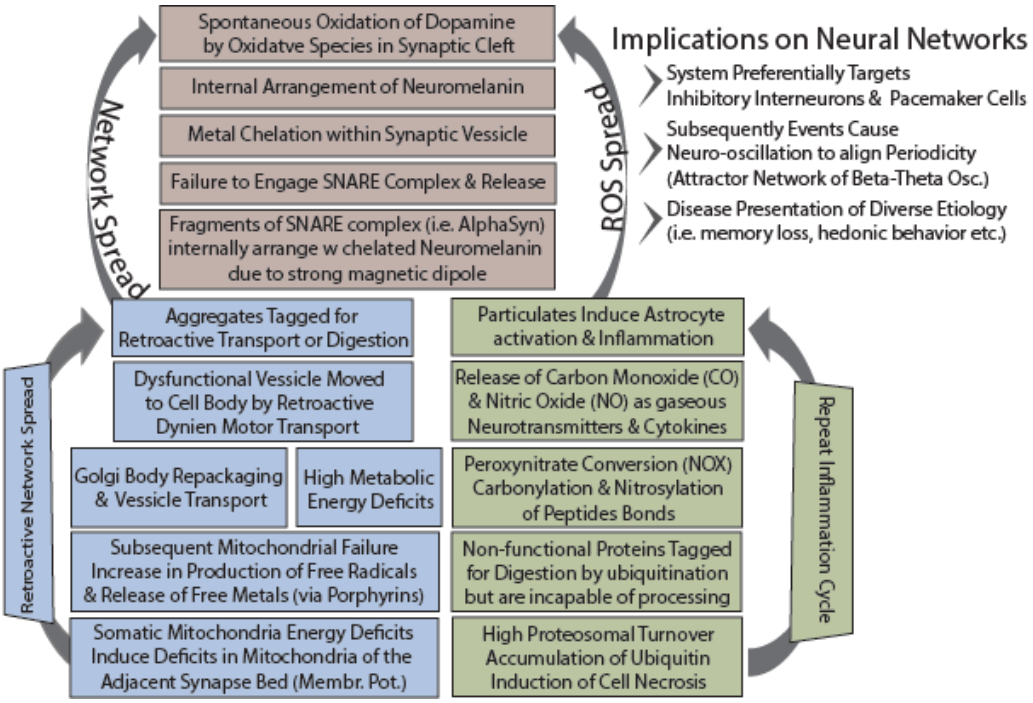

Figure 4.4 Collective Role of Neuroinflammation and Free Radicals on Parkinson's

In the above interpretation the etiology of PD involves multiple factors to facilitate retroactive spread. Above the hypothesized mechanism of PD as it relates to NM and Fe-NM is shown comprising of (1) Retroactive spread, movement of dysfunctional synaptic vesicles to the Golgi; (2) Persistent Neuro-inflammation as the result of inclusion bodies causing foreign body response by nitric oxide and 'respiratory burst' (release of free radicals). (3) These oxidized products result in proteins which are otherwise become incorporated into the proteome.

4.6. High-Throughput Application Guidance for Future Studies

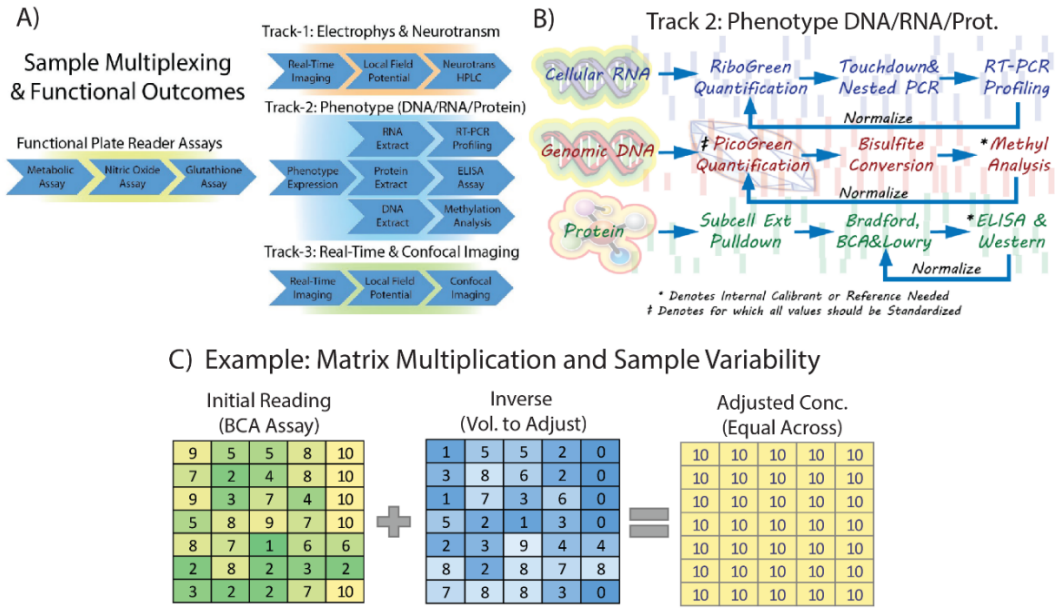

Figure 4.5 Schematic Diagram of Data-Multiplexing

(A) A sample can be processed along several tracks and (B) then readjusted to account for differences between samples. Assuming an array of samples readings all values can be adjusted using matrix multiplication to account for variability between samples. Simple ‘matrix multiplication’ would allow for adjusting all values in a 96 well plate if spectral measurements were treated as an <array> (C).

Biological systems are inherently difficult to characterize, minor variations in the parameters of (1) seeding density (2) silk sponge surface area and (3) cell survival can contribute to sample variability over time. Variability between samples would require normalization against a known internal calibrant and method file development such that other research groups could replicate results with ease. Furthermore, to emphasize the need for greater statistical significance the potential for high-throughput extraction is vital. It was found that flash-freezing and lyophilization of silk scaffolds greatly enhance the yields of retrieval towards a high-throughput processing. The Opentrons lab robotics platform was intended to be the basis for these preliminary experiments regarding multiplexing sample analysis and was intended to transition to high-throughput applications.

4.7. Ferric/Ferrous Iron Ratios in Relation to NM

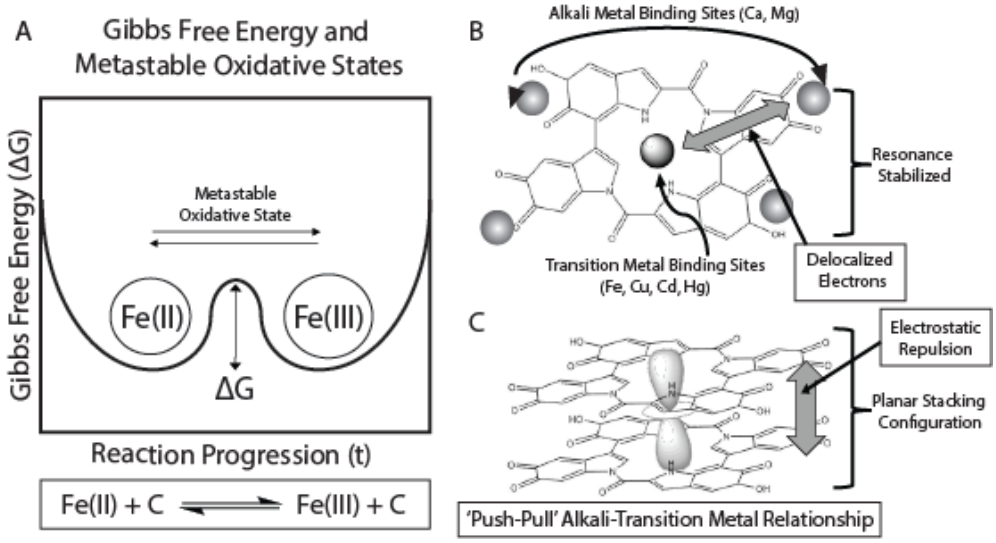

Figure 4.6 Gibbs Free-Energy Diagram of NM Molecular Configuration

(A) In a hypothetical example if the transition between oxidative states of iron were to be low enough it would facilitate exchange between the two oxidative states (B) The carboxyl groups which make up the exterior of the DHI:DHICA molecule would likely destabilize the resonance structure of the molecule (C) Lastly, electrostatic repulsion between the 'stacked planar configuration' would result in a continuously unstable structural orientation. Adapted with permission from: Phys. Rev. Lett. 97. Kaxiras, E., Tsolakidis, A., Zonios, G. and Meng, S., Structural Model of Eumelanin, (2006) [10]. Changes included redrawing of the molecule and overlay of arrows and circles.

The oscillatory phenomena of transition metals is additionally observed on an inorganic basis most notably in the Belousov–Zhabotinsky (BZ) and Briggs-Rauscher reaction (BR) reactions [285] commonly visualized with the change in oxidative state of chemical marker Ferroin. The aforementioned chemical oscillators require a transition metal catalyst (Mn, Fe, Cu, Cr, Co) which serves as a catalyst for the colorimetric changes observed. Coincidentally, many of the aforementioned transition metals are established neurotoxins at the synaptic bed [49] are chelated by neuromelanin [39] are implicated in Parkinson's disease [200, 286] and catalysis of alpha-synuclein aggregation [287, 288]. Transition metals in a 'metastable' oxidative state like the BZ reactions comprise a niche of reactions which act as harmonic oscillators between energetic states. Amplification of the chemical oscillators results in broad disturbance to the surrounding magnetic field by proximity. Changes in the oxidative state of the Fe-NM precipitate would alter the firing behaviors of surrounding neurons. A supplemental video of the Fe-NM behavior in solution has been provided to underscore the proposed electrostatic repulsion.

Chapter 5. Bibliography

1. Tang-Schomer, M.D., J.D. White, L.W. Tien, L.I. Schmitt, T.M. Valentin, D.J. Graziano, A.M. Hopkins, F.G. Omenetto, P.G. Haydon and D.L. Kaplan, *Bioengineered functional brain-like cortical tissue.* Proceedings of the National Academy of Sciences, 2014. **111**(38): p. 13811-13816.
2. Chwalek, K., M.D. Tang-Schomer, F.G. Omenetto and D.L. Kaplan, *In vitro bioengineered model of cortical brain tissue.* Nature protocols, 2015. **10**(9): p. 1362.
3. Sood, D., K. Chwalek, E. Stuntz, D. Pouli, C. Du, M. Tang-Schomer, I. Georgakoudi, L.D. Black III and D.L. Kaplan, *Fetal brain extracellular matrix boosts neuronal network formation in 3D bioengineered model of cortical brain tissue.* ACS biomaterials science & engineering, 2015. **2**(1): p. 131-140.
4. Usunoff, K., D. Itzev, W. Ovtscharoff and E. Marani, *Neuromelanin in the human brain: a review and atlas of pigmented cells in the substantia nigra.* Archives of physiology and biochemistry, 2002. **110**(4): p. 257-369.
5. Ito, S. and K. Wakamatsu, *Chemistry of mixed melanogenesis—pivotal roles of dopaquinone.* Photochemistry and photobiology, 2008. **84**(3): p. 582-592.
6. Zecca, L., C. Bellei, P. Costi, A. Albertini, E. Monzani, L. Casella, M. Gallorini, L. Bergamaschi, A. Moscatelli and N.J. Turro, *New melanic pigments in the human brain that accumulate in aging and block environmental toxic metals.* Proceedings of the National Academy of Sciences, 2008. **105**(45): p. 17567-17572.
7. Sulzer, D., *α-Synuclein and cytosolic dopamine: stabilizing a bad situation.* Nature medicine, 2001. **7**(12): p. 1280.
8. Napolitano, A., P. Manini and M. d'Ischia, *Oxidation chemistry of catecholamines and neuronal degeneration: an update.* Current medicinal chemistry, 2011. **18**(12): p. 1832-1845.
9. Meng, S. and E. Kaxiras, *Theoretical models of eumelanin protomolecules and their optical properties.* Biophysical journal, 2008. **94**(6): p. 2095-2105.
10. Kaxiras, E., A. Tsolakidis, G. Zonios and S. Meng, *Structural model of eumelanin.* Physical review letters, 2006. **97**(21): p. 218102.
11. Zucca, F.A., E. Basso, F.A. Cupaioli, E. Ferrari, D. Sulzer, L. Casella and L. Zecca, *Neuromelanin of the human substantia nigra: an update.* Neurotoxicity research, 2014. **25**(1): p. 13-23.
12. Meiser, J., D. Weindl and K. Hiller, *Complexity of dopamine metabolism.* Cell Communication and Signaling, 2013. **11**(1): p. 34.
13. Schroeder, R.L., K.L. Double and J.P. Gerber, *Using Sepia melanin as a PD model to describe the binding characteristics of neuromelanin–A critical review.* Journal of chemical neuroanatomy, 2015. **64**: p. 20-32.
14. Kim, S., P.A. Thiessen, E.E. Bolton, J. Chen, G. Fu, A. Gindulyte, L. Han, J. He, S. He and B.A. Shoemaker, *PubChem substance and compound databases.* Nucleic acids research, 2015. **44**(D1): p. D1202-D1213.
15. Zucca, F.A., R. Vanna, F.A. Cupaioli, C. Bellei, A. De Palma, D. Di Silvestre, P. Mauri, S. Grassi, A. Prinetti and L. Casella, *Neuromelanin organelles are specialized autolysosomes that accumulate undegraded proteins and lipids in aging human brain and are likely involved in Parkinson's disease.* npj Parkinson's Disease, 2018. **4**(1): p. 17.
16. Popescu, A., C.F. Lippa, V.M.-Y. Lee and J.Q. Trojanowski, *Lewy bodies in the amygdala: increase of α-synuclein aggregates in neurodegenerative diseases with tau-based inclusions.* Archives of Neurology, 2004. **61**(12): p. 1915-1919.

17. Obeso, J.A., M.C. Rodriguez-Oroz, C.G. Goetz, C. Marin, J.H. Kordower, M. Rodriguez, E.C. Hirsch, M. Farrer, A.H. Schapira and G. Halliday, *Missing pieces in the Parkinson's disease puzzle.* Nature medicine, 2010. **16**(6): p. 653.
18. Olanow, C.W., K. Kieburtz and A.H. Schapira, *Why have we failed to achieve neuroprotection in Parkinson's disease?* Annals of Neurology: Official Journal of the American Neurological Association and the Child Neurology Society, 2008. **64**(S2): p. S101-S110.
19. Pires, A.O., F.G. Teixeira, B. Mendes-Pinheiro, S.C. Serra, N. Sousa and A.J. Salgado, *Old and new challenges in Parkinson's disease therapeutics.* Progress in neurobiology, 2017. **156**: p. 69-89.
20. Harry, G.J. and E. Tiffany-Castiglioni, *Evaluation of neurotoxic potential by use of in vitro systems.* Expert opinion on drug metabolism & toxicology, 2005. **1**(4): p. 701-713.
21. Farrer, M.J., *Genetics of Parkinson disease: paradigm shifts and future prospects.* Nature Reviews Genetics, 2006. **7**(4): p. 306.
22. Schüle, B., R.A.R. Pera and J.W. Langston, *Can cellular models revolutionize drug discovery in Parkinson's disease?* Biochimica et Biophysica Acta (BBA)-Molecular Basis of Disease, 2009. **1792**(11): p. 1043-1051.
23. Pampaloni, F., E.G. Reynaud and E.H. Stelzer, *The third dimension bridges the gap between cell culture and live tissue.* Nature reviews Molecular cell biology, 2007. **8**(10): p. 839.
24. Langston, J.W. and J. Palfreman, *The case of the frozen addicts: How the solution of a medical mystery revolutionized the understanding of Parkinson's disease*. 2013: IOS Press.
25. Olanow, C. and W. Tatton, *Etiology and pathogenesis of Parkinson's disease.* Annual review of neuroscience, 1999. **22**(1): p. 123-144.
26. Dawson, T.M. and V.L. Dawson, *Molecular pathways of neurodegeneration in Parkinson's disease.* Science, 2003. **302**(5646): p. 819-822.
27. Singh, N., S. Haldar, A.K. Tripathi, K. Horback, J. Wong, D. Sharma, A. Beserra, S. Suda, C. Anbalagan and S. Dev, *Brain iron homeostasis: from molecular mechanisms to clinical significance and therapeutic opportunities.* Antioxidants & redox signaling, 2014. **20**(8): p. 1324-1363.
28. Liberatore, G.T., V. Jackson-Lewis, S. Vukosavic, A.S. Mandir, M. Vila, W.G. McAuliffe, V.L. Dawson, T.M. Dawson and S. Przedborski, *Inducible nitric oxide synthase stimulates dopaminergic neurodegeneration in the MPTP model of Parkinson disease.* Nature medicine, 1999. **5**(12): p. 1403.
29. Epstein, L., *Fifty years since silent spring.* Annual review of phytopathology, 2014. **52**: p. 377-402.
30. Bezard, E., Z. Yue, D. Kirik and M.G. Spillantini, *Animal models of Parkinson's disease: limits and relevance to neuroprotection studies.* Movement Disorders, 2013. **28**(1): p. 61-70.
31. Zhang, W., K. Phillips, A.R. Wielgus, J. Liu, A. Albertini, F.A. Zucca, R. Faust, S.Y. Qian, D.S. Miller and C.F. Chignell, *Neuromelanin activates microglia and induces degeneration of dopaminergic neurons: implications for progression of Parkinson's disease.* Neurotoxicity research, 2011. **19**(1): p. 63-72.
32. Plum, S., S. Helling, C. Theiss, R. Leite, C. May, W. Jacob-Filho, M. Eisenacher, K. Kuhlmann, H. Meyer and P. Riederer, *Combined enrichment of neuromelanin granules and synaptosomes from human substantia nigra pars compacta tissue for proteomic analysis.* Journal of proteomics, 2013. **94**: p. 202-206.
33. Zecca, L., M. Gallorini, V. Schünemann, A.X. Trautwein, M. Gerlach, P. Riederer, P. Vezzoni and D. Tampellini, *Iron, neuromelanin and ferritin content in the*

substantia nigra of normal subjects at different ages: consequences for iron storage and neurodegenerative processes. Journal of neurochemistry, 2001. **76**(6): p. 1766-1773.
34. Kalia, L.V., S.K. Kalia and A.E. Lang, *Disease-modifying strategies for Parkinson's disease.* Movement Disorders, 2015. **30**(11): p. 1442-1450.
35. Kobayashi, H., K. Fukuhara, S. Tada-Oikawa, Y. Yada, Y. Hiraku, M. Murata and S. Oikawa, *The mechanisms of oxidative DNA damage and apoptosis induced by norsalsolinol, an endogenous tetrahydroisoquinoline derivative associated with Parkinson's disease.* Journal of neurochemistry, 2009. **108**(2): p. 397-407.
36. Martin, L.J., Y. Pan, A.C. Price, W. Sterling, N.G. Copeland, N.A. Jenkins, D.L. Price and M.K. Lee, *Parkinson's disease α-synuclein transgenic mice develop neuronal mitochondrial degeneration and cell death.* Journal of Neuroscience, 2006. **26**(1): p. 41-50.
37. Samii, A., J.G. Nutt and B.R. Ransom, *Parkinson's disease.* The Lancet, 2004. **363**(9423): p. 1783-1793.
38. Karlsson, O. and N.G. Lindquist, *Melanin and neuromelanin binding of drugs and chemicals: toxicological implications.* Archives of toxicology, 2016. **90**(8): p. 1883-1891.
39. Zecca, L., F.A. Zucca, H. Wilms and D. Sulzer, *Neuromelanin of the substantia nigra: a neuronal black hole with protective and toxic characteristics.* Trends in Neurosciences, 2003. **26**(11): p. 578-580.
40. Hong, L. and J.D. Simon, *Current understanding of the binding sites, capacity, affinity, and biological significance of metals in melanin*. 2007, ACS Publications.
41. Gorell, J., C. Johnson, B. Rybicki, E. Peterson, G. Kortsha, G. Brown and R. Richardson, *Occupational exposure to manganese, copper, lead, iron, mercury and zinc and the risk of Parkinson's disease.* Neurotoxicology, 1999. **20**(2-3): p. 239-247.
42. Ward, R.J., F.A. Zucca, J.H. Duyn, R.R. Crichton and L. Zecca, *The role of iron in brain ageing and neurodegenerative disorders.* The Lancet Neurology, 2014. **13**(10): p. 1045-1060.
43. Gehrmann, J., Y. Matsumoto and G.W. Kreutzberg, *Microglia: intrinsic immuneffector cell of the brain.* Brain Research Reviews, 1995. **20**(3): p. 269-287.
44. Tjälve, H., J. Henriksson, J. Tallkvist, B.S. Larsson and N.G. Lindquist, *Uptake of manganese and cadmium from the nasal mucosa into the central nervous system via olfactory pathways in rats.* Pharmacology & toxicology, 1996. **79**(6): p. 347-356.
45. Sirois, J.E. and W.D. Atchison, *Effects of mercurials on ligand-and voltage-gated ion channels: a review.* Neurotoxicology, 1996. **17**(1): p. 63-84.
46. Das, K., S. Das and S. Dhundasi, *Nickel, its adverse health effects & oxidative stress.* Indian Journal of Medical Research, 2008. **128**(4): p. 412.
47. Dusek, P., P.M. Roos, T. Litwin, S.A. Schneider, T.P. Flaten and J. Aaseth, *The neurotoxicity of iron, copper and manganese in Parkinson's and Wilson's diseases.* Journal of Trace Elements in Medicine and Biology, 2015. **31**: p. 193-203.
48. Sanders, T., Y. Liu, V. Buchner and P.B. Tchounwou, *Neurotoxic effects and biomarkers of lead exposure: a review.* Reviews on environmental health, 2009. **24**(1): p. 15-46.
49. Sadiq, S., Z. Ghazala, A. Chowdhury and D. Büsselberg, *Metal toxicity at the synapse: presynaptic, postsynaptic, and long-term effects.* Journal of toxicology, 2012. **2012**.

50. Klang, I.M., B. Schilling, D.J. Sorensen, A.K. Sahu, P. Kapahi, J.K. Andersen, P. Swoboda, D.W. Killilea, B.W. Gibson and G.J. Lithgow, *Iron promotes protein insolubility and aging in C. elegans.* Aging (Albany NY), 2014. **6**(11): p. 975.
51. Mitra, J., V. Vasquez, P.M. Hegde, I. Boldogh, S. Mitra, T.A. Kent, K.S. Rao and M.L. Hegde, *Revisiting metal toxicity in neurodegenerative diseases and stroke: Therapeutic potential.* Neurological research and therapy, 2014. **1**(2).
52. Hornykiewicz, O., *A brief history of levodopa.* Journal of neurology, 2010. **257**(2): p. 249-252.
53. Knowles, W.S., *Application of organometallic catalysis to the commercial production of L-DOPA.* Journal of Chemical Education, 1986. **63**(3): p. 222.
54. Sacks, O., *Awakenings. 1973.* rev., Nueva York: HarperCollins, 1990.
55. Goetz, C.G., *The history of Parkinson's disease: early clinical descriptions and neurological therapies.* Cold Spring Harbor perspectives in medicine, 2011. **1**(1): p. a008862.
56. Van der Schyf, C.J., *Rational drug discovery design approaches for treating Parkinson's disease.* Expert opinion on drug discovery, 2015. **10**(7): p. 713-741.
57. Mercuri, N.B. and G. Bernardi, *The 'magic'of L-dopa: why is it the gold standard Parkinson's disease therapy?* Trends in pharmacological sciences, 2005. **26**(7): p. 341-344.
58. Pierre, J.M., *Extrapyramidal symptoms with atypical antipsychotics.* Drug safety, 2005. **28**(3): p. 191-208.
59. Ravina, B.M., S. Fagan, R. Hart, C. Hovinga, D. Murphy, T. Dawson and J. Marler, *Neuroprotective agents for clinical trials in Parkinson's disease A systematic assessment.* Neurology, 2003. **60**(8): p. 1234-1240.
60. Ilijic, E., J. Guzman and D. Surmeier, *The L-type channel antagonist isradipine is neuroprotective in a mouse model of Parkinson's disease.* Neurobiology of disease, 2011. **43**(2): p. 364-371.
61. Braak, H., K. Del Tredici, U. Rüb, R.A. De Vos, E.N.J. Steur and E. Braak, *Staging of brain pathology related to sporadic Parkinson's disease.* Neurobiology of aging, 2003. **24**(2): p. 197-211.
62. Marchetti, C., *Interaction of metal ions with neurotransmitter receptors and potential role in neurodiseases.* Biometals, 2014. **27**(6): p. 1097-1113.
63. Sharma, S., C.S. Moon, A. Khogali, A. Haidous, A. Chabenne, C. Ojo, M. Jelebinkov, Y. Kurdi and M. Ebadi, *Biomarkers in Parkinson's disease (recent update).* Neurochemistry international, 2013. **63**(3): p. 201-229.
64. Tjälve, H. and J. Henriksson, *Uptake of metals in the brain via olfactory pathways.* Neurotoxicology, 1999. **20**(2-3): p. 181-195.
65. Weinshenker, D., *Long road to ruin: noradrenergic dysfunction in neurodegenerative disease.* Trends in neurosciences, 2018.
66. Hawkes, C.H., K. Del Tredici and H. Braak, *A timeline for Parkinson's disease.* Parkinsonism & related disorders, 2010. **16**(2): p. 79-84.
67. Braak, H., E. Braak, D. Yilmazer, C. Schultz and E. Jansen, *Nigral and extranigral pathology in Parkinson's disease.* Journal of neural transmission. Supplementum, 1995. **46**: p. 15-31.
68. Witjas, T., C. Baunez, J.M. Henry, M. Delfini, J. Regis, A.A. Cherif, J.C. Peragut and J.P. Azulay, *Addiction in Parkinson's disease: impact of subthalamic nucleus deep brain stimulation.* Movement disorders: official journal of the Movement Disorder Society, 2005. **20**(8): p. 1052-1055.
69. Ramaker, C., J. Marinus, A.M. Stiggelbout and B.J. Van Hilten, *Systematic evaluation of rating scales for impairment and disability in Parkinson's disease.*

Movement disorders: official journal of the Movement Disorder Society, 2002. **17**(5): p. 867-876.
70. Braak, H., E. Ghebremedhin, U. Rüb, H. Bratzke and K. Del Tredici, *Stages in the development of Parkinson's disease-related pathology.* Cell and tissue research, 2004. **318**(1): p. 121-134.
71. Parashar, A. and M. Udayabanu, *Gut microbiota: Implications in Parkinson's disease.* Parkinsonism & related disorders, 2017. **38**: p. 1-7.
72. Visanji, N.P., P.L. Brooks, L.-N. Hazrati and A.E. Lang, *The prion hypothesis in Parkinson's disease: Braak to the future.* Acta neuropathologica communications, 2013. **1**(1): p. 2.
73. Abbott, R.D., G.W. Ross, H. Petrovitch, C.M. Tanner, D.G. Davis, K.H. Masaki, L.J. Launer, J.D. Curb and L.R. White, *Bowel movement frequency in late-life and incidental Lewy bodies.* Movement disorders: official journal of the Movement Disorder Society, 2007. **22**(11): p. 1581-1586.
74. Burke, R.E., W.T. Dauer and J.P.G. Vonsattel, *A critical evaluation of the Braak staging scheme for Parkinson's disease.* Annals of Neurology: Official Journal of the American Neurological Association and the Child Neurology Society, 2008. **64**(5): p. 485-491.
75. Ratheesh, G., L. Tian, J.R. Venugopal, H. Ezhilarasu, A. Sadiq, T.-P. Fan and S. Ramakrishna, *Role of medicinal plants in neurodegenerative diseases.* Biomanufacturing Reviews, 2017. **2**(1): p. 2.
76. Hori, Y., T. Yoshikawa, N. Tsuji, T. Bamba, Y. Aso, M. Kudou, Y. Uchida, M. Takagi, K. Harada and K. Hirata, *Phytochelatins inhibit the metal-induced aggregation of α-crystallin.* Journal of bioscience and bioengineering, 2009. **107**(2): p. 173-176.
77. Van Den Eeden, S.K., C.M. Tanner, A.L. Bernstein, R.D. Fross, A. Leimpeter, D.A. Bloch and L.M. Nelson, *Incidence of Parkinson's disease: variation by age, gender, and race/ethnicity.* American journal of epidemiology, 2003. **157**(11): p. 1015-1022.
78. Ragonese, P., M. D'amelio, G. Callari, G. Salemi, L. Morgante and G. Savettieri, *Age at menopause predicts age at onset of Parkinson's disease.* Movement disorders: official journal of the Movement Disorder Society, 2006. **21**(12): p. 2211-2214.
79. Still, C.N., *Postmenopausal Parkinsonism: brain iron overload?*, in *Parkinson's Disease*. 1977, Springer. p. 291-296.
80. Snyder, A.M. and J.R. Connor, *Iron, the substantia nigra and related neurological disorders.* Biochimica et Biophysica Acta (BBA)-General Subjects, 2009. **1790**(7): p. 606-614.
81. Bae, J.R. and B.D. Lee, *Function and dysfunction of leucine-rich repeat kinase 2 (LRRK2): Parkinson's disease and beyond.* BMB reports, 2015. **48**(5): p. 243.
82. Kubo, S.i., T. Kitami, S. Noda, H. Shimura, Y. Uchiyama, S. Asakawa, S. Minoshima, N. Shimizu, Y. Mizuno and N. Hattori, *Parkin is associated with cellular vesicles.* Journal of neurochemistry, 2001. **78**(1): p. 42-54.
83. Urrutia, P.J., N.P. Mena and M.T. Nunez, *The interplay between iron accumulation, mitochondrial dysfunction, and inflammation during the execution step of neurodegenerative disorders.* Frontiers in pharmacology, 2014. **5**: p. 38.
84. Yang, Y.X., N.W. Wood and D.S. Latchman, *Molecular basis of Parkinson's disease.* Neuroreport, 2009. **20**(2): p. 150-156.
85. Plum, S., S. Steinbach, J. Attems, S. Keers, P. Riederer, M. Gerlach, C. May and K. Marcus, *Proteomic characterization of neuromelanin granules isolated from*

human substantia nigra by laser-microdissection. Scientific reports, 2016. **6**: p. 37139.
86. Guiney, S.J., P.A. Adlard, A.I. Bush, D.I. Finkelstein and S. Ayton, *Ferroptosis and cell death mechanisms in Parkinson's disease.* Neurochemistry international, 2017. **104**: p. 34-48.
87. Do Van, B., F. Gouel, A. Jonneaux, K. Timmerman, P. Gelé, M. Pétrault, M. Bastide, C. Laloux, C. Moreau and R. Bordet, *Ferroptosis, a newly characterized form of cell death in Parkinson's disease that is regulated by PKC.* Neurobiology of disease, 2016. **94**: p. 169-178.
88. van Dijk, K.D., C.E. Teunissen, B. Drukarch, C.R. Jimenez, H.J. Groenewegen, H.W. Berendse and W.D. van de Berg, *Diagnostic cerebrospinal fluid biomarkers for Parkinson's disease: a pathogenetically based approach.* Neurobiology of Disease, 2010. **39**(3): p. 229-241.
89. Mosharov, E.V., A. Borgkvist and D. Sulzer, *Presynaptic effects of levodopa and their possible role in dyskinesia.* Movement Disorders, 2015. **30**(1): p. 45-53.
90. Baker, M., *Reproducibility crisis: Blame it on the antibodies.* Nature News, 2015. **521**(7552): p. 274.
91. Jesse, S., J. Brettschneider, S.D. Süssmuth, B.G. Landwehrmeyer, C.A. Von Arnim, A.C. Ludolph, H. Tumani and M. Otto, *Summary of cerebrospinal fluid routine parameters in neurodegenerative diseases.* Journal of neurology, 2011. **258**(6): p. 1034-1041.
92. Esteves, A., D. Arduino, D. Silva, C. Oliveira and S. Cardoso, *Mitochondrial dysfunction: the road to alpha-synuclein oligomerization in PD.* Parkinson's disease, 2011. **2011**.
93. Chan, C.S., T.S. Gertler and D.J. Surmeier, *A molecular basis for the increased vulnerability of substantia nigra dopamine neurons in aging and Parkinson's disease.* Movement Disorders, 2010. **25**(S1): p. S63-S70.
94. El-Agnaf, O.M., S.A. Salem, K.E. Paleologou, M.D. Curran, M.J. Gibson, J.A. Court, M.G. Schlossmacher and D. Allsop, *Detection of oligomeric forms of α-synuclein protein in human plasma as a potential biomarker for Parkinson's disease.* The FASEB journal, 2006. **20**(3): p. 419-425.
95. Potashkin, J., S. Blume and N. Runkle, *Limitations of animal models of Parkinson's disease.* Parkinson's disease, 2011. **2011**.
96. Gardner, P.R., I. Raineri, L.B. Epstein and C.W. White, *Superoxide radical and iron modulate aconitase activity in mammalian cells.* Journal of Biological Chemistry, 1995. **270**(22): p. 13399-13405.
97. Stadtman, E.R., *Protein oxidation and aging.* Free radical research, 2006. **40**(12): p. 1250-1258.
98. Morgan, J.C., S.H. Mehta and K.D. Sethi, *Biomarkers in Parkinson's disease.* Current neurology and neuroscience reports, 2010. **10**(6): p. 423-430.
99. Miller, D.B. and J.P. O'Callaghan, *Biomarkers of Parkinson's disease: present and future.* Metabolism, 2015. **64**(3): p. S40-S46.
100. Goldstein, D.S., C. Holmes, O. Bentho, T. Sato, J. Moak, Y. Sharabi, R. Imrich, S. Conant and B.A. Eldadah, *Biomarkers to detect central dopamine deficiency and distinguish Parkinson disease from multiple system atrophy.* Parkinsonism & related disorders, 2008. **14**(8): p. 600-607.
101. Shi, M., J. Bradner, A.M. Hancock, K.A. Chung, J.F. Quinn, E.R. Peskind, D. Galasko, J. Jankovic, C.P. Zabetian and H.M. Kim, *Cerebrospinal fluid biomarkers for Parkinson disease diagnosis and progression.* Annals of neurology, 2011. **69**(3): p. 570-580.

102. Dimitrov, J.D., T.L. Vassilev, S. Andre, S.V. Kaveri and S. Lacroix-Desmazes, *Functional variability of antibodies upon oxidative processes.* Autoimmunity reviews, 2008. **7**(7): p. 574-578.
103. Bradbury, A. and A. Pluckthun, *Standardize antibodies used in research: to save millions of dollars and dramatically improve reproducibility, protein-binding reagents must be defined by their sequences and produced as recombinant proteins, say Andrew Bradbury, Andreas Pluckthun and 110 co-signatories.* Nature, 2015. **518**(7537): p. 27-30.
104. Fasano, M., B. Bergamasco and L. Lopiano, *Is neuromelanin changed in Parkinson's disease? Investigations by magnetic spectroscopies.* Journal of neural transmission, 2006. **113**(6): p. 769-774.
105. Zecca, L. and H. Swartz, *Total and paramagnetic metals in human substantia nigra and its neuromelanin.* Journal of Neural Transmission-Parkinson's Disease and Dementia Section, 1993. **5**(3): p. 203-213.
106. Drescher, M., M. Huber and V. Subramaniam, *Hunting the Chameleon: Structural Conformations of the Intrinsically Disordered Protein Alpha-Synuclein.* ChemBioChem, 2012. **13**(6): p. 761-768.
107. Aime, S., B. Bergamasco, D. Biglino, G. Digilio, M. Fasano, E. Giamello and L. Lopiano, *EPR investigations of the iron domain in neuromelanin.* Biochimica et Biophysica Acta (BBA)-Molecular Basis of Disease, 1997. **1361**(1): p. 49-58.
108. Sulzer, D., C. Cassidy, G. Horga, U.J. Kang, S. Fahn, L. Casella, G. Pezzoli, J. Langley, X.P. Hu and F.A. Zucca, *Neuromelanin detection by magnetic resonance imaging (MRI) and its promise as a biomarker for Parkinson's disease.* NPJ Parkinson's disease, 2018. **4**(1): p. 11.
109. Kozlov, A.V., D.Y. Yegorov, Y.A. Vladimirov and O.A. Azizova, *Intracellular free iron in liver tissue and liver homogenate: studies with electron paramagnetic resonance on the formation of paramagnetic complexes with desferal and nitric oxide.* Free Radical Biology and Medicine, 1992. **13**(1): p. 9-16.
110. Nakamura, T., S. Tu, M.W. Akhtar, C.R. Sunico, S.-i. Okamoto and S.A. Lipton, *Aberrant protein s-nitrosylation in neurodegenerative diseases.* Neuron, 2013. **78**(4): p. 596-614.
111. Ottis, P., K. Koppe, B. Onisko, I. Dynin, T. Arzberger, H. Kretzschmar, J.R. Requena, C.J. Silva, J.P. Huston and C. Korth, *Human and rat brain lipofuscin proteome.* Proteomics, 2012. **12**(15-16): p. 2445-2454.
112. Beckman, J.S. and W.H. Koppenol, *Nitric oxide, superoxide, and peroxynitrite: the good, the bad, and ugly.* American Journal of Physiology-Cell Physiology, 1996. **271**(5): p. C1424-C1437.
113. Stadtman, E. and R. Levine, *Free radical-mediated oxidation of free amino acids and amino acid residues in proteins.* Amino acids, 2003. **25**(3-4): p. 207-218.
114. Buzsáki, G. and A. Draguhn, *Neuronal oscillations in cortical networks.* science, 2004. **304**(5679): p. 1926-1929.
115. Esmail, S. and D.E. Linden, *Neural networks and neurofeedback in Parkinson's disease.* Neuroregulation, 2014. **1**(3-4): p. 240.
116. Baker, S.N., *Oscillatory interactions between sensorimotor cortex and the periphery.* Current opinion in neurobiology, 2007. **17**(6): p. 649-655.
117. Du, C., W. Collins, W. Cantley, D. Sood and D.L. Kaplan, *Tutorials for electrophysiological recordings in neuronal tissue engineering.* ACS Biomaterials Science & Engineering, 2017. **3**(10): p. 2235-2246.
118. Milnor, J., *On the concept of attractor: Correction and remarks.* Communications in Mathematical Physics, 1985. **102**(3): p. 517-519.

119. Björklund, L.M., R. Sánchez-Pernaute, S. Chung, T. Andersson, I.Y.C. Chen, K.S.P. McNaught, A.-L. Brownell, B.G. Jenkins, C. Wahlestedt and K.-S. Kim, *Embryonic stem cells develop into functional dopaminergic neurons after transplantation in a Parkinson rat model.* Proceedings of the National Academy of Sciences, 2002. **99**(4): p. 2344-2349.
120. Crapo, P.M., S. Tottey, P.F. Slivka and S.F. Badylak, *Effects of biologic scaffolds on human stem cells and implications for CNS tissue engineering.* Tissue Engineering Part A, 2013. **20**(1-2): p. 313-323.
121. Trounson, A. and C. McDonald, *Stem cell therapies in clinical trials: progress and challenges.* Cell stem cell, 2015. **17**(1): p. 11-22.
122. Edmondson, R., J.J. Broglie, A.F. Adcock and L. Yang, *Three-dimensional cell culture systems and their applications in drug discovery and cell-based biosensors.* Assay and drug development technologies, 2014. **12**(4): p. 207-218.
123. Hopkins, A.M., E. DeSimone, K. Chwalek and D.L. Kaplan, *3D in vitro modeling of the central nervous system.* Progress in neurobiology, 2015. **125**: p. 1-25.
124. Lin, Q., H.L. Wong, F.-R. Tian, Y.-D. Huang, J. Xu, J.-J. Yang, P.-P. Chen, Z.-L. Fan, C.-T. Lu and Y.-Z. Zhao, *Enhanced neuroprotection with decellularized brain extracellular matrix containing bFGF after intracerebral transplantation in Parkinson's disease rat model.* International journal of pharmaceutics, 2017. **517**(1-2): p. 383-394.
125. Toledo, E.M., D. Gyllborg and E. Arenas, *Translation of WNT developmental programs into stem cell replacement strategies for the treatment of Parkinson's disease.* British journal of pharmacology, 2017. **174**(24): p. 4716-4724.
126. Moriarty, N., C.L. Parish and E. Dowd, *Primary tissue for cellular brain repair in Parkinson's disease: Promise, problems and the potential of biomaterials.* European Journal of Neuroscience, 2018.
127. Kundu, B., R. Rajkhowa, S.C. Kundu and X. Wang, *Silk fibroin biomaterials for tissue regenerations.* Advanced drug delivery reviews, 2013. **65**(4): p. 457-470.
128. Omenetto, F.G. and D.L. Kaplan, *New opportunities for an ancient material.* Science, 2010. **329**(5991): p. 528-531.
129. Guo, X., S. Chen, Y. Hu, G. Li, N. Liao, X. Ye, D. Liu and C. Xue, *Preparation of water-soluble melanin from squid ink using ultrasound-assisted degradation and its anti-oxidant activity.* Journal of food science and technology, 2014. **51**(12): p. 3680-3690.
130. Scholz, D., D. Pöltl, A. Genewsky, M. Weng, T. Waldmann, S. Schildknecht and M. Leist, *Rapid, complete and large-scale generation of post-mitotic neurons from the human LUHMES cell line.* Journal of neurochemistry, 2011. **119**(5): p. 957-971.
131. Al-Hilaly, Y.K., L. Biasetti, B.J. Blakeman, S.J. Pollack, S. Zibaee, A. Abdul-Sada, J.R. Thorpe, W.-F. Xue and L.C. Serpell, *The involvement of dityrosine crosslinking in α-synuclein assembly and deposition in Lewy Bodies in Parkinson's disease.* Scientific reports, 2016. **6**: p. 39171.
132. Viceconte, N., M.A. Burguillos, A.J. Herrera, R.M. De Pablos, B. Joseph and J.L. Venero, *Neuromelanin activates proinflammatory microglia through a caspase-8-dependent mechanism.* Journal of neuroinflammation, 2015. **12**(1): p. 5.
133. Liebscher, J.r., R. Mrówczyński, H.A. Scheidt, C. Filip, N.D. Hădade, R. Turcu, A. Bende and S. Beck, *Structure of polydopamine: a never-ending story?* Langmuir, 2013. **29**(33): p. 10539-10548.
134. Ward, R.J., F.A. Zucca, J.H. Duyn, R.R. Crichton and L. Zecca, *The role of iron in brain ageing and neurodegenerative disorders.* Lancet Neurol, 2014. **13**(10): p. 1045-60.

135. Karlsson, O. and N.G. Lindquist, *Melanin and neuromelanin binding of drugs and chemicals: toxicological implications.* Arch Toxicol, 2016. **90**(8): p. 1883-91.
136. Ambrico, M., P. Ambrico, A. Cardone, T. Ligonzo, S. Cicco, A. Lavizzera, V. Augelli and G. Farinola, *Progress towards melanin integration in bio-inspired devices.* MRS Online Proceedings Library Archive, 2012. **1467**.
137. Fedorow, H., F. Tribl, G. Halliday, M. Gerlach, P. Riederer and K.L. Double, *Neuromelanin in human dopamine neurons: comparison with peripheral melanins and relevance to Parkinson's disease.* Prog Neurobiol, 2005. **75**(2): p. 109-24.
138. Liu, Y., L. Hong, V.R. Kempf, K. Wakamatsu, S. Ito and J.D. Simon, *Ion-exchange and adsorption of Fe(III) by Sepia melanin.* Pigment Cell Res, 2004. **17**(3): p. 262-9.
139. Madaras, F., J.P. Gerber, F. Peddie and M.J. Kokkinn, *The effect of sampling methods on the apparent constituents of ink from the squid Sepioteuthis australis.* J Chem Ecol, 2010. **36**(11): p. 1171-9.
140. Rockwood, D.N., R.C. Preda, T. Yucel, X. Wang, M.L. Lovett and D.L. Kaplan, *Materials fabrication from Bombyx mori silk fibroin.* Nat Protoc, 2011. **6**(10): p. 1612-31.
141. Hopkins, A.M., E. DeSimone, K. Chwalek and D.L. Kaplan, *3D in vitro modeling of the central nervous system.* Prog Neurobiol, 2015. **125**: p. 1-25.
142. Sood, D., K. Chwalek, E. Stuntz, D. Pouli, C. Du, M. Tang-Schomer, I. Georgakoudi, L.D. Black, 3rd and D.L. Kaplan, *Fetal brain extracellular matrix boosts neuronal network formation in 3D bioengineered model of cortical brain tissue.* ACS Biomater Sci Eng, 2016. **2**(1): p. 131-140.
143. Tang-Schomer, M.D., J.D. White, L.W. Tien, L.I. Schmitt, T.M. Valentin, D.J. Graziano, A.M. Hopkins, F.G. Omenetto, P.G. Haydon and D.L. Kaplan, *Bioengineered functional brain-like cortical tissue.* Proc Natl Acad Sci U S A, 2014. **111**(38): p. 13811-6.
144. Chwalek, K., M.D. Tang-Schomer, F.G. Omenetto and D.L. Kaplan, *In vitro bioengineered model of cortical brain tissue.* Nat Protoc, 2015. **10**(9): p. 1362-73.
145. Schildknecht, S., C. Karreman, D. Poltl, L. Efremova, C. Kullmann, S. Gutbier, A. Krug, D. Scholz, H.R. Gerding and M. Leist, *Generation of genetically-modified human differentiated cells for toxicological tests and the study of neurodegenerative diseases.* ALTEX, 2013. **30**(4): p. 427-44.
146. Lotharius, J., S. Barg, P. Wiekop, C. Lundberg, H.K. Raymon and P. Brundin, *Effect of mutant α-synuclein on dopamine homeostasis in a new human mesencephalic cell line.* Journal of Biological Chemistry, 2002. **277**(41): p. 38884-38894.
147. Smirnova, L., G. Harris, J. Delp, M. Valadares, D. Pamies, H.T. Hogberg, T. Waldmann, M. Leist and T. Hartung, *A LUHMES 3D dopaminergic neuronal model for neurotoxicity testing allowing long-term exposure and cellular resilience analysis.* Archives of toxicology, 2016. **90**(11): p. 2725-2743.
148. Smirnova, L., H.T. Hogberg, M. Leist and T. Hartung, *Food for Thought…: Developmental Neurotoxicity–Challenges in the 21st Century and In Vitro Opportunities.* Altex, 2014. **31**(2): p. 129.
149. Dexter, D.T., A. Carayon, F. Javoy-Agid, Y. Agid, F.R. Wells, S.E. Daniel, A.J. Lees, P. Jenner and C.D. Marsden, *Alterations in the levels of iron, ferritin and other trace metals in Parkinson's disease and other neurodegenerative diseases affecting the basal ganglia.* Brain, 1991. **114 (Pt 4)**(4): p. 1953-75.
150. Ju, K.-Y., Y. Lee, S. Lee, S.B. Park and J.-K. Lee, *Bioinspired polymerization of dopamine to generate melanin-like nanoparticles having an excellent free-radical-scavenging property.* Biomacromolecules, 2011. **12**(3): p. 625-632.

151. Wakamatsu, K., T. Murase, F.A. Zucca, L. Zecca and S. Ito, *Biosynthetic pathway to neuromelanin and its aging process.* Pigment Cell Melanoma Res, 2012. **25**(6): p. 792-803.
152. Giasson, B.I. and V.M. Lee, *Are ubiquitination pathways central to Parkinson's disease?* Cell, 2003. **114**(1): p. 1-8.
153. Gu, Z., T. Nakamura, D. Yao, Z. Shi and S. Lipton, *Nitrosative and oxidative stress links dysfunctional ubiquitination to Parkinson's disease*. 2005, Nature Publishing Group.
154. Pompella, A., A. Visvikis, A. Paolicchi, V. De Tata and A.F. Casini, *The changing faces of glutathione, a cellular protagonist.* Biochem Pharmacol, 2003. **66**(8): p. 1499-503.
155. Rockwood, D.N., R.C. Preda, T. Yücel, X. Wang, M.L. Lovett and D.L. Kaplan, *Materials fabrication from Bombyx mori silk fibroin.* Nature protocols, 2011. **6**(10): p. 1612.
156. Chida, J., K. Yamane, T. Takei and H. Kido, *An efficient extraction method for quantitation of adenosine triphosphate in mammalian tissues and cells.* Analytica chimica acta, 2012. **727**: p. 8-12.
157. Liu, Y., L. Hong, V.R. Kempf, K. Wakamatsu, S. Ito and J.D. Simon, *Ion-exchange and adsorption of Fe (III) by Sepia melanin.* Pigment cell research, 2004. **17**(3): p. 262-269.
158. Sulzer, D., *Multiple hit hypotheses for dopamine neuron loss in Parkinson's disease.* Trends in neurosciences, 2007. **30**(5): p. 244-250.
159. Cole, N., *Metal Catalyzed Oxidation of Alpha-Synuclein-A Role for Oligomerization in Pathology?* Current Alzheimer Research, 2008. **5**(6): p. 599-606.
160. Winner, B., R. Jappelli, S.K. Maji, P.A. Desplats, L. Boyer, S. Aigner, C. Hetzer, T. Loher, M. Vilar and S. Campioni, *In vivo demonstration that α-synuclein oligomers are toxic.* Proceedings of the National Academy of Sciences, 2011. **108**(10): p. 4194-4199.
161. Hirschmann, J., T.E. Özkurt, M. Butz, M. Homburger, S. Elben, C. Hartmann, J. Vesper, L. Wojtecki and A. Schnitzler, *Distinct oscillatory STN-cortical loops revealed by simultaneous MEG and local field potential recordings in patients with Parkinson's disease.* Neuroimage, 2011. **55**(3): p. 1159-1168.
162. Bettinger, C.J., J.P. Bruggeman, A. Misra, J.T. Borenstein and R. Langer, *Biocompatibility of biodegradable semiconducting melanin films for nerve tissue engineering.* Biomaterials, 2009. **30**(17): p. 3050-3057.
163. Zhang, L., G. Yagnik, Y. Peng, J. Wang, H.H. Xu, Y. Hao, Y.-N. Liu and F. Zhou, *Kinetic studies of inhibition of the amyloid beta (1–42) aggregation using a ferrocene-tagged β-sheet breaker peptide.* Analytical biochemistry, 2013. **434**(2): p. 292-299.
164. Dong, H., W. Song, C. Wang, C. Mu and R. Li, *Effects of melanin from Sepiella Maindroni ink (MSMI) on the intestinal Microbiome of mice.* BMC microbiology, 2017. **17**(1): p. 147.
165. Streit, W.J., *Microglial senescence: does the brain's immune system have an expiration date?* Trends in neurosciences, 2006. **29**(9): p. 506-510.
166. Gröber, U., J. Schmidt and K. Kisters, *Magnesium in prevention and therapy.* Nutrients, 2015. **7**(9): p. 8199-8226.
167. Pompella, A., A. Visvikis, A. Paolicchi, V. De Tata and A.F. Casini, *The changing faces of glutathione, a cellular protagonist.* Biochemical pharmacology, 2003. **66**(8): p. 1499-1503.

168. Liddell, J.R. and A.R. White, *Nexus between mitochondrial function, iron, copper and glutathione in Parkinson's disease.* Neurochemistry international, 2017.
169. Dalle-Donne, I., G. Aldini, M. Carini, R. Colombo, R. Rossi and A. Milzani, *Protein carbonylation, cellular dysfunction, and disease progression.* Journal of cellular and molecular medicine, 2006. **10**(2): p. 389-406.
170. Brettschneider, J., K. Del Tredici, V.M.-Y. Lee and J.Q. Trojanowski, *Spreading of pathology in neurodegenerative diseases: a focus on human studies.* Nature Reviews Neuroscience, 2015. **16**(2): p. 109.
171. Spandidos, A., X. Wang, H. Wang and B. Seed, *PrimerBank: a resource of human and mouse PCR primer pairs for gene expression detection and quantification.* Nucleic Acids Res, 2010. **38**(Database issue): p. D792-9.
172. Glass, D.J., *Experimental design for biologists*. 2014: Cold Spring Harbor Laboratory Press Cold Spring Harbour, NY, USA.
173. Baker, M., *Reproducibility crisis: Blame it on the antibodies.* Nature, 2015. **521**(7552): p. 274-6.
174. Baker, M., *1,500 scientists lift the lid on reproducibility.* Nature, 2016. **533**(7604): p. 452-4.
175. Liddell, J.R. and A.R. White, *Nexus between mitochondrial function, iron, copper and glutathione in Parkinson's disease.* Neurochemistry international, 2018. **117**: p. 126-138.
176. Robertson, D., *Proposed biochemistry of Parkinson's and Alzheimer's diseases.* Medical hypotheses, 2017. **109**: p. 131-138.
177. Sheng, Z.H., *The Interplay of Axonal Energy Homeostasis and Mitochondrial Trafficking and Anchoring.* Trends Cell Biol, 2017. **27**(6): p. 403-416.
178. Fernández, E., *Biomarkers of Oxidative Stress in Parkinson's Disease*, in *Oxidative Stress and Redox Signalling in Parkinson's Disease*. 2017. p. 423-446.
179. Dalle-Donne, I., G. Aldini, M. Carini, R. Colombo, R. Rossi and A. Milzani, *Protein carbonylation, cellular dysfunction, and disease progression.* J Cell Mol Med, 2006. **10**(2): p. 389-406.
180. Arslan-Yildiz, A., R. El Assal, P. Chen, S. Guven, F. Inci and U. Demirci, *Towards artificial tissue models: past, present, and future of 3D bioprinting.* Biofabrication, 2016. **8**(1): p. 014103.
181. Daviaud, N., E. Garbayo, N. Lautram, F. Franconi, L. Lemaire, M. Perez-Pinzon and C. Montero-Menei, *Modeling nigrostriatal degeneration in organotypic cultures, a new ex vivo model of Parkinson's disease.* Neuroscience, 2014. **256**: p. 10-22.
182. Lu, X., J.S. Kim-Han, K.L. O'Malley and S.E. Sakiyama-Elbert, *A microdevice platform for visualizing mitochondrial transport in aligned dopaminergic axons.* J Neurosci Methods, 2012. **209**(1): p. 35-9.
183. O'Rourke, C., C. Lee-Reeves, R.A. Drake, G.W. Cameron, A.J. Loughlin and J.B. Phillips, *Adapting tissue-engineered in vitro CNS models for high-throughput study of neurodegeneration.* Journal of tissue engineering, 2017. **8**: p. 2041731417697920.
184. Struzyna, L.A., K.D. Browne, Z.D. Brodnik, J.C. Burrell, J.P. Harris, H.I. Chen, J.A. Wolf, K.V. Panzer, J. Lim, J.E. Duda, R.A. Espana and D.K. Cullen, *Tissue engineered nigrostriatal pathway for treatment of Parkinson's disease.* J Tissue Eng Regen Med, 2018. **12**(7): p. 1702-1716.
185. Zhuang, P., A.X. Sun, J. An, C.K. Chua and S.Y. Chew, *3D neural tissue models: From spheroids to bioprinting.* Biomaterials, 2018. **154**: p. 113-133.

186. Liebscher, J., R. Mrowczynski, H.A. Scheidt, C. Filip, N.D. Hadade, R. Turcu, A. Bende and S. Beck, *Structure of polydopamine: a never-ending story?* Langmuir, 2013. **29**(33): p. 10539-48.
187. Klosterman, L., J.K. Riley and C.J. Bettinger, *Control of heterogeneous nucleation and growth kinetics of dopamine-melanin by altering substrate chemistry.* Langmuir, 2015. **31**(11): p. 3451-3458.
188. d'Ischia, M., A. Napolitano, V. Ball, C.-T. Chen and M.J. Buehler, *Polydopamine and eumelanin: From structure–property relationships to a unified tailoring strategy.* Accounts of chemical research, 2014. **47**(12): p. 3541-3550.
189. Bartholomew, C.H., *Mechanisms of catalyst deactivation.* Applied Catalysis A: General, 2001. **212**(1-2): p. 17-60.
190. Ito, S., *A chemist's view of melanogenesis.* Pigment cell research, 2003. **16**(3): p. 230-236.
191. Benfenati, V., S. Toffanin, R. Capelli, L.M. Camassa, S. Ferroni, D.L. Kaplan, F.G. Omenetto, M. Muccini and R. Zamboni, *A silk platform that enables electrophysiology and targeted drug delivery in brain astroglial cells.* Biomaterials, 2010. **31**(31): p. 7883-7891.
192. Lill, R. and U. Mühlenhoff, *Iron–sulfur-protein biogenesis in eukaryotes.* Trends in biochemical sciences, 2005. **30**(3): p. 133-141.
193. Zucca, F., C. Bellei, S. Giannelli, M. Terreni, M. Gallorini, E. Rizzio, G. Pezzoli, A. Albertini and L. Zecca, *Neuromelanin and iron in human locus coeruleus and substantia nigra during aging: consequences for neuronal vulnerability.* Journal of neural transmission, 2006. **113**(6): p. 757-767.
194. Efremova, L., S. Schildknecht, M. Adam, R. Pape, S. Gutbier, B. Hanf, A. Bürkle and M. Leist, *Prevention of the degeneration of human dopaminergic neurons in an astrocyte co-culture system allowing endogenous drug metabolism.* British journal of Pharmacology, 2015. **172**(16): p. 4119-4132.
195. Ali, I., T. Khan and S. Omanovic, *Direct electrochemical regeneration of the cofactor NADH on bare Ti, Ni, Co and Cd electrodes: the influence of electrode potential and electrode material.* Journal of Molecular Catalysis A: Chemical, 2014. **387**: p. 86-91.
196. Ramsey, A.J., P.J. Hillas and P.F. Fitzpatrick, *Characterization of the active site iron in tyrosine hydroxylase redox states of the iron.* Journal of Biological Chemistry, 1996. **271**(40): p. 24395-24400.
197. Belmonte, L. and S.S. Mansy, *Metal catalysts and the origin of life.* Elements, 2016. **12**(6): p. 413-418.
198. Neumann, M., *The pathological mechanisms leading to neurodegeneration and cell death in frontotemporal dementia.* Alzheimer's & Dementia: The Journal of the Alzheimer's Association, 2011. **7**(4): p. S805.
199. Pissadaki, E.K. and J.P. Bolam, *The energy cost of action potential propagation in dopamine neurons: clues to susceptibility in Parkinson's disease.* Frontiers in computational neuroscience, 2013. **7**: p. 13.
200. Dexter, D., A. Carayon, F. Javoy-Agid, Y. Agid, F. Wells, S. Daniel, A. Lees, P. Jenner and C. Marsden, *Alterations in the levels of iron, ferritin and other trace metals in Parkinson's disease and other neurodegenerative diseases affecting the basal ganglia.* Brain, 1991. **114**(4): p. 1953-1975.
201. Humphries, M.D., J.A. Obeso and J.K. Dreyer, *Insights into Parkinson's disease from computational models of the basal ganglia.* J Neurol Neurosurg Psychiatry, 2018: p. jnnp-2017-315922.
202. Hutchison, W.D., J.O. Dostrovsky, J.R. Walters, R. Courtemanche, T. Boraud, J. Goldberg and P. Brown, *Neuronal oscillations in the basal ganglia and movement*

disorders: evidence from whole animal and human recordings. Journal of Neuroscience, 2004. **24**(42): p. 9240-9243.
203. Maguire, M. and G. Maguire, *Gut dysbiosis, leaky gut, and intestinal epithelial proliferation in neurological disorders: towards the development of a new therapeutic using amino acids, prebiotics, probiotics, and postbiotics.* Reviews in the neurosciences, 2018.
204. O'mahony, S., G. Clarke, Y. Borre, T. Dinan and J. Cryan, *Serotonin, tryptophan metabolism and the brain-gut-microbiome axis.* Behavioural brain research, 2015. **277**: p. 32-48.
205. Blanchard-Fillion, B., D. Prou, M. Polydoro, D. Spielberg, E. Tsika, Z. Wang, S.L. Hazen, M. Koval, S. Przedborski and H. Ischiropoulos, *Metabolism of 3-nitrotyrosine induces apoptotic death in dopaminergic cells.* Journal of Neuroscience, 2006. **26**(23): p. 6124-6130.
206. Sugama, S., B. Conti and Y. Kakinuma, *Effect of chronic stress in the onset of Parkinson's disease: possible role of microglial cells in neuroinflammation.* J. Neurol. Disord, 2015. **2**(1).
207. Paul, R., B.C. Phukan, A.J. Thenmozhi, T. Manivasagam, P. Bhattacharya and A. Borah, *Melatonin protects against behavioral deficits, dopamine loss and oxidative stress in homocysteine model of Parkinson's disease.* Life sciences, 2018. **192**: p. 238-245.
208. Dufek, M., M. Hamanová, J. Lokaj, D. Goldemund, I. Rektorová, Z. Michálková, K. Sheardova and I. Rektor, *Serum inflammatory biomarkers in Parkinson's disease.* Parkinsonism & related disorders, 2009. **15**(4): p. 318-320.
209. Tufekci, K.U., S. Genc and K. Genc, *The endotoxin-induced neuroinflammation model of Parkinson's disease.* Parkinson's disease, 2011. **2011**.
210. Lee, C.R., J.C. Patel, B. O'neill and M.E. Rice, *Inhibitory and excitatory neuromodulation by hydrogen peroxide: translating energetics to information.* The Journal of physiology, 2015. **593**(16): p. 3431-3446.
211. Wu, X., C. Yang, J. Ge and Z. Liu, *Polydopamine tethered enzyme/metal–organic framework composites with high stability and reusability.* Nanoscale, 2015. **7**(45): p. 18883-18886.
212. Oja, S.S., R. Janáky, V. Varga and P. Saransaari, *Modulation of glutamate receptor functions by glutathione.* Neurochemistry international, 2000. **37**(2-3): p. 299-306.
213. Abe, K., K. Nakanishi and H. Saito, *The anticonvulsive effect of glutathione in mice.* Biological and Pharmaceutical Bulletin, 1999. **22**(11): p. 1177-1179.
214. Morris, G., G. Anderson, O. Dean, M. Berk, P. Galecki, M. Martin-Subero and M. Maes, *The glutathione system: a new drug target in neuroimmune disorders.* Molecular neurobiology, 2014. **50**(3): p. 1059-1084.
215. Paoletti, P. and J. Neyton, *NMDA receptor subunits: function and pharmacology.* Current opinion in pharmacology, 2007. **7**(1): p. 39-47.
216. Ishigami, M., K. Hiraki, K. Umemura, Y. Ogasawara, K. Ishii and H. Kimura, *A source of hydrogen sulfide and a mechanism of its release in the brain.* Antioxidants & redox signaling, 2009. **11**(2): p. 205-214.
217. Vandiver, M.S. and S.H. Snyder, *Hydrogen sulfide: a gasotransmitter of clinical relevance.* Journal of molecular medicine, 2012. **90**(3): p. 255-263.
218. Singh, N., D. Das, A. Singh and M.L. Mohan, *Prion protein and metal interaction: physiological and pathological implications.* Current issues in molecular biology, 2010. **12**(2): p. 99.
219. Devos, D., C. Moreau, J.C. Devedjian, J. Kluza, M. Petrault, C. Laloux, A. Jonneaux, G. Ryckewaert, G. Garçon and N. Rouaix, *Targeting chelatable iron*

as a therapeutic modality in Parkinson's disease. Antioxidants & redox signaling, 2014. **21**(2): p. 195-210.
220. Sofic, E., P. Riederer, H. Heinsen, H. Beckmann, G. Reynolds, G. Hebenstreit and M. Youdim, *Increased iron (III) and total iron content in post mortem substantia nigra of parkinsonian brain.* Journal of neural transmission, 1988. **74**(3): p. 199-205.
221. Kim, N.-H., S.-J. Park, J.-K. Jin, M.-S. Kwon, E.-K. Choi, R.I. Carp and Y.-S. Kim, *Increased ferric iron content and iron-induced oxidative stress in the brains of scrapie-infected mice.* Brain research, 2000. **884**(1-2): p. 98-103.
222. Riederer, P., E. Sofic, W.D. Rausch, B. Schmidt, G.P. Reynolds, K. Jellinger and M.B. Youdim, *Transition metals, ferritin, glutathione, and ascorbic acid in parkinsonian brains.* Journal of neurochemistry, 1989. **52**(2): p. 515-520.
223. Quintana, C. and L. Gutiérrez, *Could a dysfunction of ferritin be a determinant factor in the aetiology of some neurodegenerative diseases?* Biochimica et Biophysica Acta (BBA)-General Subjects, 2010. **1800**(8): p. 770-782.
224. Milardi, D. and E. Rizzarelli, *Neurodegeneration: metallostasis and proteostasis*. 2011: Royal Society of Chemistry.
225. Scemes, E. and C. Giaume, *Astrocyte calcium waves: what they are and what they do.* Glia, 2006. **54**(7): p. 716-725.
226. Halassa, M.M., T. Fellin and P.G. Haydon, *Tripartite synapses: roles for astrocytic purines in the control of synaptic physiology and behavior.* Neuropharmacology, 2009. **57**(4): p. 343-346.
227. Zhang, H. and A.E. Cohen, *Optogenetic approaches to drug discovery in neuroscience and beyond.* Trends in biotechnology, 2017. **35**(7): p. 625-639.
228. Hammond, C., H. Bergman and P. Brown, *Pathological synchronization in Parkinson's disease: networks, models and treatments.* Trends in neurosciences, 2007. **30**(7): p. 357-364.
229. Khabarova, E.A., N.P. Denisova, A.B. Dmitriev, K.V. Slavin and L. Verhagen Metman, *Deep Brain Stimulation of the Subthalamic Nucleus in Patients with Parkinson Disease with Prior Pallidotomy or Thalamotomy.* Brain sciences, 2018. **8**(4): p. 66.
230. Blomstedt, P., T. Taira and M. Hariz, *Rescue pallidotomy for dystonia through implanted deep brain stimulation electrode.* Surgical neurology international, 2016. **7**(Suppl 35): p. S815.
231. MacKay-Lyons, M., *Central pattern generation of locomotion: a review of the evidence.* Physical therapy, 2002. **82**(1): p. 69-83.
232. Marder, E. and D. Bucher, *Central pattern generators and the control of rhythmic movements.* Current biology, 2001. **11**(23): p. R986-R996.
233. Joers, V., M.G. Tansey, G. Mulas and A.R. Carta, *Microglial phenotypes in Parkinson's disease and animal models of the disease.* Progress in neurobiology, 2017. **155**: p. 57-75.
234. Jaffrey, S.R., H. Erdjument-Bromage, C.D. Ferris, P. Tempst and S.H. Snyder, *Protein S-nitrosylation: a physiological signal for neuronal nitric oxide.* Nature cell biology, 2001. **3**(2): p. 193.
235. Seneviratne, U., A. Nott, V.B. Bhat, K.C. Ravindra, J.S. Wishnok, L.-H. Tsai and S.R. Tannenbaum, *S-nitrosation of proteins relevant to Alzheimer's disease during early stages of neurodegeneration.* Proceedings of the National Academy of Sciences, 2016: p. 201521318.
236. Van der Worp, H.B., D.W. Howells, E.S. Sena, M.J. Porritt, S. Rewell, V. O'Collins and M.R. Macleod, *Can animal models of disease reliably inform human studies?* PLoS medicine, 2010. **7**(3): p. e1000245.

237. Varas, M., M. Pérez, O. Ramírez and S.R. de Barioglio, *Melanin concentrating hormone increase hippocampal synaptic transmission in the rat.* Peptides, 2002. **23**(1): p. 151-155.
238. Lu, Z.-h., S. Fukuda, Y. Minakawa, A. Yasuda, H. Sakamoto, S. Sawamura, H. Takahashi and N. Ishii, *Melanin concentrating hormone induces hippocampal acetylcholine release via the medial septum in rats.* Peptides, 2013. **44**: p. 32-39.
239. Williams, G., C. Bing, X.J. Cai, J.A. Harrold, P.J. King and X.H. Liu, *The hypothalamus and the control of energy homeostasis: different circuits, different purposes.* Physiology & behavior, 2001. **74**(4-5): p. 683-701.
240. Guyon, A., G. Conductier, C. Rovere, A. Enfissi and J.-L. Nahon, *Melanin-concentrating hormone producing neurons: activities and modulations.* Peptides, 2009. **30**(11): p. 2031-2039.
241. Saito, Y., M. Cheng, F.M. Leslie and O. Civelli, *Expression of the melanin-concentrating hormone (MCH) receptor mRNA in the rat brain.* Journal of comparative Neurology, 2001. **435**(1): p. 26-40.
242. Ferreira, J.G.P., J.C. Bittencourt and A. Adamantidis, *Melanin-concentrating hormone and sleep.* Current opinion in neurobiology, 2017. **44**: p. 152-158.
243. Siletti, C.E., C.A. Zeiner and J.M. Bhatnagar, *Distributions of fungal melanin across species and soils.* Soil Biology and Biochemistry, 2017. **113**: p. 285-293.
244. Cordero, R.J. and A. Casadevall, *Functions of fungal melanin beyond virulence.* Fungal Biology Reviews, 2017. **31**(2): p. 99-112.
245. Shoham, S. and S.M. Levitz, *The immune response to fungal infections.* British journal of haematology, 2005. **129**(5): p. 569-582.
246. Smith, A.D., B.L. Logeman and D.J. Thiele, *Copper acquisition and utilization in fungi.* Annual review of microbiology, 2017. **71**: p. 597-623.
247. Partlow, B.P., C.W. Hanna, J. Rnjak-Kovacina, J.E. Moreau, M.B. Applegate, K.A. Burke, B. Marelli, A.N. Mitropoulos, F.G. Omenetto and D.L. Kaplan, *Highly tunable elastomeric silk biomaterials.* Advanced functional materials, 2014. **24**(29): p. 4615-4624.
248. Applegate, M.B., B.P. Partlow, J. Coburn, B. Marelli, C. Pirie, R. Pineda, D.L. Kaplan and F.G. Omenetto, *Photocrosslinking of silk fibroin using riboflavin for ocular prostheses.* Advanced Materials, 2016. **28**(12): p. 2417-2420.
249. Hopkins, A.M., L. De Laporte, F. Tortelli, E. Spedden, C. Staii, T.J. Atherton, J.A. Hubbell and D.L. Kaplan, *Silk hydrogels as soft substrates for neural tissue engineering.* Advanced functional materials, 2013. **23**(41): p. 5140-5149.
250. McKinlay, A.C., R.E. Morris, P. Horcajada, G. Férey, R. Gref, P. Couvreur and C. Serre, *BioMOFs: metal–organic frameworks for biological and medical applications.* Angewandte Chemie International Edition, 2010. **49**(36): p. 6260-6266.
251. Zhou, H.-C., J.R. Long and O.M. Yaghi, *Introduction to metal–organic frameworks*. 2012, ACS Publications.
252. Yaghi, O.M., M. O'keeffe, N.W. Ockwig, H.K. Chae, M. Eddaoudi and J. Kim, *Reticular synthesis and the design of new materials.* Nature, 2003. **423**(6941): p. 705.
253. Xi, J., Y. Xia, Y. Xu, J. Xiao and S. Wang, *(Fe, Co)@ nitrogen-doped graphitic carbon nanocubes derived from polydopamine-encapsulated metal–organic frameworks as a highly stable and selective non-precious oxygen reduction electrocatalyst.* Chemical Communications, 2015. **51**(52): p. 10479-10482.
254. Lian, X., Y. Fang, E. Joseph, Q. Wang, J. Li, S. Banerjee, C. Lollar, X. Wang and H.-C. Zhou, *Enzyme–MOF (metal–organic framework) composites.* Chemical Society Reviews, 2017. **46**(11): p. 3386-3401.

255. Keskin, S. and S. Kızılel, *Biomedical applications of metal organic frameworks.* Industrial & Engineering Chemistry Research, 2011. **50**(4): p. 1799-1812.
256. Zheng, H., Y. Zhang, L. Liu, W. Wan, P. Guo, A.M. Nyström and X. Zou, *One-pot synthesis of metal–organic frameworks with encapsulated target molecules and their applications for controlled drug delivery.* Journal of the American chemical society, 2016. **138**(3): p. 962-968.
257. Chang, L., J. Li, X. Duan and W. Liu, *Porous carbon derived from Metal–organic framework (MOF) for capacitive deionization electrode.* Electrochimica Acta, 2015. **176**: p. 956-964.
258. Sheberla, D., J.C. Bachman, J.S. Elias, C.-J. Sun, Y. Shao-Horn and M. Dincă, *Conductive MOF electrodes for stable supercapacitors with high areal capacitance.* Nature materials, 2017. **16**(2): p. 220.
259. Shen, S., Y. Wu, Y. Liu and D. Wu, *High drug-loading nanomedicines: progress, current status, and prospects.* International journal of nanomedicine, 2017. **12**: p. 4085.
260. Wilms, H., P. Rosenstiel, J. Sievers, G.N. DEUSCHL, L. Zecca and R. Lucius, *Activation of microglia by human neuromelanin is NF-κB dependent and involves p38 mitogen-activated protein kinase: implications for Parkinson's disease.* The FASEB journal, 2003. **17**(3): p. 500-502.
261. Gao, H.-M., J.-S. Hong, W. Zhang and B. Liu, *Distinct role for microglia in rotenone-induced degeneration of dopaminergic neurons.* Journal of Neuroscience, 2002. **22**(3): p. 782-790.
262. Magin, C.M., D.L. Alge and K.S. Anseth, *Bio-inspired 3D microenvironments: a new dimension in tissue engineering.* Biomedical Materials, 2016. **11**(2): p. 022001.
263. Heathman, T.R., A.W. Nienow, M.J. McCall, K. Coopman, B. Kara and C.J. Hewitt, *The translation of cell-based therapies: clinical landscape and manufacturing challenges.* Regenerative medicine, 2015. **10**(1): p. 49-64.
264. Dalton, A.C. and W.A. Barton, *Over-expression of secreted proteins from mammalian cell lines.* Protein science, 2014. **23**(5): p. 517-525.
265. Baker, M., *Is there a reproducibility crisis? A Nature survey lifts the lid on how researchers view the'crisis rocking science and what they think will help.* Nature, 2016. **533**(7604): p. 452-455.
266. Grist, S.M., S. Gawad, L. Yu, L. Chrostowski and K.C. Cheung, *3D Cell Culture with Integrated Oxygen Control and Measurement.* CMBES Proceedings, 2018. **37**.
267. Howells, D., M.J. Porritt, J. Wong, P. Batchelor, R. Kalnins, A. Hughes and G. Donnan, *Reduced BDNF mRNA expression in the Parkinson's disease substantia nigra.* Experimental neurology, 2000. **166**(1): p. 127-135.
268. Liu, H., Y. Zhou, S. Chen, M. Bu, J. Xin and S. Li, *Current sustained delivery strategies for the design of local neurotrophic factors in treatment of neurological disorders.* asian journal of pharmaceutical sciences, 2013. **8**(5): p. 269-277.
269. Grist, S.M., J.C. Schmok, A.D. Gaxiola and K.C. Cheung. *Microfluidic platform with integrated thin-film optical oxygen sensors for transient hypoxia*. in *New Circuits and Systems Conference (NEWCAS), 2016 14th IEEE International*. 2016. IEEE.
270. Al-Zyoud, W., R. Bater, T. Awad, O. Yasin and A. Al-Zaben. *Bioreactor for biopharmaceutical production: Simple controlled environment design*. in *2018 IEEE 4th Middle East Conference on Biomedical Engineering (MECBME)*. 2018. IEEE.

271. Vespa, P., M. Bergsneider, N. Hattori, H.-M. Wu, S.-C. Huang, N.A. Martin, T.C. Glenn, D.L. McArthur and D.A. Hovda, *Metabolic crisis without brain ischemia is common after traumatic brain injury: a combined microdialysis and positron emission tomography study.* Journal of Cerebral Blood Flow & Metabolism, 2005. **25**(6): p. 763-774.
272. Wang, Z., S.N. Wang, T.Y. Xu, Z.W. Miao, D.F. Su and C.Y. Miao, *Organoid technology for brain and therapeutics research.* CNS neuroscience & therapeutics, 2017. **23**(10): p. 771-778.
273. Kratochwil, N.A., W. Huber, F. Müller, M. Kansy and P.R. Gerber, *Predicting plasma protein binding of drugs: a new approach.* Biochemical pharmacology, 2002. **64**(9): p. 1355-1374.
274. Manzanares, J.A., A.-K. Rimpelä and A. Urtti, *Interpretation of ocular melanin drug binding assays. Alternatives to the model of multiple classes of independent sites.* Molecular pharmaceutics, 2016. **13**(4): p. 1251-1257.
275. Pelkonen, L., U. Tengvall-Unadike, M. Ruponen, H. Kidron, E.M. del Amo, M. Reinisalo and A. Urtti, *Melanin binding study of clinical drugs with cassette dosing and rapid equilibrium dialysis inserts.* European Journal of Pharmaceutical Sciences, 2017. **109**: p. 162-168.
276. Araújo, M., R. Viveiros, T.R. Correia, I.J. Correia, V.D. Bonifácio, T. Casimiro and A. Aguiar-Ricardo, *Natural melanin: A potential pH-responsive drug release device.* International journal of pharmaceutics, 2014. **469**(1): p. 140-145.
277. Giasson, B.I. and V.M.-Y. Lee, *Are ubiquitination pathways central to Parkinson's disease?* Cell, 2003. **114**(1): p. 1-8.
278. Brundin, P., R. Melki and R. Kopito, *Prion-like transmission of protein aggregates in neurodegenerative diseases.* Nature Reviews Molecular Cell Biology, 2010. **11**(4): p. 301.
279. Taylor, D., *Inactivation of transmissible degenerative encephalopathy agents: a review.* The Veterinary Journal, 2000. **159**(1): p. 10-17.
280. Collins, S.J., V.A. Lawson and C.L. Masters, *Transmissible spongiform encephalopathies.* The Lancet, 2004. **363**(9402): p. 51-61.
281. Eigen, M., *Prionics or the kinetic basis of prion diseases.* Biophysical chemistry, 1996. **63**(1): p. A1-A18.
282. Velez-Pardo, C., M. Jimenez Del Rio, H. Verschueren, G. Ebinger and G. Vauquelin, *Dopamine and iron induce apoptosis in PC12 cells.* Pharmacology & toxicology, 1997. **80**(2): p. 76-84.
283. Giese, R.W. and B.L. Vallee, *Metallocenes. Novel class of reagents for protein modification. I. Maleic anhydride iron tetracarbonyl.* Journal of the American Chemical Society, 1972. **94**(17): p. 6199-6200.
284. Erker, G., *Bio-organometallic chemistry, ansa-metallocenes, and frustrated Lewis pairs: functional group chemistry at the group 4 bent metallocenes.* Organometallics, 2011. **30**(3): p. 358-368.
285. Imbihl, R. and G. Ertl, *Oscillatory kinetics in heterogeneous catalysis.* Chemical Reviews, 1995. **95**(3): p. 697-733.
286. Normandin, L. and A.S. Hazell, *Manganese neurotoxicity: an update of pathophysiologic mechanisms.* Metabolic brain disease, 2002. **17**(4): p. 375-387.
287. Uversky, V.N., J. Li and A.L. Fink, *Metal-triggered structural transformations, aggregation, and fibrillation of human α-synuclein a possible molecular link between parkinson' s disease and heavy metal exposure.* Journal of Biological Chemistry, 2001. **276**(47): p. 44284-44296.
288. Cole, N.B., D.D. Murphy, J. Lebowitz, L. Di Noto, R.L. Levine and R.L. Nussbaum, *Metal-catalyzed oxidation of α-synuclein helping to define the*

relationship between oligomers, protofibrils, and filaments. Journal of Biological Chemistry, 2005. **280**(10): p. 9678-9690.